DETAILED MODELLING OF FLUID-PARTICLE INTERACTION IN SEDIMENT TRANSPORT WITH APPLICATIONS IN RIVERS

Oldouz Payan

Submitted in accordance with the requirements for degree of

Doctor of Philosophy

The University of Leeds

School of Civil Engineering

February, 2015

The candidate confirms that the work submitted is her own and that appropriate credit has been given where reference has been made to the work of others.

This copy has been supplied on the understanding that it is copyright material and that no quotation from the thesis may be published without proper acknowledgement.

The right of Oldouz Payan to be identified as Author of this work has been asserted by her in accordance with the Copyright, Designs and Patents Act 1988.

Acknowledgments

Abstract

Flood risks, channel and bank erosions are directly related to the sediment transport discharge, its understanding and control. Moreover the prediction of sediment entrainment, transport and deposition, predicting the river bed-form (e.g. ripples and dunes) changes is an important research field due to its substantial practical worth. The prediction process of sediment transport over bed-forms in open-channel flow is strongly affected by the complex turbulence structures. Witnessing effects of small and large turbulent scales on particles while considering inter-particle collisions remain challengeable. On the other hand it is clear that, not only the movement of sediments at river beds is influenced by turbulent flows the but also on most cases the solid particles have a direct impact on the flow regime. One of the tasks remain in this regard is to measure the aforementioned effects, on a very small scales where the momentum exchange at the particulate scales occurs.

In order to study such challenges in a more faithful approach, four-way coupling through open source code of CFD-DEM (a coupling code between Computational Fluid dynamics (CFD) and Discrete Element Method (DEM)), is demonstrated in this research for bed-load sediment transport on a particulate scale. Understanding the fluid-particle interaction for application in rivers where the presence of micro and macro turbulent structures in the fluid plays a significant role, have been the focus of this study. Furthermore this thesis is furnished by conducting numerical and experimental investigations to obtain better understanding of turbulent flows in geometries similar to river bed-forms, e.g. dune-form and bar-form.

This research demonstrates that complexity of particle-laden turbulent flows is a result of particle-fluid, fluid-particle, particle-particle and particle-structures that takes place close to bed. Turbulence and near-bed flow velocity along with its irregular risings and fallings have a direct impact on the sediment particles motion. By utilising Large Eddy Simulation (LES) turbulent modelling, turbulent scales are captured. Moreover inter-particle collision of sediments has been highlighted by the means of four-way coupling. Consequently the effect of fluid on the particles and vice versa is

demonstrated. It is revealed that the presence of sediment particles in turbulent flows affect the fluid motion along with its accompanying turbulent activities. Particles are lifted as a result of applied forces from eddies and significant influence is therefore captured on the moving particles that are in the vicinity of eddies. The effects that sediments apply on the turbulent structures in the flow have also been captured due to momentum exchange between particle and fluid phase. This has been shown by the means of fluctuation variations at the location of interacting particles.

Keywords: Sediment transport, Bed-load, LES, Four-way coupling, CFD-DEM

Table of Contents

List of Tables

List of Figures

List of Abbreviations

ADV	Acoustic Doppler Velocimeter
CFD	Computational Fluid Dynamics
CFD-DEM	Coupling code between CFD and DEM
DEM	Discrete Element Method
DNS	Direct Numerical Simulation
LES	Large Eddy Simulation
FDM	Finite Difference Method
FEM	Finite Element Method
FVM	Finite Volume Method
N-S	Navier Stokes equations
OpenFOAM	Open source Field Operation And Manipulation
PIV	Particle Image Velocimetry
RANS	Reynolds Average Navier Stokes

Preface

Detailed computational modelling of fluid particle interaction with the presence of turbulent flow structures is important and yet challenging with applications of sediment transport in rivers. Four way coupling procedure to simulate bed-load sediment transport is aimed to be the focus of this this research that has been carried out at the School of Civil Engineering, University of Leeds.

This thesis has been furnished in 6 chapters which provides insight to interaction between fluid and particles at the particulate scales. Chapter 1 consist of the previous works on the sediment transport and turbulent flows along with motivation and objectives for carrying out this research. Chapter 2 to is dedicated to experimental investigations in geometries similar to river bed-forms, e.g. bar-form. Third chapter gives insight to numerical method, CFD and DEM tools used in this research. Furthermore numerical results in both CFD (fluid phase) and CFD-DEM (particle-laden flow) have been reported in Chapter 4. Findings and discussions of the results have been included in Chapter 5. Finally conclusion and potential future works have been addressed in Chapter 6 of this thesis.

Oldouz Payan

February 2015

Leeds, UK

Chapter 1 Introduction

1.1 Sediment transport in open channels

1.1.1 Introduction

Sediment transport is a time dependant phenomena and such unsteadiness is described by Hsü (2004) as the process of sand deposition on a river bed at one flood, and the high likelihood of sediments to be carried away by the next flood. The natural processes of erosion, transportation and sedimentation shown in Figure 1-1 relate to the interaction between sediment and the surrounding fluid.
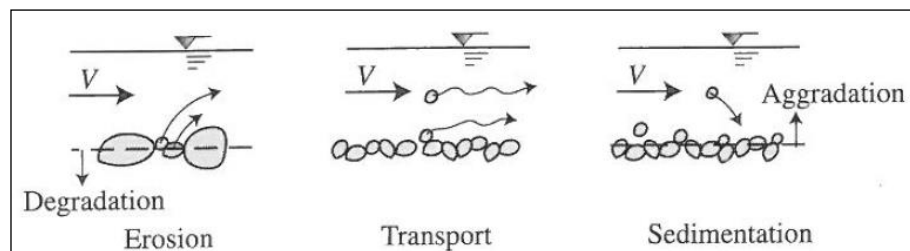
Figure 1-1: processes of erosion, transportation and sedimentation (Julien 2010)

Furthermore, capturing either stationary or moving sediments interactions with small and large coherent structures of eddies where is caused by relatively random phenomena of turbulence, remains the biggest challenge of hydrodynamics problems. The small and large scale turbulent structures play a significant role in sediment entrainment. Describing such complexity of sediment transport process, fluid motion with the presence of small and large turbulent scales is the key factor to find a more specific, accurate and universal function. In other words, the prediction process of sediment transport over bed-forms in open-channel flow is strongly affected by the complex turbulence structures caused by flow separations that occur as part of the process. The three dimensionality of turbulence and its effect on the morphological process form a complex problem which remains to be investigated in greater details. Another challenge lies in this area is the absence of sediment transport physical models at very small scales where the momentum exchange at the particulate scales happens. Such a

drawback makes the prediction of small-scale sedimentary processes difficult. It is understood that complexity of particle-laden turbulent flows are a result of different movement patterns such as rolling, sliding and saltation close and distant from bed. Turbulence and near-bed velocity along with its irregular risings and fallings have a direct impact on the sediment particles motion. Conversely the presence of sediment particles in turbulent flows may affect the fluid motion along with its accompanying turbulent activities. Moreover, inter-particle collision of sediments have been highlighted in many studies, experimentally where have led to different results as to whether grains elastically rebound or if the collisions are viscously damped or even if the mixture of both processes are involved Niño and García (1994); Murphy and Hooshiari (1982); Sckine (1992) and Abbott and Francis (1977). Furthermore Schmeeckle, Nelson *et al.* (2001) state that the inter-particle collision is inevitable and also can be important but not dominant in the process of momentum and energy transport in the flow.

1.1.2 Background

A river is a natural waterway that flows towards another river, an ocean, or a lake. Being part of the hydrological cycle, a significant amount of sedimentation entrainment occurs with the flow of water on different moveable beds. Throughout geological time, sediment transport and depositional processes, have shaped the Earth's surface and landscape. This is a result of the interaction between natural fluid motions and either stationary or in-motion particles in the flow. Such interaction and sediment movement was explained by Bagnold (1988) by carrying out various experiments. The river flow is simply is not a laminar one and the sediment transport itself is a very complex system which, covers the fluid-particles interaction topic. It is clear that, not always movement of sediments at river beds are influenced by turbulent flows the but also on most occasions the solid particles have a direct impact on the flow regime and fluids motion. Considering rivers as a branch of hydraulic science, this field and its problems have been developed through time. Sedimentation, which is referred to the motion of solid particles, cause severe engineering and environmental problems (Julien 2010). Flood risks, channel and bank erosions are directly related to the sediment transport discharge, its understanding and control. Moreover the prediction of sediment pick-up, transport and deposition, predicting the river bed-form (e.g. ripples and dunes) changes or hydraulic roughness of the river, is an important research field due to its significant practical value.

Uncertain questions on sediment transport have been tried to be answered in the past by many researches and contributors. Approaches executed by the investigators has been carried out from two main angles of deterministic and statistical views where the former involves with the mean flow properties and the latter with theory of turbulent stress variations. After Shields (1936), who was a pioneer in including a threshold of motion in a sediment transport formula, many researches such as White (1940); Coleman (1967); Wiberg and Smith (1987); Zanke (1990); Ling (1995); Dey (1999); Dey and Debnath (2000); McEwan and Heald (2001); Paphitis (2001); Papanicolaou *et al.* (2001); Kleinhans and van Rijn (2002); Wu and Chou (2003); Dey and Papanicolaou (2008), addressed the same concept of developing motion to

be a function of the mean bed shear stress. In contrast to such view other investigators such as Einstein and El-Samni (1949); Nelson *et al.* (1995); Cheng and Chiew (1999), and many more dealt with sediment transport with a non-deterministic approach.

The study of flow in open channels in a physical and mathematical approach started by Leonardo Da Vinci in 1500, the Italian experimentalist and engineer who showed eddies in his art sketches. This great interest of water motion was then carried out by another scientist Galileo Galilei through experiments. Galileo's student, Benedetto Castelli, who explained the continuity law in more details in his book in 1628, was credited as being the founder of river hydraulics afterward. Later on in the seventeenth century, Sir Isaac Newton introduced the law of viscosity where the proportionality of shear stress and the velocity gradient was stated in his proposal. Newton's work was continued by Prandtl where the shear stress relationship was used to create assumptions for turbulent flows. However in the eighteenth century, Daniel Bernoulli and Leonard Euler derived mathematical description of fluid mechanics, the excellence of equations were not to its maximum until Navier-Stokes equations (N-S) were derived by Claude-Louis Navier in 1822 and George Stokes in 1845 (Graf 1984; Anderson Jr 2005; Wright and Crosato 2011).

Different methods and studies have been used since the sixteenth century to predict the behaviour of fluid-particles interaction in river and the problems that are caused by sedimentation in rivers. Albert Brahams was the first to describe initiation of sediment motion. Such qualitative and remarkable contribution of N-S equations was then continued by other engineering scientists such as Bossut and Chezy. Later in the nineteenth century Shields (1936) empirically proposed a relationship between shear velocity, U^* (ms^{-1}) and critical shear stress, τ_c (Pa) which is still one of the most used in sediment transport problems.

Developing sediment transport equations have continuously being done since the 16th century up to present mostly concentrating on suspended, bed load transport and shear stresses with little focus on the presence of

turbulence. Turbulent effects in natural streams have not just been ignored to a great deal, but also have only been modelled in the past rather than resolved principally in regards with fluid-particles interaction.

Van Rijn (1984-a) was one of the pioneers in the computation of bed-load transport. Through investigating the motion of the bed-load particles and to establish simple expressions for the particle characteristics and transport rate both for small and large particles, a remarkable conclusion was obtained based on a verification study using 580 flume and field data. Expressions for bed-load thickness layer and bed-load concentration were determined. He concluded that the proposed equations predict a reliable estimate of the bed-load transport in the particle range 200-2,000 µm. This resulted in a score of 77% of the predicted bed-load transport rates in the range of 0.5-2.0 times the measured values. He then accomplished a further investigation on the parameters that control the suspended load transport. In his analysis a relationship which specifies the reference concentration that yields good results for predicting the sediment transport for fine particles (100-500 *µm*) was proposed, alongside many other objectives (Van Rijn 1984-b).

The suspended load transport (q_s) according to his method is computed from equation (1-1) while the bed-load transport *(q_b)*, is computed as given in his initial work. For comparison also formulas of Engelund and Hansen (1967) and Einstein (1942) were used.

$$q_s = F\bar{u}dc_a \tag{1-1}$$

in which $\bar{u}$ = mean flow velocity; d = flow depth; and c_a = reference concentration. For the precise definition of F-factor and reference concentration you can refer to the work done by Van Rijn (1984-b).

More researchers such as Einstein and El-Samni (1949); Paintal (1971); Nelson *et al.* (1995); Cheng and Chiew (1999) and Papanicolaou *et al.* (2002) have dealt with sediment entrainment based on stochastic approaches. Schmeeckle and Nelson (2003) applied Direct Numerical Simulation (DNS) for bed-load transport while taking into account for lift force on sediment transport simulations as a challenge.

6

Also, in general, investigation in this field have either been carried out by analytical considerations i.e. constructing a physical model (experiment) or by a numerical simulation of the reality e.g. a designed structure. Despite the fact that analytical solutions are only found for more simplified problems and unconnected from practical cases but fundamental findings of such approach can accurately be used for a broader and perhaps universal models. On the other hand, taking into account for all the mentioned complexity in the area, numerical models have advantages of being cost-effective compared to experimental investigations.

There are two approaches for further insight into the investigation of sediment transport in rivers. The first approach is the numerical calculation using Euler-Lagrange approach where fluid phase (water) is treated as a continuum by solving Navier-stokes (N-S) equations. While the dispersed phase is solved by tracking particles through the calculated flow field; and the second approach is the Euler-Euler approach where both the fluid and solid phase are treated mathematically as a continuum. Such method performs particle tracking by focusing on the control volume, which treats sediment as a continuous scalar field and is concerned with its concentration at fixed points. Only the first approach has been used in this literature. In the Euler-Lagrangian approach, the continuum (water) is solved by a mathematical model called Large Eddy simulation (LES), explained in details in later sections of this thesis, while the dispersed phase (sand) is solved by integrating the force balance on the particle, which is written in the Lagrangian frame of reference. Schematic Figure 1-2 shows a particle being tracked in a control volume. Furthermore this method has been used in a lot of different sediment transport studies, such as Pedinotti, Mariotti *et al.* (1992), Elghobashi and Truesdell (1993), Wang and Maxey (1993), Yang and Lei (1998), Dorgan and Loth (2004) and Bosse, Kleiser *et al.* (2006); where the centre of attention has been on only the features close to the bed-load rather than suspended sediments. Observing sediment transport in the flow, as a discrete phase rather than a continuum phase, have been done by the Discrete Phase Modelling (DPM) approach and also Discrete Element Modelling (DEM) in different studies by Heald, McEwan and Tait (2004); Drake and Calantoni (2001); McEwan and Heald (2001); McEwan, Heald

and Goring (1999); Jefcoate and McEwan (1997) and Calantoni, Todd Holland and Drake (2004). The Eulerian approach has been used alternatively where the study of sediment transport in suspension has been the core of investigation, in particular in laboratory and also field works Wu, Rodi *et al.* (2000); Zedler and Street (2001); Zedler and Street (2006) and Byun and Wang (2005). Such an approach was concerned with one-way coupling where only flow affects the particles, and ignores the two-way coupling where fluid-particle interactions are of interest. Despite all other past studies that have been focusing on the transport of finite number of particles using the Lagrangian particle tracking approach; the work of Chou and Fringer has been done while having unlimited sediment pickup from the channel bed. This has also enabled the Eulerian approach to be used as a result of low concentration sediment in simulation where assumed that particles with no separate dynamics and are following the flow. In such method fine-scale particle physics in turbulent flow is ignored; as Chou and Fringer (2008) believes that the study of fine sediment suspensions may not be practical using the Lagrangian particle tracking approach where the motion of each particle must be calculated at each very small time step and this has a high computational loading.
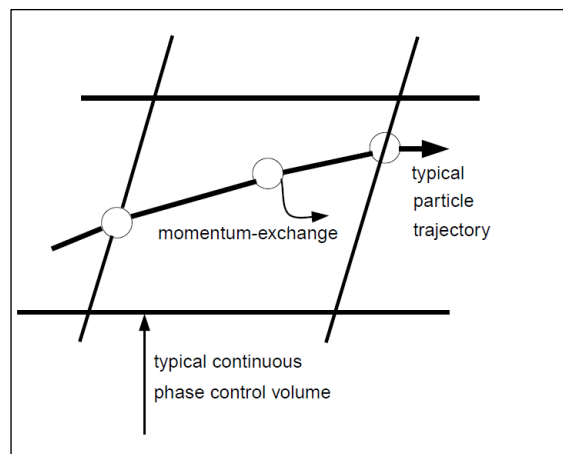
Figure 1-2: Interphase exchange of momentum between particle to fluid (ANSYS Fluent 2009)

Another way to look at the interaction details happening between particle and fluid is to bring the range of coupling into the picture. So basically when

the particle-laden flow is considered as dilute enough so the surrounding fluid feels no effect from the presence of particles, term of one-way coupling can be described. Nonetheless at the time that particles do not behave like passive containments, the energy distribution of the surrounding fluid are likely to be affected to a great deal by the turbulence in a particle-laden turbulent flow. This results in the behaviour of particles being changed by turbulence and in return the fluid turbulence is altered too. When this happens then term of two-way coupling is used. For the two-way coupling occurrences to take place, enough particles must be present so the momentum exchange between the discrete phase (particles) and the continuous phase (fluid) changes the carrier phase dynamics. Yeoh, Cheung and Tu (2013) bring to attention the importance of particle-particle interactions in turbulent flows where terminology of four-way coupling is expanded in the framework of kinetic energy. Inter-particle collisions have been determined using terms of particle relaxation time (τ_p) and the characteristics time of collisions (τ_c).
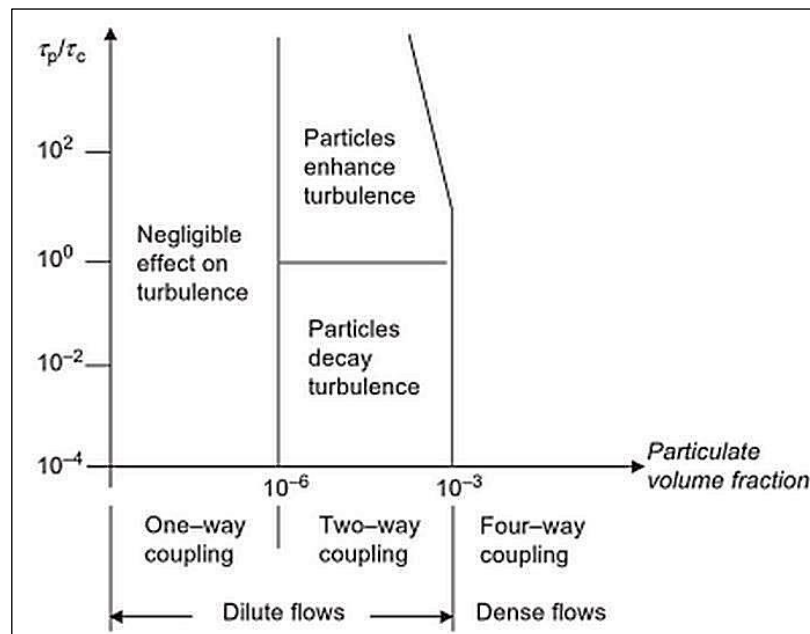
Figure 1-3: Proposed map for particle-turbulence modulation (Elghobashi 1994; Yeoh, Cheung and Tu 2013)

Dilute and dense regimes are given by $\frac{\tau_p}{\tau_c} \ll 1$ and $\frac{\tau_p}{\tau_c} \gg 1$ respectively. Figure 1-3 indicates that if particle volume fractions are less than 10^{-6}, there

is no influence of particles expected to be inserted to the turbulence of the fluid. For particle volume fractions between 10^{-6} and 10^{-3} turbulence is increased by particles; and if the volume fraction is greater than 10^{-3} the motion of particles is significantly controlled by inter-particle interactions. The three phases mentioned are referred to as very dilute, dilute and dense flows in respect to the particle volume fractions.

Acknowledging the major features of turbulent fluid–particle flows is of importance to sediment transport. Despite their importance, little is known about the influence of inter-particle collisions on the particle and fluid phase characteristics in the context of energy cascade by the means of small and large turbulent scales through a flume. Vreman *et al.* (2009) states that the four-way coupled simulations contain stronger coherent particle structures. It is thus essential to include the particle–particle interactions in numerical simulations. Again similar to Figure 1-3, Tsuji (2000) classifies particle–laden flows into three general categories with respect to their inter-particle collisions: dilute (collision-free) flows, medium concentration (collision-dominated) flows, and dense (contact-dominated) flows. A recent work where the four-way coupling has been studied been done by Afkhami *et al.* (2015). Unlike the current study their work focuses on dilute and medium concentration flows where is only valid for particles of low Stokes number. Furthermore the effects of gravity and fluid turbulence, respectively in both horizontal and vertical wall-bounded dilute turbulent flows have not been acknowledged.

It is believed that the change in turbulence intensity and dissipation due to particle presence can be studied in great detail once turbulence phenomena is captured accurately and this has been covered in the section below.

1.2 Turbulence & Large Eddy Simulation (LES)

1.2.1 Turbulence

An vast uniform bulk of fluid can be considered by a density ρ and molecular transport coefficients such as the viscosity μ. This bulk of fluid can be set into various kinds of motion. It is a well-known point that under appropriate settings, some of these motions' characteristics such as velocity at any given time and position in the fluid are not found to be the same when they are measured several times under apparently equal settings. The velocity takes unsystematic values which are not determined by a controllable data of flow, although it is believed that the average properties of the flow field are determined exclusively by the data. Batchelor (1953) states that "fluctuating motions of this kind are said to be turbulent". The concept of turbulence has been the core of investigation by many people such as Taylor (1938); Von Karman (1948); Kolmogorov (1941) and followed up by many more people such as Townsend (1980); Monin and Yaglom (2007) in the later years.

Many flows occurring in nature and in engineering applications are turbulent. Taking into account for turbulence, this can be done by either a deterministic approach or a statistical method. Irregularity, diffusivity (rapid mixing and increased rate of momentum, heat and mass transfer), dissipation (viscos losses) and also continuum phenomenon (turbulent length scales that are ordinary far larger than any molecular length scale), are the characteristics of turbulent flows (Tennekes and Lumley 1972).

Turbulence modelling is one of the elements in Computational Fluid Dynamics (CFD). Very precise mathematical theories have been evolved by many clever engineers, Prandtl, Taylor, von Karman and many others whose focus of work was on combination of simplicity with physical insight. Using their work as a gauge, an ideal model should introduce the minimum amount of complexity while capturing the essence of turbulence (Wilcox 1993). Therefore as the effects of turbulence in the CFD simulation cannot perfectly be represented, a turbulence model needs to be used. Presence of small and large scale turbulent structures (Figure 1-4) have been taken into account by the very early turbulence modelling in 1895 when Reynolds

(1895) published his research on turbulence using the time-averaged Navier-Stokes equation.
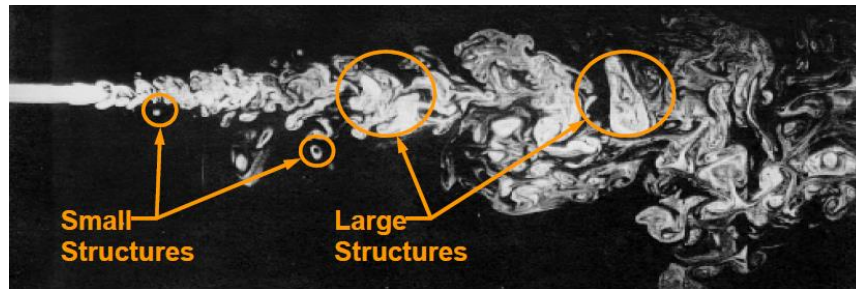
Figure 1-4: Random but presence of patterns to the motion as eddies dissipate (ANSYS UK 2010)

Turbulent flows are categorized by an unlimited number of time and length scales and so turbulence can be considered to be composed of eddies of different sizes. An eddy can be described as to be measured of a turbulent motion restricted within a region of different sizes and they range from the flow length-scale L to the smallest eddies. Each eddy has a Reynolds number, and for large eddies, R_e is large, i.e. viscos effects are negligible. The large eddies are not stable and therefore transferring energy to the smaller eddies while they break down. This process continues repeatedly where the smaller eddies also experience the same process. This energy cascade continues until the Reynolds number is sufficiently small and eventually energy is vanished by viscos effects (Pope 2000). At this time the eddy motion is stable, and molecular viscosity is responsible for dissipation. This is shown well and clearly by the hypothesis of the energy cascade mechanism presented by Richardson in 1922 (Figure 1-5). This British meteorologist described this process in verse as: "Big whorls have little whorls, which feed on their velocity; and little whorls have lesser whorls, and so on to viscosity" (Richardson 2007).
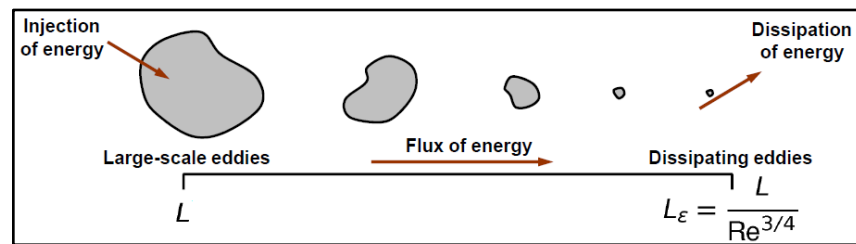
Figure 1-5: Energy Cascade (ANSYS UK 2010)

In principle, the time-dependant, three-dimensional Navier-Stokes equation contains all of the physics of a given turbulent flow. Important early contributions were made by several researchers, most notably by Von Karman (1930a). In up-to-date terms, it is referred to a mixing-length model as a zero-equation model of turbulence where by definition, an n-equation model indicates a model that requires solution of **n** number of additional differential transport equations in addition to those articulating conservation of mass, momentum and energy. The ability of forecasting properties of turbulent flows then was enriched and so a more realistic mathematical description of the turbulent stresses was developed by Prandtl (1945). A modelled differential equation approximating the exact equation for k as the kinetic energy of the turbulent fluctuations was suggested. If the velocity at a particular point in the real turbulent fluid flow is recorded, the instantaneous velocity (U) at any point in time would be $U = \bar{U} + u'$ (Figure 1-6). Turbulent Kinetic energy, k, is defined as the sum of the three fluctuating velocity components: $k = 0.5\,(\overline{u'^2} + \overline{v'^2} + \overline{w'^2})$ where the time average of the fluctuating velocities are zero, $\overline{u'} = 0$ but, the Root Mean Square (RMS) of fluctuating parts are not necessarily zero , $\overline{u'^2} \neq 0$.
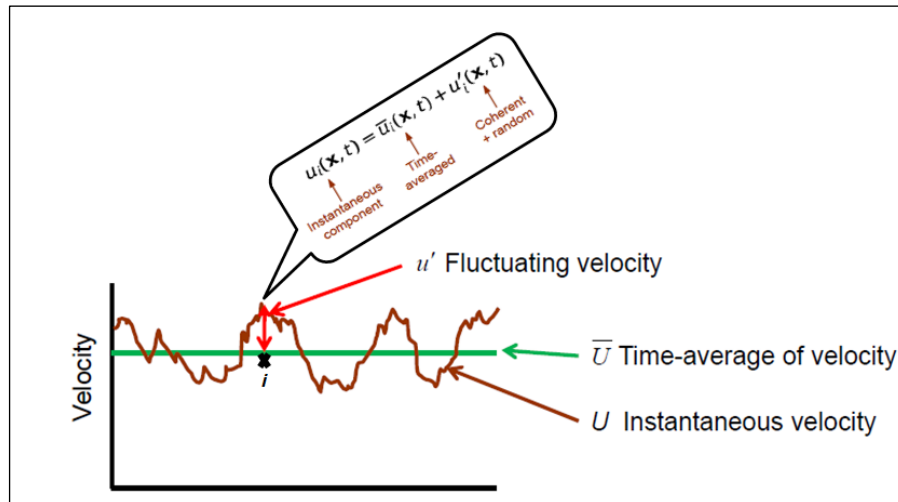
Figure 1-6: Velocity decomposition (ANSYS UK 2012)

Nowadays this is known as one-equation model of turbulence. Since this model was known as an "incomplete" due to hardships of introducing a flow length scale, Kolmogorov (1942) then introduced the first complete turbulence model. Such models have not been without excellence and in fact have proven to be of great value in many engineering applications. Kolmogorov introduced a second parameter ω, that is referred to as the rate of dissipation of energy in unit volume and time. This model is termed as a two-equation model of turbulence and due to the unavailability of computers for solving its nonlinear differential equations, this was not applied for almost a quarter century. A second-order closure approach was then originated by Rotta (1951) to accommodate effects such as streamline curvature, rigid-body rotation and body forces that were not accounted for the eddy-viscosity models properly (Wilcox 1993). During these years most CFD methods were restricted to certain types of flow where mainly time and space derivatives were approximated by using the Finite difference Method (FDM). The coming age of computers in 1960's made the four classes of turbulence models to be developed extensively. First methods applicable to general 3D flows were developed in 1960's and 1970's. This started with the Primitive Variable Methods (PVM) that involved solving for primitive variables of velocity (U, V, W) and Pressure (P) as well as Finite Volume Method (FVM) (Versteeg and Malalasekera 2007). The two main research group contributed into such development were the Las Alamos National

Laboratory, (Harlow and Amsden) in 1968 and the Imperial College of London in 1972, (Patankar and Spalding 1972).

1.2.2 Turbulence modelling: Large Eddy Simulation (LES)

Computational fluid Dynamics (CFD) is the science of predicting fluid flow and related phenomena by numerical solution of the mathematical equations which govern these processes. CFD analysis complements experimentations. In addition it reduces the total effort required in the laboratory. As analysis begins with a mathematical model of a physical problem, hence conservation of mass, momentum, and energy are to be satisfied throughout the region of interest. Also in some cases some simplifying assumptions are made in order to make the problem tractable while providing appropriate initial and boundary conditions for the problem. These points all are covered in chapter 3 of the thesis.

General motion of turbulent flow is described by the Navier-Stokes (N-S) equations which were first formulated by Claude-Louis Navier and George Gabriel Stokes in the 19th century. The application of these equations within CFD tools such as ANSYS fluent has made it very convenient to explore more insight into physical problems.

Having said that, the generation of eddies in the flow is caused by random phenomena of turbulence; simulating process and capturing either stationary or moving sediments interactions with small and large coherent structures remains the biggest challenge of hydrodynamics problems. As mentioned before the small and large scale turbulent structures play a significant role in sediment entrainment. Describing such complexity of sediment transport process, fluid motion with the presence of small and large turbulent scales is the key factor to find a more specific, accurate and universal function.

Predicting every fluctuating motion in the flow is feasible by resolving them directly; known as the Direct Numerical Simulation (DNS) approach. This means that the whole range of space-based and time-based scales of the turbulence must be resolved. All the spatial scales of the turbulence must be resolved in the computational mesh, from the smallest dissipative scales

(Kolmogorov scales), up to the integral scale L, associated with the motions containing most of the kinetic energy. But this is very expensive and intensive computationally as it requires a lot of time and computing powers. The grid must be very fine and the time-step to be very small. The higher the Reynolds number the higher these demands will be. Another main turbulence model used by engineers is called Reynolds-averaged Navier Stokes (RANS) where equations are solved for time-averaged flow behaviour and the magnitude of turbulent fluctuations. RANS based models are shown in Figure 1-7.
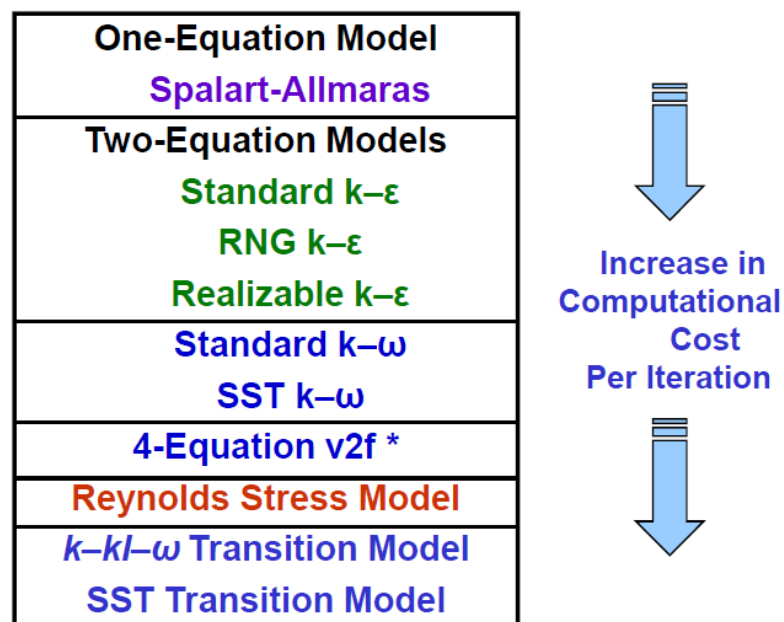
Figure 1-7: RANS based models(ANSYS UK 2012)
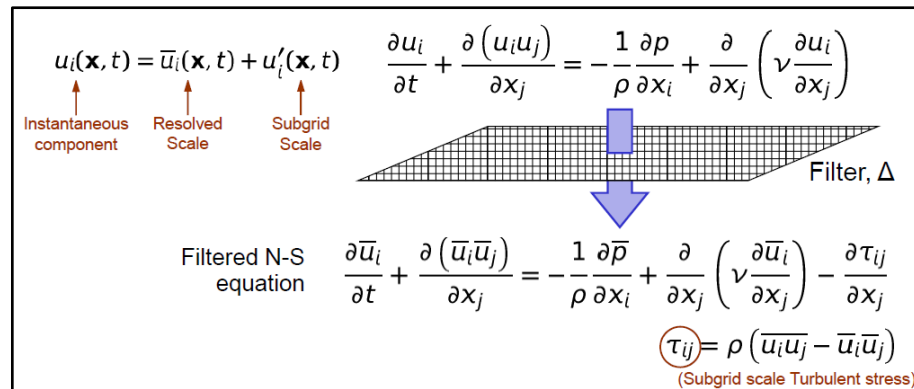
Some limitations and disadvantages of using RANS based models for different case studies are pointed out below. These reasons have been the motivation behind applying a more appropriate turbulence model of Large Eddy Simulation (LES) on the cases covered in Chapter 4 of this thesis.

Bernard (1986) and Mansour, Kim and Moin (1989) have stated that the k-ε model fails to be in good agreement with experimental results in the vicinity of the wall and boundary region and so they need modification to make reasonable predictions. More recently Berdanier (2011) has carried out a comparison study on a diffuser type of geometry, using the experimental data of Buice (1997) as a benchmark. Such study set out to compare the results from turbulence models of varying complexity and their ability to accurately resolve the locations of detachment and reattachment, as well as

the velocity profiles through the diffuser. This resulted in that none of the models were able to accurately resolve the wall shear stress values on the flow separating wall. Moreover ANSYS UK (2012) points out the limitations of each RANS based turbulence model. It is stated that using the Spalart-Allmaras (S-A) model, is not a reliable one for predicting the decay of turbulence, standard K-epsilon model results in extreme K production near separation point, and so not accurate prediction in the region close to walls where k and ε display large peaks. Additionally Reynolds Stress Model (RSM) have been witnessed to perform better where turbulence is highly anisotropic and so 3D effects are present. Although this was done through attempts of avoiding the shortcoming of the eddy-viscosity model, the computational cost is higher and RSMs do not always provide greater performance over k-ε and k-ω models.

Above mentioned shortcomings on the RANS based turbulence models available have been motivations behind implementing a Large Eddy Simulation (LES) on the case studies in this thesis. In LES Larger eddies are explicitly solved in the calculation and are resolved through using appropriate fine grid while taking into account of smaller eddies implicitly through a sub-grid scale model (Smagorinsky 1963). This can be described as separating the velocity field into a resolved and sub-grid part. The resolved part of the flow field signify the "large" eddies, while the subgrid part of the velocity represent the "small scales". The challenge however remains to identify a range with the most suitable filter width, in terms of Kolmogorov "-5/3 law" for the energy spectrum distribution (Kolmogorov 1941) where small eddies and dissipation becomes important at the smallest scale. Kolmogorov length scale is defined as $= \sqrt[4]{v^3/\varepsilon}$. As a consequence of filtering or averaging processes, some unknown variables such as turbulent stress, τ_{ij}^* will remain, which needs to be modelled using Sub-Grid Scale modelling (SGS) (Figure 1-8). Such modelling can be done through different methods such as eddy viscosity model, scale similarity model, and mixed model, Chung (2010). By implementing LES to model the turbulence regime, SGS effect is modelled in a recent study by Nabi *et al.* (2010) using a dynamic sub-grid scale model. The sensitivity and accuracy of such turbulence modelling becomes notable when the results obtained from

turbulence modelling is expected to be implemented on the particulate phase of the simulation. Eventually the aim is to use the coupled solved data from turbulence LES modelling to be used for determining the pick-up and deposition of the sediments, instead of empirical relations. This is critically something that has not been taken care of in the aforementioned study. Formulations of LES have been covered in chapter 3 of this thesis.

Figure 1-8: Filtering N-S equations to solve for LES turbulence model (ANSYS UK 2012)

1.3 Sediment transport

The basic process of sediment transport can be explained by the movement of particles in which the particles will only start to move if the applied shear force by the moving fluid is greater than the natural resistance force on the particle. The applied shear force on the particle is illustrated by experiments that increase from zero, τ_0, where particle motion starts, to u, where sediment motion of the bed load type occurs. Particles of such features are normally referred to as the discrete phase in the numerical investigations. This is because they can sometimes be taken care of separately as a discrete phenomenon, while being influenced by the fluid phase effects around them. The suspension load also initiates when a further increase of τ_0 leads the finer particles to be swept up in the fluid. This process can also be explained by the equilibrium momentum in equation of $a.F_L + b.F_D = a.F_w + c.F_c$ according to Figure 1-9, where the forces acting on the centre of the protruding particle include the fluid drag (F_D) and lift (F_L), particle self-

weight (F_w) and the inter-particle cohesion (F_c) at each grain contact which is normally ignored in the past. This deficiency of sediment transport simulations has been covered in the present study by carrying out a four-way coupling numerical simulation and is explained in more detail in Chapter 3. In the equation, a, b and c are the lever arms of the forces about point P where the motion of grain upon entrainment starts.

The fluid drag (F_D) in the above equation can be replaced with the mean bed shear stress that is applied at the grain projected area or even through another shear stress definition, $\tau_0 = \frac{f}{\delta}\rho U_{mean}$ that involves a drag coefficient and the mean velocity at the particle level applied over the projected area.

The shear stress equation above includes a non-dimensional small empirical coefficient called Darcy-Weisbach friction coefficient (f), fluid density (ρ), the boundary layer thickness (δ), and the mean time-averaged velocity over the whole boundary layer (U_{mean}). Moreover knowing that the lift force is more difficult to define and is normally ignored in an attempt to predict the entrainment threshold, it can be identified through the Bernoulli equation which predicts a difference in pressures on the upper and lower surface of grains which cause them to be lifted (Figure 1-10). A recent study by Schmeeckle *et al.* (2007) has shown that typical formulas for shear-induced lift based on Bernoulli's principle poorly predicts the vertical force on near-bed particles.
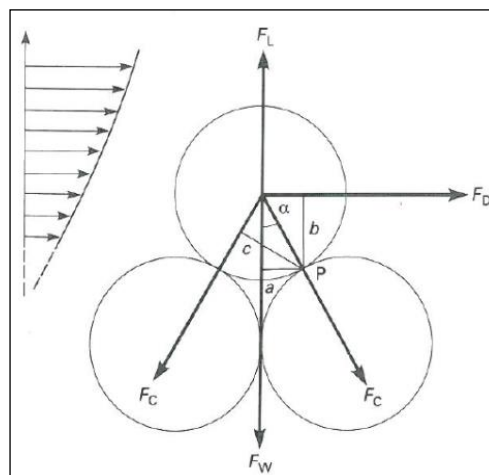
Figure 1-9:Forces acting on a particle resting on a granular bed subject to a steady current (Pye 1994)
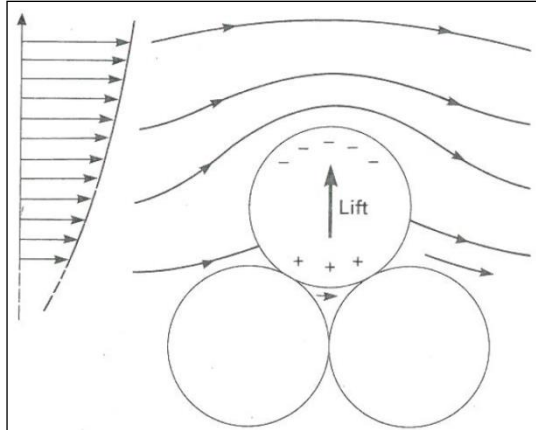
Figure 1-10:Lift force due to the Bernoulli influence on a particle on a granular bed subject to fluid shear. The fluid pressure is greater on the underside of the particle (plus signs), where the fluid velocity is lower than the upper surface (minus signs), high velocity obtains (Pye 1994)

The current study has overcome the problem of poorly defined lift force exerted on the particles. This has been achieved by defining a set of equations used as a source term in the equation of particle motion explained in Chapter 3 of this thesis.

Motion of particles occurs in the three forms of rolling, sliding and sometimes jumping which is referred as saltation. As such motion normally takes place close to bed; it is called the sediment transport of bed load. According to Van Rijn (1984-a) it happens when the value of the bed-shear velocity just exceeds the critical value for initiation of motion, the particles will be rolling and sliding or both, in continuous contact with the bed. For increasing values of the bed-shear velocity, the particles will be moving along the bed by more or less regular jumps, which are called saltation.

The governing equation methods are categorised based on fluid properties such as (1) viscosity that forms into shear stress relationship (Du-Boys-type), (2) discharge relationship (Schoklitsch-type) and (3) statically consideration of lift force (Einstein-type) (Graf 1984). Pye (1994) states that Du-Boys in 1879, was the first to show interest in prediction of bed-load flux rate by developing the idea of exerting shear force on bed-grains in which cause the displacement of stream bed in the direction of energy gradient.

Attempts to predict bed-load have been taken several directions such as empirically, semi-theoretically or even theoretically. Meyer-Peter and Muller's empirical bed-load relationship that was derived from field and laboratory flume data was perhaps the most widely used empirically (Meyer-Peter and Müller 1948). Hans Einstein's probabilistic approach and complex formulas, that explained that entrainment occurs when the local instantaneous lift force exceeds the immersed weight of an individual particle was another well-known semi-theoretical set of equations (Einstein 1942). Another theoretical approach which was different to Einstein's was then adopted by Bagnold (1988) first in 1966, where he believed the rate of work by sediment transport should be related to the rate of energy expenditure. Furthermore Engelund and Hansen developed another empirical formula to compute the bed-load transport under a current (Engelund and Hansen 1967). This formula was later used to compute the total load. Moreover Van Rijn again developed other equations for computation of suspended and bed-load transport which was in agreement with Du-Boys and Bagnold assumptions and findings rather than Einstein's; using about 800 data including field observations and flume experiments (Van Rijn 1984-a; 1984-b). Van Rijn's equations (Van Rijn 1993) have still been used for validation purposes as well as fundamental equations in many works where experiments dominate the research (Feurich and Olsen 2011).

Van Rijn (1984-a) states that when the value of the bed-shear velocity exceeds the fall velocity of the particles, the sediment particles can be lifted to a level at which the upward turbulent forces will be comparable with or of higher order than the submerged weight of the particles and as a result the particles may go into suspension phase.

Agreeing with Bagnold's findings and also considering Einstein's work more critically, later on Van Rijn illustrated equations of motions. Using Figure 1-11, where the forces acting on a saltating particle were shown to be a downward force due to its submerged weight (F_G) and hydrodynamic fluid forces, which could be resolved into a lift force (F_L), a drag force (F_D); were used to compute the reference concentration for the suspended load. Particle fall velocity and sediment diffusion coefficient has been stated to be

the main controlling hydraulic parameters for suspension phase were then studied in more details by Van Rijn (Van Rijn 1984-b).
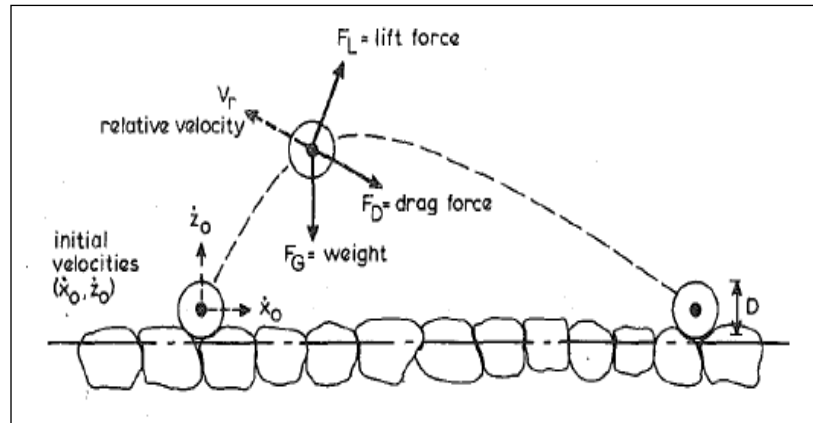
Figure 1-11: Definition sketch of particle saltation (Van Rijn 1984 (a))

Interactions between isotropic and homogenous turbulent structures and particles have been studied to a great deal by using numerical simulation in the works of Elghobashi and Truesdell (1993), Wang and Maxey (1993), Yang and Lei (1998) and Bosse, Kleiser *et al.* (2006); however the concept of suspension of particles by the turbulence is not well understood; knowing that the entrainment of sediment following the suspension of particles by turbulence is a very common phenomenon in rivers.

The link between the sediment transport in the suspension phase with the large coherent turbulent structures has been highlighted by Ikezaki, M.W. *et al.* (1999) in an experimental work. It is illustrated experimentally by sediment simulation and the presentation of a two-dimensional velocity field that indicates the sediment concentration is highly time-varying. The separation region is again found to be playing an important role on sediment trapping in the interior flow layer. Sediment suspension is also maintained by the large turbulent structures that are generated between the reattachment point and the midpoint of the stoss of the dune. Such suspension process lasts until the strength and coherency of vortical structures has not been weakened due to topographic acceleration (velocity increase) over the dune crest.

Another further development in the instantaneous transport of bed-load sediment have been achieved by Schmeeckle (1999) by combining the work of Ashida (1972); where a semi-theoretical method for calculating a dynamic friction coefficient and critical shear stress have been derived considering the force and motion of individual grains; with the work of Wiberg and Smith (1985); Sckine (1992) and Niño and García (1994) which saltation models were derived. This has been done by applying a simple model of momentum loss during collision of a saltating particle with the bed to calculate the dynamic friction coefficient per number of moving grains. From this a total shear stress reduction by moving particles, a reduced downstream velocity and also the instantaneous drag on a particle have been derived empirically. Such variable drag forces for mixed-grains have been used to simulate a three-dimensional bed. Then reasonable transport rate prediction was concluded by the dynamic boundary condition when such results were coupled with a grain motion simulation. Schmeeckle (1999) also concludes that on one hand the "Bagnold boundary condition" which is the basis of the bed-load sediment transport model works poorly at low transport stages and on the other hand at higher transport stages, empirically, have shown that entrainment prediction cannot be done properly.

So far generally these predictions have been done either by modelling a big domain of river and its topography mostly assuming the fixed bed or by considering a smaller area of any open-channel flows with other simplified assumptions. River hydraulics and sediment transport field then became the centre of studies in 20th century by describing the formation of dunes in river beds by Austrian Exner in 1925 with quantitative terms and later by Engels in 1929 who continued in laboratories specially designed for river and channel problems. Sediment problems were again studied by D. Guglielmini in the Italian school of hydraulics in 1960 through field observation (Graf 1984).

Even more recently such sediment transport prediction has been done in studies using the advanced numerical and computing techniques such as Direct Numerical Simulation (DNS). Despite the fact that such a model is quite expensive in respect to computation and time, Schmeeckle and Nelson

(2003) have carried out their work by directly inegrating the equations of motion of each particle of a simulated mixed-grain size sediment bed. The flux of the bed-load sediment is calculated as a uniform function of boundary shear stress which is a time-averaged quantity; where not always the vertical transport of momentum in the flow at an instant is linked with the forces on the sediment bed. Furthermore Schmeeckle and Nelson (2003) have completed an adjustment of the Bagnold boundary condition at low transport stages that have accounted for temporal and spatial variability of near bed turbulence by developing a model where each particle moves in response to the local and temporally variable velocity field. It is stated that such modification has been carried out to overcome the problem of overprediction in sediment flux. Overprediction is due to a high dynamic friction coefficient that is determined by Van Rijn (1984-a), Wiberg and Smith (1985), Sckine (1992), Lee (1994), Niño and García (1994) in the formulation of particle equations of motion and also the saltating particles trajectories simulation.

In the past 15 years significant developments have been obtained by an understanding of the fluid dynamics associated with alluvial dunes through laboratory works, field investigation and also numerical models. Flow separation zones over dunes and their effect on the boundary layers structure have been looked at in more comprehensive principles. Considering that sediment motion and the rate of sediment entrainment have been influenced by the composition of the river bed and vice versa, it is good to take this into account with respect to dune development and migration. Moreover, as a result the relationships of turbulent structures and sediment transport over dunes have been more deeply understood.

Studies that were carried out on different bed-forms in rivers have contributed significantly on turbulence phenomena and dune-related problems as well as its link to sediment transport. According to McLean and Smith (1979); McLean (1990); McLean, Nelson and Wolfe (1994); Maddux *et al.* (2003a); Bennett and Best (1995); Bridge (2003) and Kleinhans (2004) five major regions of flow structure are created in flow over river asymmetric cross sectional dunes in a river (Figure 1-12). These regions are as below:

1. Flow separation zone
2. Shear layer where the large-scale turbulence is generated in the form of Kelvin-Helmholtz instabilities in this layer
3. Flow expansion in the dune leeside
4. Internal boundary layer
5. Maximum horizontal velocity region,
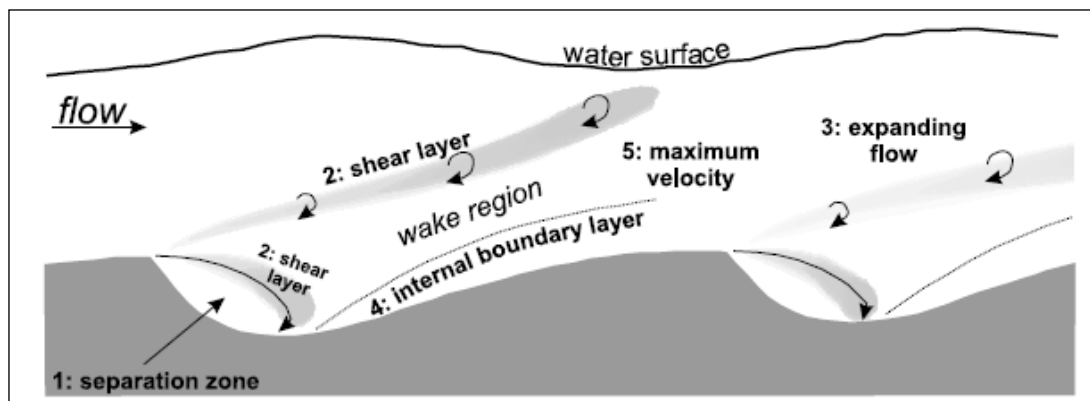
Figure 1-12: Schematic diagram of the principal regions of flow over asymmetrical dunes (Best 2005a)

Best (2005a), ASCE Task Force (2002, 2005) and Fedele and Garcia (2001) have stated that the generation of such flow structures over river dunes has important implications for flow resistance and bed shear stress where estimation of such features helps the sediment transport prediction. According to Kostaschuk, Villard and Best (2004); Villard and Kostaschuk (1998); McLean, Wolfe and Nelson (1999a) & (1999b); Fedele and Garcia (2001) and Kostaschuk, Villard and Best (2004) such shear stress estimations can directly be linked to sediment transport equations.

Furthermore it is understood that the first two zones are the main factors in generating turbulence over dunes. This is also supported by Hasbo (1995) that flow separation zone, which directly has an effect on the leeside Reynolds stress magnitude and, drag coefficient and more importantly the dispersal patterns of sediment, is influenced by the obliquity of the dune crest. Such random phenomena (turbulence) are generated due to the flow

velocity gradient where it refers to Reynolds stress. These local flow turbulence structures are termed as coherent flow structures that are defined by quadrant analysis, that has been developed by several studies. Stoesser, Frohlich *et al.* (2003) stated that quadrant analysis by Lu and Willmarth (1973) is the most widely used approach. Knowing that flow velocities can be split into a mean part ($\overline{u_i}$) and a fluctuating part (u_i') mathematically ($u_i = \overline{u_i} + u_i'$); coherent structures are classified in four regions based on their sign of stream-wise (u') and wall-normal (w' or v') velocity fluctuating components. The fluctuation velocity components are classified in four regions of Q_1, Q2, Q3 and Q_4 where distinguished as below: (Dwivedi, Melville and Shamseldin 2010) (Figure 1-13).

1. Q_1 that are called outward interactions (u' > 0 and w' > 0)
2. Q_2 that are called ejections (u' < 0 and w' > 0)
3. Q_3 that are called inward interactions (u' < 0 and w' < 0)
4. Q_4 that are called sweeps (u' > 0 and w' < 0)
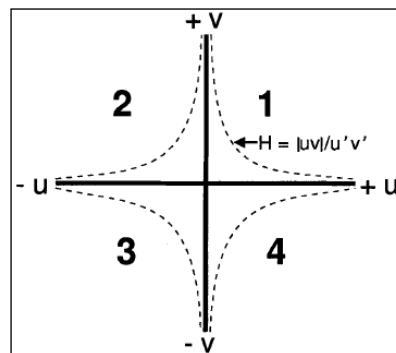
Figure 1-13: Quadrants of the instantaneous *uv* plane (Bennett and Best 1995)

Nelson, McLean and Wolfe (1993) suggest quadrant-4 events (sweeps) dominate bed-load sediment transport, having obtained some findings about the flow turbulent structures based on the quadrant analysis mentioned above. It is also known that the macro-turbulent events are the dominant mechanism for the suspension of sediment over dune beds (Jackson 1976; Schmeeckle 1999; Shimizu, Schmeeckle and Nelson 2001; Venditti and Bennett 2000).

ASCE Manual 54, "Sedimentation Engineering" (V. A. Vanoni, ed.) was issued in 1975 (Garcia (2008); Vanoni (2006)). The manual has been a valuable source of information concerning sedimentation engineering for three decades. Marcelo García (2008) of the University of Illinois is spearheading the effort to issue a revised manual. Adversely Papanicolaou *et al.* (2008) states that in many applications, integral model limitations do not allow precise simulation of a method independently of data input and model calibration. An explanation for this is believed to be that the eddy viscosity models that are frequently used in solving the governing hydrodynamic equations of turbulent flows include some degree of empiricism in their formulations. The issue is a mixture of motives for sediment transport models. They rely heavily on experimental and field information and whose formulations involve a high degree of empiricism. As a result, currently no dependable and complete theoretical methods can define the two-phase modelling of sediment transport. It is not surprising therefore that Dawdy and Vanoni (1986) in their investigation of some of the available 1D hydrodynamic/sediment transport models concluded that most of the movable bed models were found not to lead to completely satisfactory results. Moreover the study done by Papanicolaou *et al.* (2008) indicates that most of the 1D models assume that a stage of equilibrium exists with respect to sediment transport and that the nature of sediment entrainment is deterministic without a stochastic process i.e. presence of turbulence has not been acknowledged. However, 2D and 3D hydrodynamic/sediment transport models normally deals with the reference concentration of sediment near the bed and consequently simulating the term for sediment diffusion because of turbulent motion. Furthermore the users of the multidimensional models, deal with problems in determining the source term of the advection-diffusion equation and the effects of sediment motion on near-bed turbulent flow characteristics. After the publication of Manual 54 in 1975, the use of integrated computer programs for numerical modelling of sediment erosion, transport, and deposition in time and space became increasingly common (Garcia 2008). Some are one-dimensional, typically applied for evaluation of sedimentation processes along rivers and channels. Others are two- or three-dimensional, typically applied for evaluation of

sedimentation processes in broad floodplains, estuaries, coastal regions, and stratified water bodies.

The origin of macro-turbulence that has been linked to the shear layer development in the dune lee and also flow separation is again highlighted by Best (2005b), Hardy and Best *et al.* (2010). Also the interaction between flow structures and sediment entrainment holds the key for understanding and predicting the transport and erosion of particles. Moreover the importance of such macro-turbulence in relation to the occurrence of dunes and their distinction to other bed-forms have been stressed by Jackson (1976) and Bennett and Best (1995). Furthermore Schmeeckle (1999),Ikezaki *et al.* (1999), Bennett and Best (1995),Best (2005b),Hardy *et al.* (2007), Hardy *et al.* (2009) and many others have shown interest on the link between such macro-turbulence and sediment transport, and yet there are questions to be answered.

Therefore here a high-resolution 3D numerical model for morphodynamic processes on small temporal and spatial turbulence scales, based on Large Eddy simulation (LES) has been developed. In this study, fluid phase in the particle-laden flow has played a role in the incompressible single-phase, therefore the general form of governing N-S equations shown below as equation (1-2) and (1-3) are derived based on the conservation laws of momentum and mass. Also isothermal flow is assumed; therefore the equation for conservation of energy is not needed. Detailed formulation for the continuous phase (water) and the solid phase (sediments) are covered in Chapter 3 of this thesis.

$$\frac{\partial(\rho u_i)}{\partial t} + \frac{\partial(\rho u_i u_j)}{\partial x_j} = -\frac{\partial P}{\partial x_i} + \mu \frac{\partial^2 u_i}{\partial x_i x_j} \tag{1-2}$$

$$\frac{\partial \rho}{\partial t} + \frac{\partial}{\partial x_i}(\rho \, \bar{u}_i) = 0 \tag{1-3}$$

1.4 Summary of work

1.4.1 Research gap

Despite the significant contribution of the mentioned empirical, semi-theoretical and even theoretical equations in prediction of bed-load and suspended load transport; still a lot of viewpoints are remained to look from in this area. However knowing that the formulas of Du-Boys, Einstein, Engelund and Hansen, Van Rijn, and others are the basis for understanding long-term rates of sediment transport and also fundamental to present day engineering problems, but the processes of obtaining such relationships remain empirical and specific to its own boundaries of assumption.

Interest in finding an equation with universal application remains rigorous and demanding in this field. The initiation and also more importantly the influence of flow turbulent structures on the entrainment of sediment into both suspended and bed-load transport; have been studied extensively through various sources such as qualitative laboratory results as well as field observations. Despite the fact that in some applications in which sediment transport models incorporate a various degree of simplification to be computationally feasible, it is necessary to give extra care to the role of turbulence where is important.

Hence in order to capture micro-scale changes happen in a particle-laden flow where detailed mapping of the turbulent microstructure is required, and also studying the effect of sediments on the turbulent features is a research gap. Referring to a 4-way coupling where include all aspects of fluid-particle, particle-fluid, particle-particle and finally particle-structure interaction in a three-dimensional numerical modelling is an area of focus in this thesis.

1.4.2 Objectives of the thesis

Having identified the knowledge gap as studying the influence of turbulence on sediments present in the river, detailed modelling is needed to closely study the behaviour and interaction of large and small scale turbulence with sediment presence and movements in the river bed. Furthermore, understanding direct and indirect relationship of such findings with flood

events; the motivation for carrying out this research has been increased significantly. An advantage of computational models is that they can be adapted to different physical domains more easily than physical models, which are typically constructed to represent site-specific conditions. Another advantage of computational models is that they are not subject to distortion effects of physical models when a solution can be obtained for the same flow conditions i.e. identical Reynolds and Froude numbers, same length scale in the three directions, etc. as those present in the field.

A common approach by researchers has been to use computational hydrodynamic or sediment transport models, in general where this involves the numerical solution of one or more of the governing differential equations of continuity, momentum, and energy of fluid, along with the differential equation for sediment continuity. But in order to study the matter faithfully, a different approach has been used in this research. This involves solving the exact motion of equations for particles (Lagrangian approach) where to be coupled i.e. four-way coupling for accommodating all the effects from particle; with the fluid governing equations.

In summary the aim of this thesis is to understand the fluid-particle interaction for application in rivers where the presence of micro and macro-scale features in the fluid plays a significant role. These features are directly and significantly influenced by the chaotic phenomenon of turbulence which involves a lot of large and small turbulent scales that need to be captured in a more precise way than it has been in the past. This is to be accomplished by different turbulent modelling techniques such as LES. The effect of captured turbulent scales on the particles and vice versa is also to be studied consequently. The objectives of this thesis by mainly carrying out a numerical investigation as well as conducting experimental investigation are outlined below:

1. Running 3-D model with LES turbulence model and capture small and large turbulent scales
   - Focusing on turbulent scales close to bed
   - Using LES model so all the velocity and pressure fluctuations of the flow regime are taken into account with less

assumptions in comparison with the RANS approach and less cost in comparison with the DNS approach

2. Validating models with experimental investigations

    - Capturing the turbulent scales at the bed region
    - Comparing the experimental results with the numerical findings

3. Inserting sediments in models and take into account of four-way coupling i.e. fluid-particle, particle-fluid, particle-particle and particle-structure

    - Using DEM numerical approach to study the behaviour of the sediments without the presence of fluid close to bed
    - Adding the fluid to the DEM results and study the coupled behaviour of bed-load using CFD-DEM coupling approach

4. Study the effects that flow field has on the particles close to bed

    - Comparing the turbulent scales generated at the bed-load in both cases of "with" or "without" particles' presence in the fluid, at the same time frame

5. Investigating the possibility of effect that sediments apply on the turbulent structures in the flow

    - Interpreting the different flow turbulent intensities captured in the regions where sediments are present

Chapter 2 Experimental investigation

2.1 Introduction

This chapter consists of experimental works carried out in the Fluid Dynamics Laboratory at the University of Hull in the United Kingdom for validation purposes of the numerical method set up of this research. Due to the laboratory limitations in using a Particle Image Velocimetry (PIV) as an optical method of obtaining instantaneous velocity measurements; an Acoustic Doppler Velocimeter (ADV) called Vectrino-II has been used instead. The main difference between PIV and ADV technique is that PIV produces two-dimensional or even three-dimensional vector fields, while the other techniques measure the velocity at a point. Experimental model set up has been constructed as a bar-form (negative slope) with a height of 0.15m and a 30 degrees angle for the slope. The flume includes the upstream which is set to have a fairly long length of 2 meter and 3 meters long for the downstream. Velocity profiles have been obtained at various locations along the flume and have been used for validating numerical results.

2.2 Acoustic Doppler Velocimeters (ADV)

Acoustic Doppler Velocimeters (ADV) were introduced in 1993. Since then, Lane et al. (1998); Nikora and Goring (1998); Puertas, Pena and Teijeiro (2003); Nikora and Goring (2000) and many other researchers have widely used ADV for the measurement of velocity fields in turbulent flows. Velocimeters are categorised as a special class of high-resolution 3D devices performed to study rapid velocity fluctuations in the laboratory (Figure 2-1) or in the ocean (Figure 2-2). These instruments have at least three focused beams to measure rapid minor scale changes in 3D velocity in a small point (Nortek As 2013).
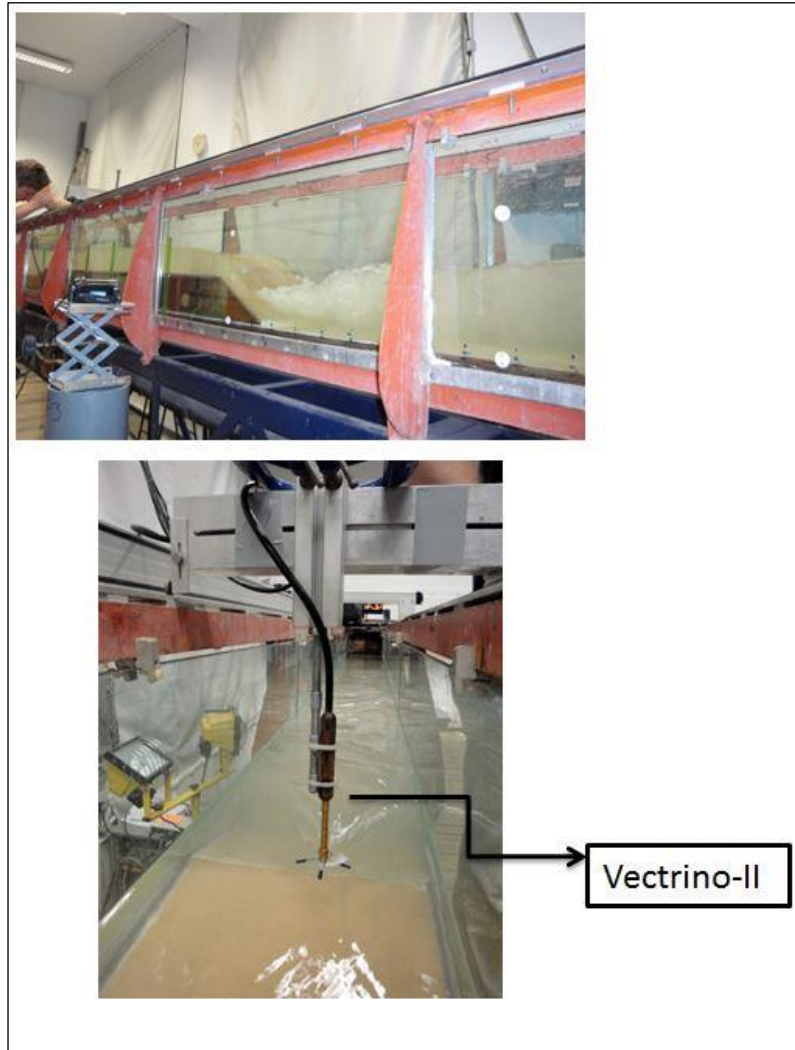
Figure 2-1: ADV in the laboratory (Taken by author)
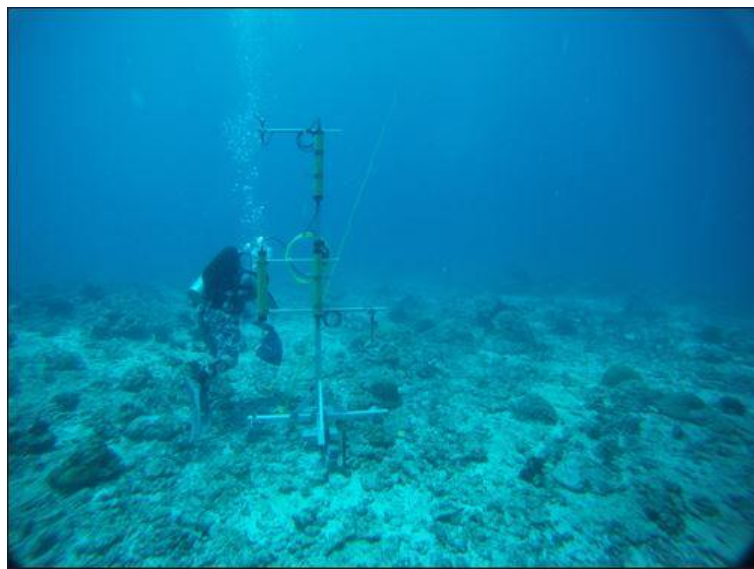
Figure 2-2: ADV in the Ocean

The Vector is a field instrument intended for measurements of high sampling rates in 3D velocity, applied for boundary layer, turbulence and surf zone measurements as well as measurements in very low flow areas. Furthermore Vectrino is utilised in hydraulic laboratories to measure turbulence and 3D velocities in physical models and flumes (Figure 2-3). A profiling version of the Vectrino is known as the Vectrino Profiler which has a 3 cm profiling zone (Figure 2-4).
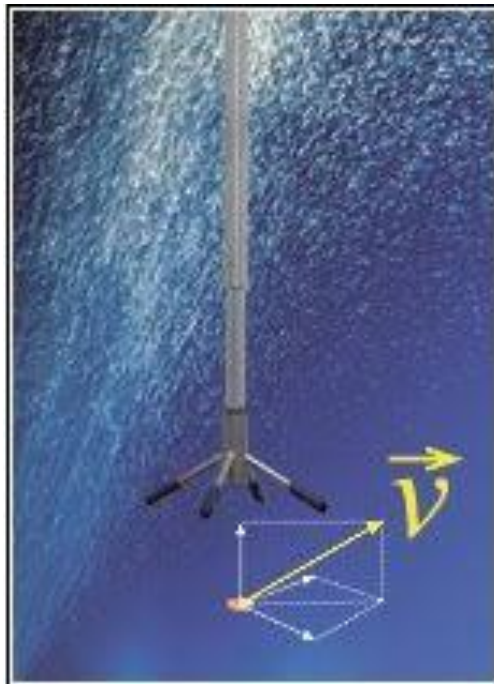
Figure 2-3: Vectrino (Nortek As 2013)
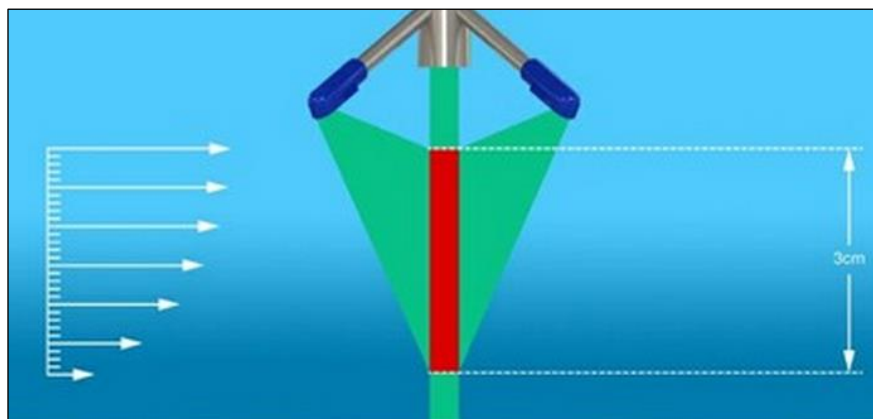
Figure 2-4: A profiling version of the Vectrino with a 3 cm profiling zone (Nortek As 2013)

All Acoustic Doppler Velocimeters operate based on sending a short acoustic pulsation from the transmit part. The echo is detected by each of the acoustic receiver parts once the pulse travels through the focus point for the receiver beams. Then in order to discover the Doppler shift the echo is analysed. Also the scaling is attuned with the measured speed of sound in the liquid (henceforth the measurement of temperature), and the velocity vector is transferred to a PC at a speedy rate (Figure 2-5) (Nortek As 2013; Nortek AS User Guide 2012).

Figure 2-5: The velocity vector is sent to a PC at a rapid rate (Nortek As 2013)

The ADV is able to record the 3D instantaneous velocity at any given spatial point. A comprehensive technical description of the ADV is provided by Kraus, Lohrmann and Cabrera (1994); Cea, Puertas and Pena (2007) . The user guide is also helpful to fix the experimental setup (Nortek AS User Guide 2012).

The 3D mean velocity, the turbulent kinetic energy, the Reynolds stresses, and the power spectrum are obtained by using the instantaneous data registered with an ADV. The Doppler noise and the aliasing of the signal are known as the main reasons of error when raw ADV velocity data are processed. These problems have been addressed in recent years by several ADV users (García *et al.* 2004b; Goring and Nikora 2002; Lane *et al.* 1998; Nikora and Goring 1998; Wahl 2000).

The Doppler noise was reported by Lohrmann, Cabrera and Kraus (1994) once turbulence measurement is carried out with any Doppler-based

backscatter system. The fluid features in addition to the flow conditions such as flow velocity, presence of particles in the flow, and turbulence are factors which indicate the level of importance of the Doppler noise. Due to the Doppler noise, the turbulent kinetic energy obtained by ADV is greater than the real turbulent kinetic energy of the flow. In order to remove the noise effects from turbulence measurements calculated from ADV dataset, some procedures have been proposed by number of investigators such as García *et al.* (2004a); Goring and Nikora (2002); Nikora and Goring (1998); Voulgaris and Trowbridge (1998).

Nikora and Goring (1998) who studied the ADV measurements of turbulence under numerous flow conditions, has obtained some notable conclusions. There are as follow:

- Due to the sensor geometry, the noise in the vertical component is up to 30 times smaller than the noise in the two horizontal components
- bubbles increase the noise significantly
- Presence of high turbulence level escalate the noise level critically

The aerification effects of the ADV velocity measurements has also been reported by Liu, Zhu and Rajaratnam (2002) and Frizell (2004) who revealed a major drop in the ADV performance due to presence of air bubbles (Cea, Puertas and Pena 2007). Nikora and Goring (1998) introduced a method for decreasing the Doppler noise. Even though in this technique the Doppler components are measured in still water taken from the flow of interest, and these values are used in order to modify the velocity measurements in the flow under study; this methodology is not suitable for resolving the noise problem in highly turbulent flows with a large concentration of bubbles. Cea, Puertas and Pena (2007) claims that it is clearly due to different properties of flowing water and still water.

2.3 **Vectrino-II**

The Vectrino-II uses the Doppler effect to measure current velocity. The Doppler effect is the change in tone that is heard when either the source of a sound or the listener is in motion. When a vehicle with an alarm is heard, the tone is higher when the vehicle is coming towards us, and lower when it is moving away. The change in tone indicates how fast the vehicle is moving. (Nortek AS User Guide 2012)

The Vectrino-II sends short pairs of sound pulses, collects their echoes and eventually, processes the change in tone or frequency of the returned sound (Nortek AS User Guide 2012) (Figure 2-6).
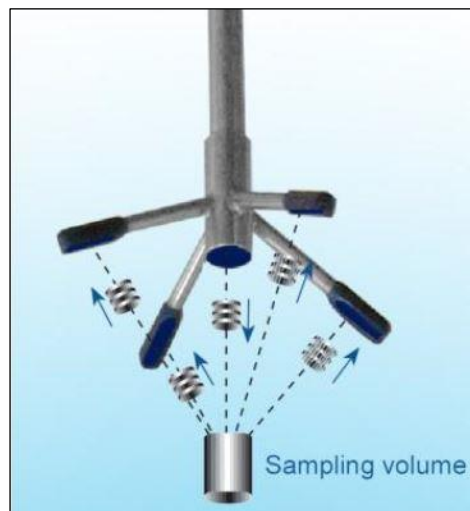
Figure 2-6: The Vectrino-II velocimeter operating principle

It is worth to mention that sound does not reflect from water, but from suspended particles of a dye that solves in water. These seeding particles move with the same average speed as the water. The velocity that is measured is thus the velocity of the water.

The Vectrino is different from standard Doppler profilers and current meters. It performs as a bistatic sonar. This means that different beams are used to transmit and receive pulses. The short pairs of sound pulses are sent through a central beam and collected through four beams displaced off to the side. Figure 2-7 depicts how the beams meet each other 50 mm from the transmitter. The produced velocity profile is given by this intersection and time range. The transmit transducer sends a short pulse that transits the

profiling region of approximately 30-80 mm and the receivers collect returned echoes from this pulsed time range. Vectrino-II uses four receivers, all focused on the same zone, to capture the three velocity components from that region.
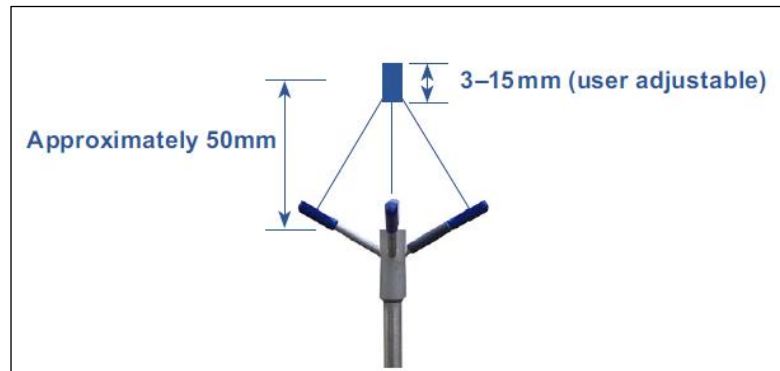
Figure 2-7: Transmitter and Beams arrangements (Nortek AS User Guide 2012)

2.4 **Bar-form experiment**

Experimental investigation has been carried out in the Fluid Dynamics Laboratory at the University of Hull in the United Kingdom. This laboratory was established in 2002 as a part of the Hull Institute for Mathematical Science and Applications at the Department of Mathematics. In August 2006 the Laboratory moved to the Department of Engineering. Flume shown in Figure 2-8 and Figure 2-9 has been used to carry out my investigation experimentally and numerically. Several measurements of velocity values have been obtained, using Vectrino-II (Figure 2-10), which is positioned in one locations on the upstream section (X=0.5m), in two locations on the slope (X=0.55m & X=0.7m), and in six locations (X=0.8m, 1.00m, 1.2m, 1.4m, 1.6m & 1.8m) downstream section. The position of X=0.00 m is 0.5 meter away from the brink point at X=0.5m (Figure 2-13).

Figure 2-8: Bar-form Flume set up (Taken by the author at the University of Hull-Fluid Dynamics Laboratory)
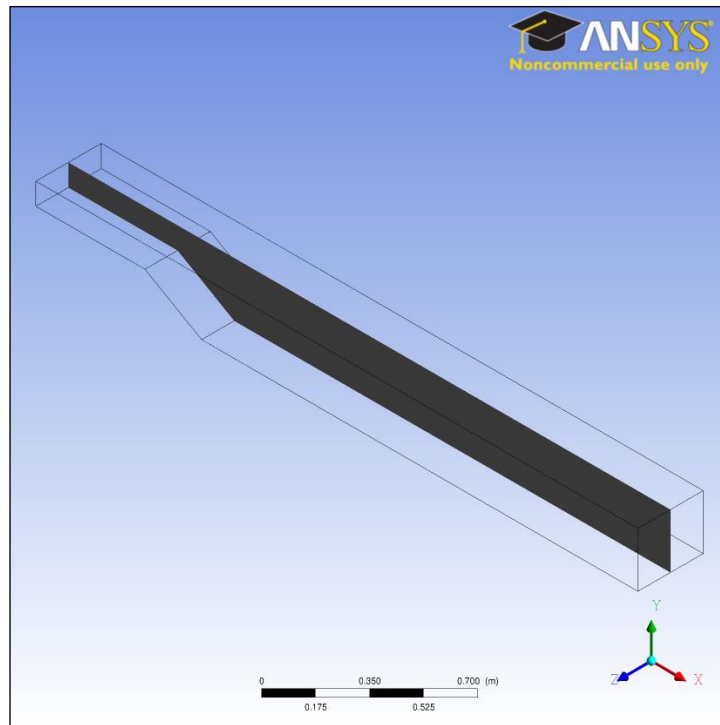
Figure 2-9: Bar-form model (drawn by the author)
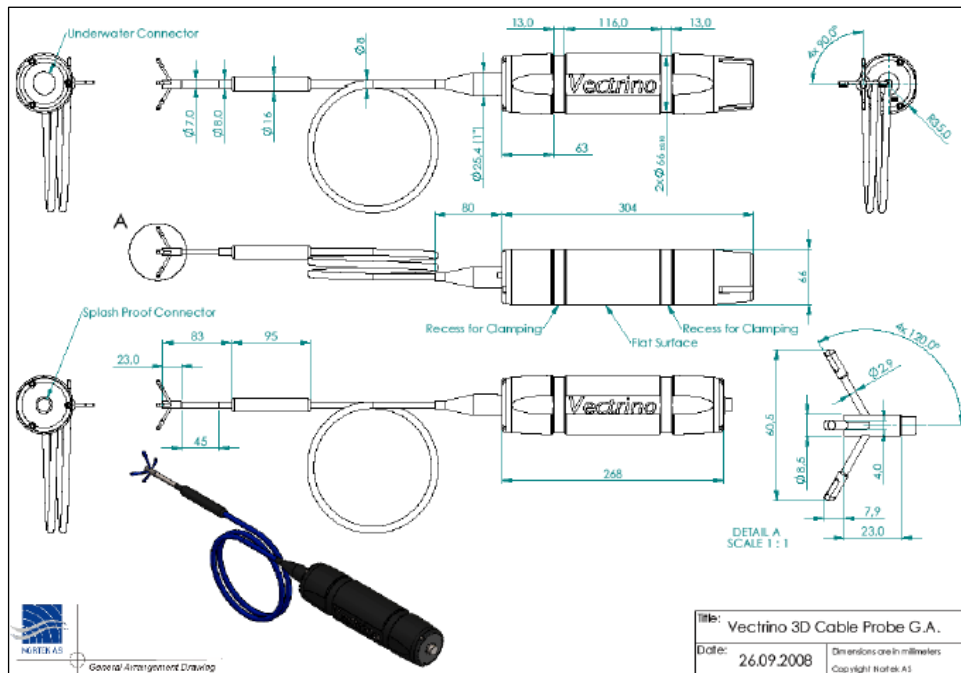
Figure 2-10: Vectrino-II used for my experimental works in Fluid Dynamics Laboratory at Hull University (Nortek AS User Guide 2012)

Vectrino-II has been configured using the software user guide (MIDAS Data Acquisition Software 2012) to carry out the experimental works (Figure 2-11).
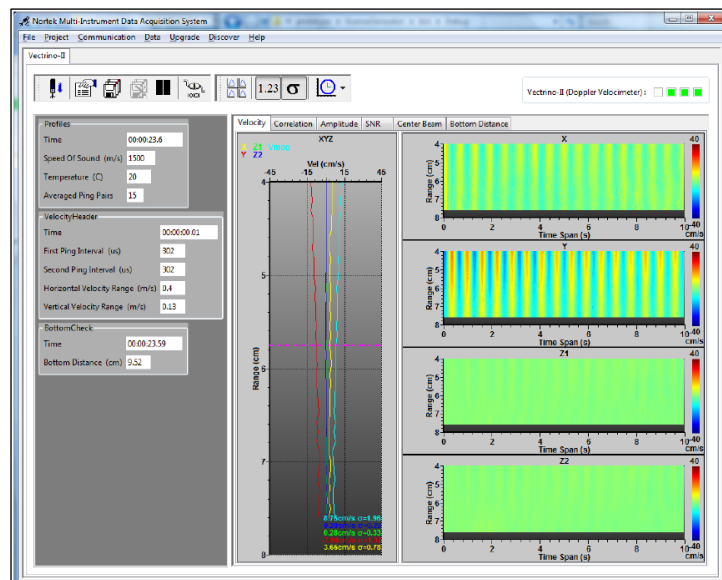
Figure 2-11: Vectrino-II Configuration sample (MIDAS Data Acquisition Software 2012)

2.4.1 Geometry set-up

Experimental model set up has been constructed as a bar-form (negative slope) with a height of 0.15m and a 30 degrees angle for the slope. The flume includes the upstream which is set to have a fairly long length of 2 metres and 3 metres long for the downstream. The current investigation has been done with the below specifications: (Figure 2-12)

- Investigated section of flume dimensions : length = 2.76 m, inlet depth = 0.1 m, outlet depth = 0.25m and width = 0.3 m
- Water velocity: 0.5 m/s
- f = 25 HZ
- Inlet upstream water depth : 0.1 meter
- upstream investigated length: 0.5 meter
- slope horizontal length: 0.26 meter
- downstream investigated length: 2 meter
- Downstream water depth: 0.25 meter
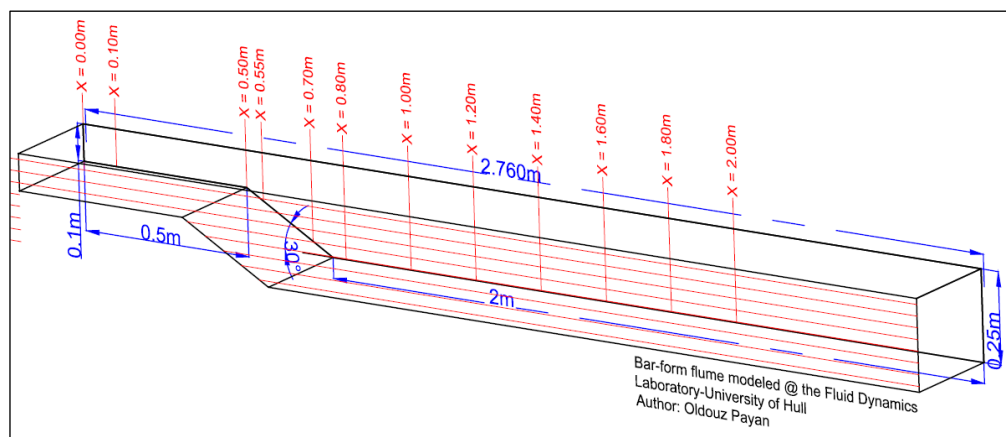
Figure 2-12: Experimental model set up (Drawn by the author)
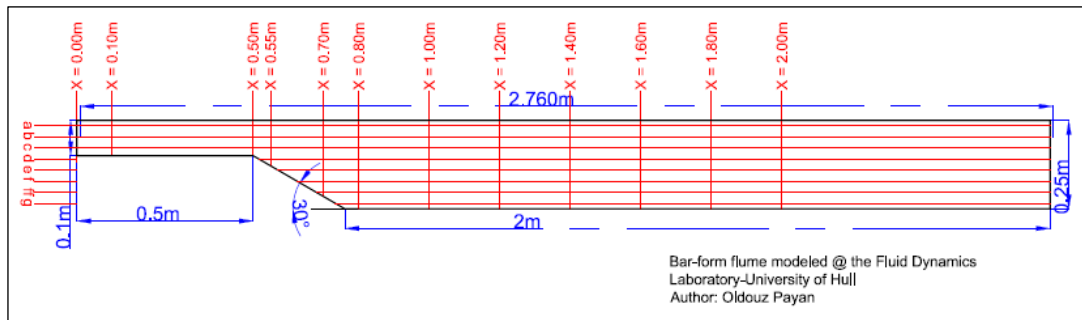
Figure 2-13: Positions of Vectrino-II shown by the lines for measurement readings
(Drawn by the author)

2.4.2 Filtering process

The Vectrino velocity gives many results with errors and also false signal links between signal frequency and sampling frequency. In order to obtain the acceptable data few filtering steps have been carried out for the Vectrino-II velocity post-processing phase. These steps are 2-D space threshold filtering phase (Parkhurst *et al.* 2011), space threshold filtering (Wahl 2003) and correlation threshold filtering (Zedel and Hay 2010). These are applied within fully vectorized MATLAB code developed by Robert E. Thomas (Thomas, McLelland and Frostick 2013) who is the research assistant at the Department of Geography, Environment & Earth Sciences, University of Hull. Raw data of the current experimental investigation carried out for this research, have been provided based on the aforementioned process.

2.4.3 Conclusion

Time averaged velocity profile on the studied locations alongside the bar-form model in the flume has obtained. The readings have gone few stages of filtering i.e. phase unwrapping, spike and correlation filtering; which has been referenced in the section 2.4.2 of this Chapter.

The graphs of velocity profiles have been plotted using the velocity Vectrino-II readings taken on points which are the intersections of horizontal levels through water depth and vertical interval distances (Figure 2-14). These graphs, that are the time averaged velocity values with taking into account of the turbulence statistics readings, have been drawn and compared with the numerical modelling results shown in chapter 4.
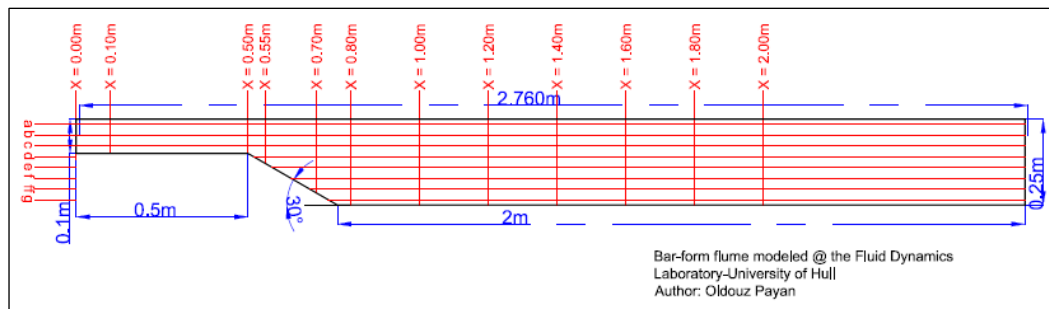
Figure 2-14: Intersection points of Vectrino-II measurements

Chapter 3 Numerical modelling

This chapter introduces the basics of fluid dynamics, and the modelling approaches for capturing the interaction between the turbulence and sediments while being transported in the flume. Large Eddy Simulation (LES) as turbulence modelling has been the core of this research. Initially the Navier-stokes (N-S) equation is considered and then an insight into essentials of the turbulence phenomena is provided. This has been accompanied by the appropriate equations and formulations that are used for the numerical modelling of cases investigated in this study. CFD tools such as ANSYS Fluent commercial software and open source codes of Open-Foam (simulating the fluid phase) and Discrete Element Method (DEM) (simulating the particle phase) have been used for the numerical modelling study in this thesis. Furthermore CFD-DEM which couples the fluid and particle phases has been used in order to utilise four-way coupling of fluid-particle interaction of the sediment transport phenomena. Details of all the CFD packages have been explained in depth in this chapter.

3.1 Theory of CFD and DEM modelling

The science of fluid and particles motion has been predicted, investigated and analysed numerically in the form of mathematical equations. In this section the tools and methods used for this study has been explained in detail.

3.1.1 CFD modelling

The general motion of turbulent flow is described by the Navier-Stokes (N-S) Equations where was first formulated by Claude-Louis Navier and George Gabriel Stokes, in the 19th century. Years later computer-based tools of Computational Fluid Dynamics (CFD) have been found to use the N-S governing equations and found to be satisfactory tools to contribute towards knowledge gap and related questions in the field. As a consequence of Newton's second law, the change of momentum on a fluid element is caused by external forces which leads to the equation of motion, in which is shown by equation (3-2).

The N-S equations are an expression of the physical laws of conservation of mass, momentum and energy. For the general form of these equations we refer to Batchelor (2000).The general and non-filtered N-S continuity and momentum equations that are the starting point for the flow analysis are as follow:

$$\frac{\partial \rho}{\partial t} + \frac{\partial \rho u_j}{\partial x_j} = 0 \tag{3-1}$$

$$\frac{\partial(\rho u_i)}{\partial t} + \frac{\partial(\rho u_i u_j)}{\partial x_j} = -\frac{\partial P}{\partial x_i} + \mu \frac{\partial^2 u_i}{\partial x_j x_j} + \rho f_i \tag{3-2}$$

Where $x_i's$ are the coordinates, P is the pressure, t the time, ρ the density, u_i the velocity component in x_i-direction and f_i the volume force in x_i-direction.

Sagaut (2001) states that CFD is the study of fluids in flow by numerical simulation where the partial differential N-S equations are solved numerically. He adds that the basic idea is to use appropriate algorithms to find solutions to the equations describing the fluid motion.

Knowing that over the past few decades dealing with knowledge gaps in hydrodynamics of river have been progressed significantly from empirical methods to theoretical ones and even more advanced to equation and computer based systems; the numerical solutions that can be obtained through equations and computer-based techniques can be coupled and used for validation in experimental studies. In order to get accurate solution from such complex partial differential equations which are described for the open-channel flow, motion of particle and hydrodynamic problems; such equations needs to be defined for digital computer-based techniques. There are some factors that need to be taken into account while using N-S system of equations in simulations. On one hand due to complexity of the N-S equations as being non-linear Partial Differential Equations (PDE) that treats the fluid domain as a continuum, should be considered by simplifying the equations. Moreover Beaman (2010) states that , knowing only simple flows have been directly solved at a very low Reynolds number, in order to simplify such complexity, the N-S equations are simplified and used to get solutions. Such complexity can be resolved mathematically by the action of "Discretization". This is a process of changing the continuous model or

equation to be discrete mathematically. Finite Difference Method (FDM), Finite Volume Method (FVM) and Finite Element Method (FEM) are three numerical ways of discretization. A more detailed formulation of these methods have been well explained by Chung (2010) and also CFD based on FVM is explained by Versteeg and Malalasekera (2007).

On the other hand using different approaches of using N-S system of equations to solve for turbulence simulations comes into consideration. Knowing that small and large turbulent scales are generated in an anisotropic manner, to obtain a result of maximum quality and to take into account of all the space-time scales of the process, the space-time resolution scale of the numerical result must be at least as fine as that of the continuous problem. Sagaut (2001) illustrated well, that such solution may be very limited of freedom by taking the case of the simplest turbulent flow, i.e. one that is statistically homogeneous and isotropic, where the solution of the exact problem contains significantly different mixing-length scales. In order to obtain a stable solution a very fine mesh resolution that involves high computational cost is required so all range of spatial and temporal scales of turbulence can be resolved instead of having any turbulence models in the simulation. This is called Direct Numerical Simulation (DNS). Such approach is called deterministic method where no randomness is involved. The challenge to solve turbulent flow, using a laminar solver, typically results in a time-unsteady solution, which fails to converge properly.

Another approach is to use a mathematical technique for turbulence solving system called Reynolds decomposition; where the average and fluctuating parts of a quantity are separated as $u = \overline{U} + u'$ where u' is the unresolved part and $\overline{U}$ is the large scale part that can be defined through an averaging system. By applying such technique of Reynolds decomposition to the N-S equation and making it as a time-averaged equation, Reynolds Average Navier Stokes (RANS) equation is created and therefore a non-linear extra term called Reynolds stress tensor, $\overline{u_i u_j}$, that owes to the fluctuating velocity field, is introduced where requires additional unknown variables to close up the RANS equation. This additional modelling has created various turbulent modelling process, zero-equation models (e.g. Prandtl mixing length model)

(Prandtl 1945), one-equation model and two-equation models such as k-ε (k-epsilon) and k-ω (k-omega) models (Chung 2010; Wilcox 1993).

Another approach to model the turbulence is to pick out certain scales that will be represented directly in the simulation process while other smaller ones can be parameterized instead. This refers to a compromise between DNS and RANS and is called LES. As mentioned earlier, the large-scale eddies are computed and small scales are modelled. It is important to minimise the errors that are involved in the mathematical model for the LES problem where the main issue is to remove the small scale of the exact solution (Figure 3-1). This should be done to the extent that the approximations of exact solution to the equations, on the computational grid, become the best possible one while solving the discrete version of the problem.
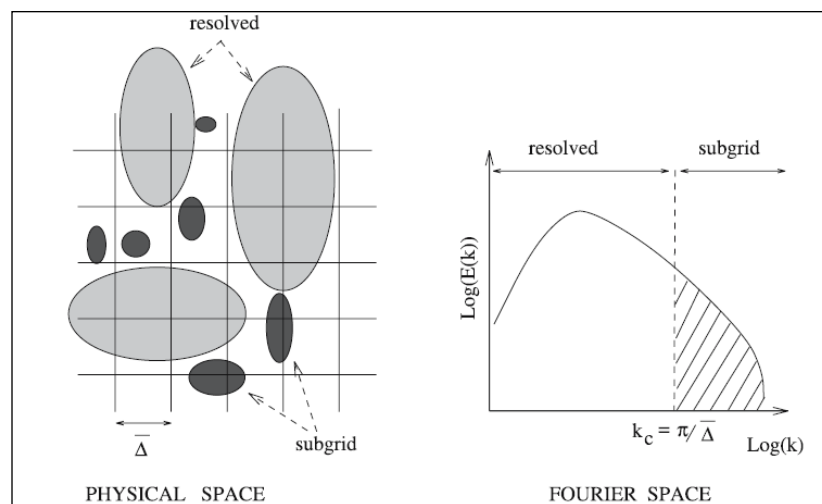
Figure 3-1: Schematic view of the simplest scale separation operator (Sagaut 2001)

3.1.2 DEM modelling

Contact detection models are based on cell encapsulation in CFD tools such as OpenFOAM, and not on specific particle separation distances. Therefore the framework is suited more for dilute systems where contact is of secondary importance and the particle phase does not feed-back on the flow. Thus in order to overcome such shortcoming, implementation of more

heavy duty Discrete Element Method (DEM) code on the models considered in this study. By doing this a more sophisticated outcome on the detailed fluid-particle interactions is enabled.

The DEM accounts for individual particle trajectories in Lagrangian frames of reference and was introduced by Cundall and Strack in the late 1970's (Kloss *et al.* 2009; Goniva *et al.* 2010). Trajectories are computed by solving translational equation (3-3) in which is the general equation of motion for a single particle (Kloss *et al.* 2009; Goniva *et al.* 2010; Fan and Zhu 2005; Fluent 6.2-User Guide 2005).

$$m_p \frac{dU_p}{d_t} = F_D + F_{GB} + F_V + F_P + F_B + F_S + F_M + F_c + F_{...} \tag{3-3}$$

Particle contact, Cohesion, rolling friction and collision models on which DEM modelling in LIGGGHTS is based, are derived from Hertzian non-linear and Hookean non-linear collision theories, of which the Hertzian formulation was adopted in this study (Johnson 1987). A soft sphere spring dashpot model is used with normal and tangential stiffness and damping, based on particle overlap and relative normal and tangential velocities. Particle overlap is generally limited to less than 0.5% of particle diameter. Furthermore various contact schemes may be selected such as those which include or exclude tangential damping, rolling friction and cohesion. Velocity Verlet integration was implemented in this study. The algorithm is detailed in equations (3-4 to 3-7) (Plimpton, Pollock and Stevens 1997).

$$x(t + \Delta t) = x(t) + v(t)\Delta t + \frac{1}{2} a (\Delta t)^2 \tag{3-4}$$

$$v\left(t + \frac{\Delta t}{2}\right) = v(t) + \frac{a(t)\Delta t}{2} \tag{3-5}$$

$$a(t + \Delta t) = \frac{\sum_k F_k}{m_p} \tag{3-6}$$

$$v(t + \Delta t) = v\left(t + \frac{\Delta t}{2}\right) + \frac{a(t+\Delta t)\Delta t}{2} \tag{3-7}$$

The algorithm updates particle velocity and position, computing a full time-step displacement advance eq. (3-4) and a half time-step velocity advance eq. (3-5) using velocity and acceleration from a previously computed timestep or initialized values. The acceleration term in equation (3-6) is computed by solving Newton's equation of motion. The last step (3-7)

involves completing the velocity integration by advancing the remaining half step. Verlet integration position error is of the order $\sim \Delta t^4$.

3.1.2.1 Forces

The general equation of motion for a single particle has been expressed as in equation (3-3) where the forces on the RHS of the equation are in order and by subscript the drag force F_D, gravity buoyancy force F_{GB}, virtual mass force also known as the carried or added mass force F_V, pressure gradient force F_P, Basset force F_B, Saffman force and Magnus force which are combined into a single lift force term F_{SM}, collision force F_C, which is comprised of the normal F_n equation (3-8) and tangential F_t equation (3-9) force components, and other forces F including magnetic, electrostatic, etc. (Kloss *et al.* 2009; Kloss *et al.* 2012; Loth and Dorgan 2009; Goniva *et al.* 2010; Fan and Zhu 2005; Fluent 6.2-User Guide 2005)

$$\boldsymbol{F}_n = -k_n \delta x_{p,n} + c_n u_{p,n} \tag{3-8}$$

$$k_n = \frac{4}{3} E^* \sqrt{R^* \delta_n} \tag{3-9}$$

$$c_n = -2 \sqrt{\frac{5}{6}} \beta \sqrt{\frac{3}{2} k_n m^*} \geq 0 \tag{3-10}$$

$$\frac{1}{m^*} = \frac{1}{m_1} + \frac{1}{m_2} \tag{3-11}$$

$$\delta_n = R_1 + R_2 - r \tag{3-12}$$

$$\frac{1}{E^*} = \frac{1 - v_1^2}{E_1} + \frac{1 - v_2^2}{E_2} \tag{3-13}$$

$$\frac{1}{R^*} = \frac{1}{R_1} + \frac{1}{R_2} \tag{3-14}$$

$$\beta = \frac{ln(e)}{\sqrt{ln^2(e) + \pi^2}} \tag{3-15}$$

$$\boldsymbol{F}_t = min \left\{ \left| k_t \int_{t_{c,0}}^{t} u_{p,t} dt + c_t u_{p,t} \right|, \mu_c \boldsymbol{F}_n \right\} \tag{3-16}$$

$$\boldsymbol{F}_t \leq \mu_c \boldsymbol{F}_n \tag{3-17}$$

$$k_t = 8 G^* \sqrt{R^* \delta_n} \tag{3-18}$$

$$c_t = -2\sqrt{\frac{5}{6}}\beta\sqrt{\frac{3}{2}k_t m^*} \geq 0 \tag{3-19}$$

$$\frac{1}{G^*} = \frac{2(2+v_1)(1-v_1)}{E_1} + \frac{2(2+v_2)(1-v_2)}{E_2} \tag{3-20}$$

Where m_i is the mass of particles, R_i is the raduis or particles, E_i is the Young modulus of particles, v_i is the Poisson ratio, r is the distance between centers of particle and G^* is the shear modulus.

Cause of drag force F_D equation (3 -21) is due to a pressure gradient which is involved with fluid particle velocity slip as well as viscous shears on the particle surface. The drag coefficient C_D is sensitive to particle Reynolds number, particle shape, size, material properties and adjacent particles. Moreover continuous phase vorticity and particle rotation have been identified as the two primary mechanisms attributing to particle lift phenomena (Loth and Dorgan 2009). The lift forces (3-22) of Magnus and Saffman based on particle rotation and shearing velocity gradients across the particle respectively, have been combined to produce equations (3-22).

Saffman lift force may be attributed to a pressure gradient which is set up across a sphere because of a difference in flow speed at opposite sides of the particle (Loth and Dorgan 2009). The velocity shear induced lift force may become relevant near wall boundaries. The Magnus lift force may also be attributed to a pressure gradient which asserts itself across a rotating sphere as a result of fluid entrainment on one side. Lift induced through particle rotation becomes negligible compared with drag when the particle is small or when spin velocity is low (Fan and Zhu 2005).

$$\boldsymbol{F}_D = \frac{2C_D}{4d_p}\frac{m_p\,\rho_f}{\rho_p}\left|U_f - U_p\right|\left(U_f - U_p\right) \tag{3-21}$$

$$\boldsymbol{F}_{SM} = \frac{3}{4}\frac{m_p\,\rho_f}{\rho_p\,d_p}C_L\,|U_r|\,\frac{U_r \times \omega}{|\omega|} \tag{3-22}$$

where ρ_f and ρ_p are densities of fluid and particle respectively, U_f and U_p are velocities of fluid and particle respectively, d_p is the diameter of particle, U_r is the reletive velocity between fluid and particle velocity, ω is the curl of fluid velocity.

3.2 **Modelling tools**

CFD tools such as ANSYS Fluent commercial software and open source codes of OpenFOAM have been used for simulating the fluid flow. LIGGGHTS open source code as Discrete Element Method (DEM) tool has been utilised to simulate the particle phase of flow in this thesis. This section is divided into two sub-sections of ANSYS Fluent software and open source code where more insight of how the turbulent structures in the flow and also fluid-particle interaction is studied numerically. Figure 3-2 shows OpenFOAM as the CFD solver and LIGGGHTS as DEM solver and is a schematic flow-chart of how such modelling tools handle the data exchange between the fluid and particulate phase.
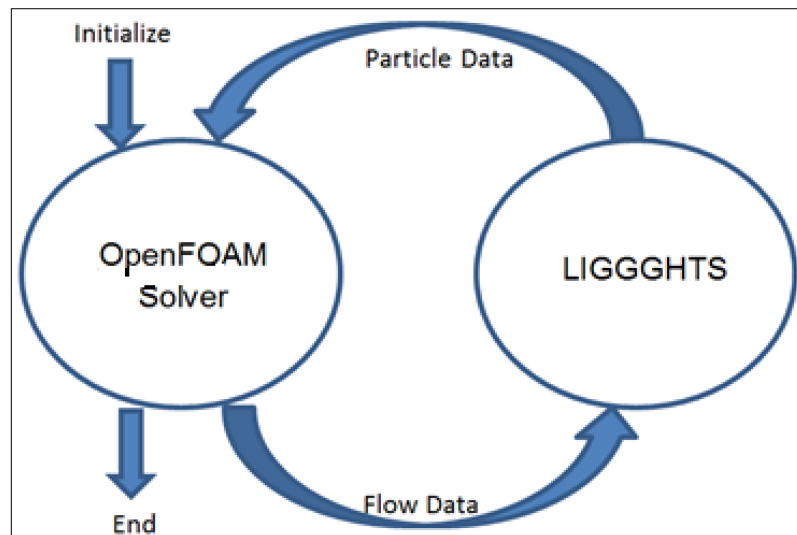
Figure 3-2: Open Source Codes coupling process

3.2.1 **ANSYS FLUENT 14.0**

3.2.1.1 **Meshing**

Grid generation has a strong impact on model accuracy. The most important consideration to follow when generating high quality CFD grids is that the relevant shear layers to be covered by at least 10 cells normal to the layer. A structured mesh in wall-normal direction has been used for all the wall bounded flow cases. Since turbulence plays a dominant role in the transport of mean momentum and other parameters, it is learned that turbulence quantities in turbulent flows ought to be properly resolved since high

accuracy is required. Due to the strong interaction of the mean flow and turbulence, the numerical results for turbulent flows tend to be more susceptible to grid dependency than those for laminar flows. Therefore regions where the mean flow changes rapidly have been resolved with sufficient fine meshes. For LES implementation in FLUENT, the wall boundary conditions have been implemented using a law-of-the-wall approach. This means that there are no computational restrictions on the near-wall mesh spacing. However, as pointed out earlier a very fine near-wall mesh spacing on the order of $y^+ = 1$ has been used.

3.2.1.2 Near-wall region

Knowing the bed of each 3-D geometries considered in chapter 4 of the thesis has been introduced as a wall with slip conditions where the viscosity-affected region, for a wall-resolved LES, it is recommended to use a mesh with a grid spacing scaling with $\Delta x^+ \approx 40$, $\Delta y^+ \approx 20$, $\Delta z^+ \approx 20$ where x is the stream-wise, y the wall-normal and z the span-wise direction (e.g. channel flow). In this study, appointing meshing nodes in the boundary layer was done by making the wall-normal resolution to be like for a finely resolved RANS simulation, meaning a near wall resolution of $\Delta y+ \approx 1$. Doing this has made the near-wall region to be resolved all the way down to the wall. Despite the fact that there are wall-functions available to be used, but because the viscosity-affected region will be not resolved, so instead the near-wall model approach has been used (Figure 3-3). Turbulence near a wall concept shows that the velocity changes rapidly (Figure 3-4).
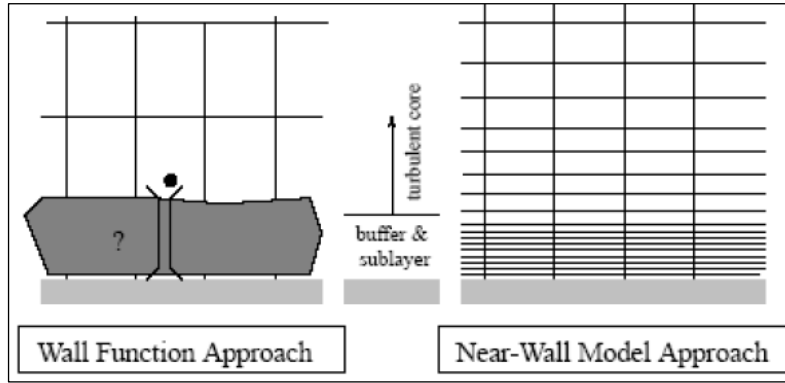
Figure 3-3: Near-Wall Region (ANSYS UK 2012)
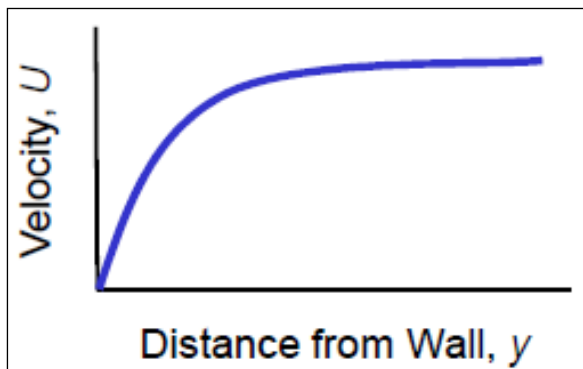
Figure 3-4: Velocity Profile

The same graph then can be plotted using log scale axes and making the wall distance (y) dimensionless as well as the velocity, u, (Figure 3-5)
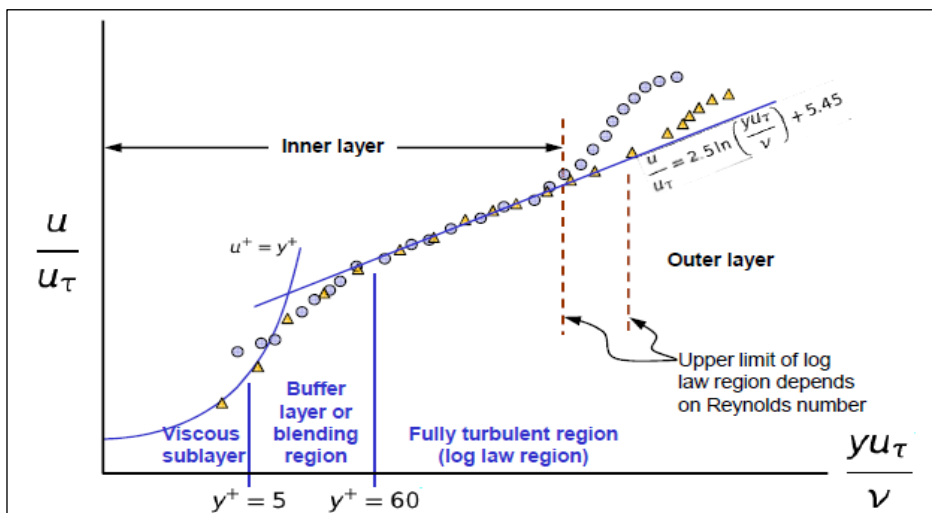
Figure 3-5: Subdivisions of near-wall region(Salim and Cheah 2009)

Values of y^+ close to the lower bound ($y^+ \approx 30$) are most desirable for wall functions whereas $y^+ \approx 1$ are most desirable for near-wall modelling (viscous

region) where most of the smaller eddies are generated and dissipated. The more we get closer to the y^+ = 1 on graph of Figure 3-5, the more we need to have smaller grid cells and accuracy in capturing and resolving small-turbulence scales. This is referred to DNS approach which involves high computational costs.

Using a high Reynolds number (R_e) for all of the case studies in chapter 4; a "Wall Function" is set to be used for the first part of simulation using RANS. This in simple word means that first grid cell (y) needs to be in the range of acceptable y+ that lies between 30 and 300 where the flow is turbulent. This option is available for all RANS-based models and it will create a much more realistic initial field for the LES run. As ANSYS Fluent (2009) suggests to start by running a steady state flow simulation using a Reynolds-averaged turbulence model until the flow field is reasonably converged and then use the 'solve/initialize/init-instantaneous-vel' text command to generate the instantaneous velocity field out of the steady-state RANS results. This command has been executed before LES is enabled. This will help in reducing the time needed for the LES simulation to reach a statistically stable mode. Predicting near-wall cell size has been carried out by performing a hand calculation at the start of meshing stage. Assumptions and formulations have been followed using steps suggested by ANSYS UK (2010) for obtaining the range for y^+.

3.2.1.3 Continuous/carrier phase

Turbulent flows are characterized by eddies with a wide range of length and time scales. The largest eddies are typically comparable in size to the characteristic length of the mean flow. The smallest scales are responsible for the dissipation of turbulence kinetic energy (ANSYS Fluent 2009).

It is possible, in theory, to directly resolve the whole spectrum of turbulent scales using an approach known as Direct Numerical Simulation (DNS) where no modelling is required in DNS. However DNS solves the exact N-S equations without involving any formulation constant assumptions or modelling and hence is very computationally extensive so is not feasible for this investigation.

On the other hand using a Reynolds Average Navier Stokes (RANS) for simulations, eddies are assumed to be isotropic turbulence which is not the case near-wall and hence the accuracy is affected. Therefore this approach is not suitable for this study where a lot of small and large scale turbulent eddies that has effect of transport of sediment.

LES is mainly used for unsteady flows as it minimizes empiricism in turbulence modelling and instead the relevant larger turbulent eddies are resolved and the flow field is represented accurately and directly while small eddies are modelled. Knowing that turbulent spectrum cannot be resolved down to the dissipative scales (Kolmogorov scales) and so energy has to be dissipated from the spectrum at the grid limit (Figure 3-6), using LES provides viscous dissipation and so makes the small eddies to be dissipated. To achieve this goal, Smagorinsky Sub-Grid Scale Model is utilised and explained in more details in this chapter.

Figure 3-6: LES conceptual graph (ANSYS UK 2012)

The rationale behind LES is summarized as follows: (ANSYS UK 2010)

- Momentum, mass, energy, and other passive scalars are transported mostly by large eddies.

- Large eddies are more problem-dependent. They are dictated by the geometries and boundary conditions of the flow involved.

- Small eddies are less dependent on the geometry, tend to be more isotropic, and are consequently more universal.

- The chance of finding a universal turbulence model is much higher for small eddies.

3.2.1.3.1 Governing equations

Isothermal flow has been assumed; therefore the equation for conservation of energy is not needed. It is also known that the compressibility of water is negligible. Knowing that in this study, the fluid phase in the particle-laden flow has played a role of the incompressible single-phase, therefore the governing N-S equations shown below could be derived based on the conservation laws of mass and momentum.

$$\frac{\partial(\rho u_i)}{\partial t} + \frac{\partial(\rho u_i u_j)}{\partial x_j} = -\frac{\partial P}{\partial x_i} + \mu \frac{\partial^2 u_i}{\partial x_j x_j} \tag{3-23}$$

For incompressible flow, considering of the constant property for the fluid and expressing that each elemental volume of fluid parcel conserves its volume as it moves in the flow, therefore continuity equation and N-S equation are filtered and so the new equations are obtained as below.

$$\frac{\partial}{\partial x_i}(\rho \, \bar{u}_i) = 0 \tag{3-24}$$

and

$$\frac{\partial}{\partial t}(\rho \bar{u}_i) + \frac{\partial}{\partial x_j}(\rho \, \overline{u_i u_j}) = \frac{\partial}{\partial x_j}\left(\mu \frac{\partial \sigma_{ij}}{\partial x_j}\right) - \frac{\partial \bar{p}}{\partial x_i} - \frac{\partial \tau_{ij}}{\partial x_j} \tag{3-25}$$

where σ_{ij} is the stress tensor due to molecular viscosity defined by

$$\sigma_{ij} \equiv \left[\mu\left(\frac{\partial \bar{u}_i}{\partial x_j} + \frac{\partial \bar{u}_j}{\partial x_i}\right)\right] - \frac{2}{3}\mu \frac{\partial \bar{u}_l}{\partial x_l}\delta_{ij} \tag{3-26}$$

And τ_{ij} is the sub-grid-scale stress defined by

$$\tau_{ij} \equiv \rho\overline{u_i u_j} - \rho \, \bar{u}_i \, \bar{u}_j \tag{3-27}$$

The nonlinear filtered advection term $\overline{u_i u_j}$ is the chief cause of difficulty in Large Eddy Simulation(LES) modelling. It requires knowledge of the unfiltered velocity field, which is unknown, so it must be modelled. The filtered N-S equations are given as below

$$\frac{\partial \bar{u_i}}{\partial t} + \frac{\partial}{\partial x_j}\left(\bar{u}_i\,\bar{u}_j\right) = -\frac{1}{\rho}\frac{\partial \bar{p}}{\partial x_i} + 2v\frac{\partial}{\partial x_j}\,\bar{S}_{ij} - \frac{\partial \tau_{ij}}{\partial x_i} \tag{3-28}$$

Therefore following a Boussinesq hypothesis as in RANS models, computing subgrid-scale turbulent stresses can be achieved as follow

$$\tau_{ij} = \frac{1}{3}\,\tau_{kk}\,\delta_{ij} - 2\mu_t \bar{S}_{ij} \tag{3-29}$$

Where μ_t is the subgrid-scale turbulent viscosity and is modelled based on a simple model first proposed by Smagorinsky (Smagorinsky 1963). The isotropic part of eq. (3-29) τ_{kk} is not modelled, but instead added to the filtered static pressure term. $\bar{S}_{ij}$ is the rate-of-strain tensor for the resolved scale defined by

$$\bar{S}_{ij} \equiv \frac{1}{2}\left(\frac{\partial \bar{u}_i}{\partial x_j} + \frac{\partial \bar{u}_j}{\partial x_i}\right) \tag{3-30}$$

In the Smagorinsky-Lilly model, the eddy-viscosity is modelled by

$$\mu_t = \rho L_s^2\,|\bar{S}| \tag{3-31}$$

where L_s is the mixing length for subgrid-scales and $|\bar{S}| \equiv \sqrt{2\bar{S}_{ij}\bar{S}_{ij}}$. In ANSYS FLUENT, L_s is computed using

$$L_s = \min(\,kd,\,C_s V^{1/3}\,) \tag{3-32}$$

Where k is the von Kàrmàn constant, d is the distance to the closest wall, C_s is the Smagorinsky constant, and V is the volume of the computational cell.

3.2.1.4 Periodic flows

Periodic flow occurs when the physical geometry of interest and the expected pattern of the flow solution have periodically repeating nature. Periodic flow has been modelled in case studies in chapter 4 using commercial software ANSYS FLUENT (Version 14.0.0, ANSYS, Inc., Canonsburg, PA, USA). A pressure gradient have been utilised across the transnationally periodic boundaries, resulting in "fully developed" or "stream-wise-periodic" flow in the unsteady-state simulation. This is something very critical and useful for achieving objectives of this thesis due to the nature of

large scale turbulence structures in the flow. Another advantage of using Periodic Boundary Conditions (PBC) for the case studies is to save a great deal of computation cost when using LES turbulence model. But due to occurrence of problems while using PBC settings with introducing additional mass for the discrete phase (e.g. particles), see point 4 mentioned below, implementing the two models are achieved otherwise with less sophistication. Limitations are explained in both in the Fluent User guide (2011) (Version 14.0.0, ANSYS, Inc., Canonsburg, PA, USA) as well as in Chapter 22 of older version of Fluent User guide (2009). The shortcomings mentioned in the user guide are listed below.

1. Stream-wise periodic flow cannot be modelled when the discrete phase model is used.
2. When tracking particles in parallel, the DPM model cannot be used with any of the multiphase flow models (VOF, mixture or Eulerian) if the shared memory option is enabled.
3. No net mass addition through inlets/exits or extra source term is allowed.
4. Species can be modelled only if inlet/exits (without net mass addition) are included in the problem.
5. Discrete phase and multiphase modelling are not allowed.
6. Steady Particle tracks can be modelled only if the particles have a possibility to leave the domain without generating incomplete trajectories.
7. While Eulerian multiphase can be modelled with transitional PBC, mass flow rate specification method cannot be used. However, a constant pressure gradient can be specified.

3.2.2 Open source codes modelling

The open source codes used in this study are OpenFOAM and LIGGGHTS where the former deals with the fluid phase and the latter with the particulate phase of case studies.

3.2.2.1 OpenFOAM software

OpenFOAM is a continuum mechanics library written in C++ and developed on Linux that was begun to develop in the late 1980's at the Imperial College of London by H. Weller, G. Tabor, H. Jasak and C. Fureby (Weller *et al.* 1998) and became available to public as open source code in 2004 and has been under continuous development since. OpenFOAM is based on finite volume where regular cell elements have been accommodated for the case studies in chapter 4 where OpenFOAM has been used to model LES incompressible turbulence flows. The CFD code is supplemented with many functions and solvers which are useful for data extraction, mesh generation and manipulation, analysis and pre and post-processing. Furthermore it can produce output in a number of different formats for compatibility with external visualization applications. Literature have shown that OpenFOAM compares well with commercial packages such as FLUENT and has a good track record with respect to non-linear and strongly coupled problems.

3.2.2.2 LIGGGHTS software

LIGGGHTS is an open source code that has been used to model the particulate flows in this study. LIGGGHTS is a more recent DEM code based on the previous molecular dynamics code LAMMPS (Large-scale Atomic/Molecular Massively Simulator). It stands for LAMMPS Improved for General Granular and Granular Heat Transfer Simulations. LIGGGHTS was developed by numerous members of the Christian Doppler Laboratory on Particulate Flow Modelling (CDLPFM) at the Johannes Kepler University (JKU) Linz in Austria (Kloss *et al.* 2011). LAMMPS is a classic molecular dynamics C++ code which can be used to model atomic, polymeric, metallic, biological, granular and coarse grained systems in solid, liquid or gaseous states using a variety of force fields and boundary conditions (Plimpton *et al.* 1990).

3.2.2.3 CFD-DEM

CFDDEM is a coupling code to couple between Computational Fluid Dynamics (CFD) Software (OpenFOAM) and Discrete Element Modelling (DEM) Software (LIGGGHTS). The major contributor of the code is Christof Goniva (Kloss et *al.* 2011). The CFD-DEM code has complete four-way coupling capability and has been used for this study which is to simulate detailed modelling of sediment transport in applications with rivers. Currently the code is limited to transient incompressible flows. To implement the CFD-DEM coupling, the DEM solver (LIGGGHTS) and an OpenFOAM® CFD solver are being run consecutively, each pausing calculation after a predefined number of time-steps for the purpose of data exchange. Inside the "time loop", the DEM solver is periodically called to calculate the particles' positions and velocities.

Figure 3-7 is a flowchart showing the steps of the coupling routine where the fluid continuum was modelled through Large Eddy Simulation (LES), supplemented by Smagorinsky Subgrid scale model. The momentum exchange between continuous and discrete phases is considered for in the N-S equations by presenting a discrete R_{sl} particle momentum exchange field and a void fraction α_f which pre-multiplies all terms in the original N-S equations. The modified continuity and N-S (momentum) equation take the form of equations (3-33) and (3-34) respectively.

$$\frac{\partial \alpha_f}{\partial t} + \boldsymbol{\nabla} \cdot \left(\alpha_f \, \overline{\boldsymbol{U}} \right) = 0 \tag{3-33}$$

$$\frac{\partial \alpha_f \overline{\boldsymbol{U}}}{\partial t} + \alpha_f \boldsymbol{\nabla} \cdot (\overline{\boldsymbol{U}} \otimes \overline{\boldsymbol{U}}) = -\left(\alpha_f \boldsymbol{\nabla} \cdot \mathbf{R} - \alpha_f \boldsymbol{\nabla} \cdot 2\upsilon \overline{\boldsymbol{D}}\right) - \boldsymbol{R}_{sl} - \alpha_f \frac{\boldsymbol{\nabla}\bar{P}}{\rho_f} + \alpha_f \boldsymbol{F}$$

(3-34)

where $\alpha_f \boldsymbol{\nabla} \cdot \mathbf{R} - \alpha_f \boldsymbol{\nabla} \cdot 2\upsilon \overline{\boldsymbol{D}} = -\boldsymbol{\nabla}^2 \left(\alpha_f \, \upsilon_e \overline{\boldsymbol{U}} \right) - \boldsymbol{\nabla} \cdot \left[\alpha_f \, \upsilon_e \, \boldsymbol{dev} \, (\boldsymbol{\nabla} \overline{\boldsymbol{U}}^T) \right]$.

The R_{sl} momentum exchange field due to numerical reasons is split into explicit and implicit terms as in equations (3-35) and (3-36) respectively.

$$R_{sl} = \frac{K_{sl} \, (\boldsymbol{U}_f - \boldsymbol{U}_p)}{\rho_f} \tag{3-35}$$

$$\mathbf{K}_{sl} = \frac{\boldsymbol{F}_i}{|\boldsymbol{U}_f - \boldsymbol{U}_p| \, V_{cell}} \tag{3-36}$$

where $\boldsymbol{F}_i = \sum_{f=1}^{N} \boldsymbol{F}_f$.

Figure 3-7 shows the steps of coupling between CFD and DEM software. This is accomplished by sequential alternating CFD-DEM runs. First velocity and position of particle are computed by DEM solver. In this step LIGGGHTS considers all the forces are exerted on each particle by fluid (e.g. drag, etc.), other particles (e.g. contact force) and other sources (e.g. magnetic fields, etc.) then integrates the motion equation in order to calculate velocity and position of the particle. CFD-DEM by having position and velocity of particles is able to compute void fraction value as well as the momentum exchange terms. Now modified N-S equations can be solved by CFD-DEM solver in order to compute the exerted fluid force on the particles. Then CFD-DEM sends the calculated fluid force to DEM solver to compute new position and velocity of particles. The aforementioned procedure lasts when termination time condition has been encountered.
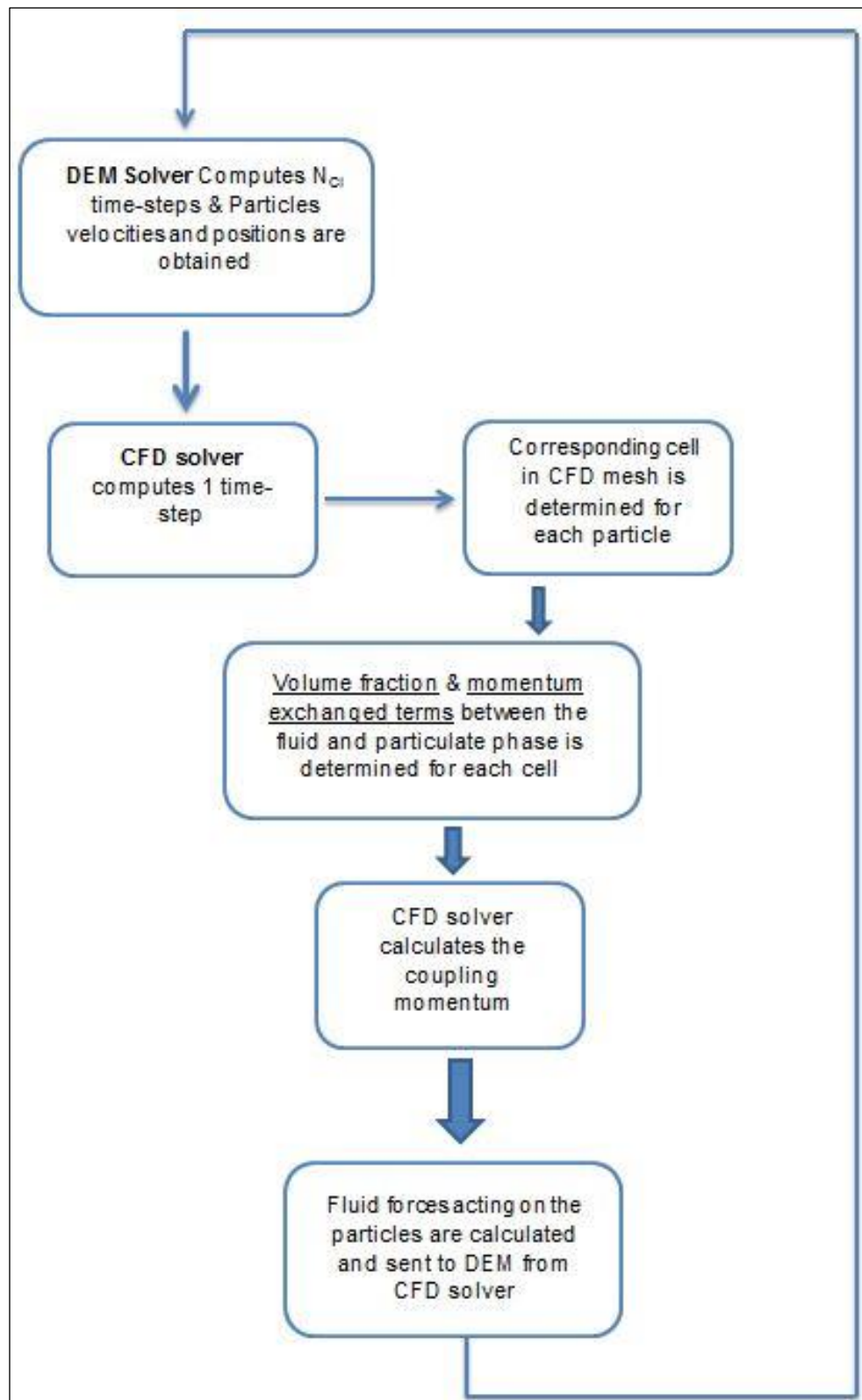
Figure 3-7: CFD-DEM flowchart, N_{CL} is coupling interval (Drawn by author)

3.2.2.4 Governing equations

Governing equations to be solved by CFD solver in OpenFOAM has been considered as incompressible N-S equation. In this regards continuity (3-37) and momentum (3-38) equations have been given as follow:

$$\nabla \cdot U = 0 \tag{3-37}$$

$$\frac{\partial U}{\partial t} + \nabla \cdot (U \otimes U) - \nabla \cdot 2\upsilon D = -\frac{1}{\rho}\nabla p \tag{3-38}$$

where $D = \frac{1}{2}(\nabla U + \nabla U^{T})$. In order to simulate turbulent flow Large Eddy Simulation (LES) modelling has been used. New sets of filtered equations (3-39) & (3-40) are formed as below to utilised LES modelling.

$$\boldsymbol{\nabla} \cdot \bar{\mathbf{U}} = 0 \tag{3-39}$$

$$\frac{\partial \bar{\bar{\mathbf{u}}}}{\partial t} + \nabla \cdot (\bar{\mathbf{U}} \otimes \bar{\mathbf{U}}) + \nabla \cdot \mathbf{B} - \nabla \cdot 2\upsilon\bar{\mathbf{D}} = -\frac{1}{\rho}\nabla\bar{\mathbf{p}} \tag{3-40}$$

After the filtering procedure an extra term of **B** is generated where called the subgrid scale (SGS) stress tensor. This is equation (3-41).

$$\boldsymbol{B} = \overline{\mathbf{U} \otimes \mathbf{U}} - \bar{\mathbf{U}} \otimes \bar{\mathbf{U}} \tag{3-41}$$

Turbulence modelling consists of finding convenient and physically correct representations for **B**. LES model used in this study is Dynamic Smagorinsky-Lilly model where the **B** term has been given as

$$\mathbf{B} = \frac{2}{3}k\mathbf{I} - 2\nu_{t}\bar{\mathbf{D}}_{D} \tag{3-42}$$

where $\bar{\mathbf{D}}_{D} = \bar{\mathbf{D}} - \frac{1}{3}tr(\bar{\mathbf{D}})\mathbf{I}$, $\nu_{t} = C_{D}\Delta^{2}\|\bar{\mathbf{D}}\|^{2}$, and $k = C_{I}\Delta^{2}\|\bar{\mathbf{D}}\|^{2}$; knowing that C_{D} and C_{I} are constant. Δ is the function of cell size (Fureby *et al.* 1997).

3.2.2.5 Mesh

For the CFD tool of OpenFOAM a mesh has been developed in using the standard OpenFOAM blockMesh functionality with a corresponding blockMeshDict file (Weller, Greenshields and Janssens 2014).

For the DEM tool of LIGGGHTS an external mesh generator called Gmesh has been applied. G Mesher (Gmsh) is an open-source three-dimensional finite element grid generator with a build-in Computer Aided Design (CAD) engine and post-processor (Geuzaine and Remacle 2009).

3.2.2.6 Time step

Discrete Element Method is very sensitive to time step selection. This is due to capture contact phenomena either between particles or between particles and surface boundaries. Two time steps' benchmarks have been considered. The first one called Rayleigh time which is time needed by Rayleigh wave to travel the diameter of a particle (Kloss *et al.* 2012; Kruggel-Emden *et al.* 2008; Goniva *et al.* 2010). A good time step is to be 20% of Rayleigh time. Rayleigh time principle is described by equation (3-43).

$$T_R = \pi R \left(\frac{\rho p}{G}\right)^{\frac{1}{2}} (0.1631v + 0.8766) \tag{3-43}$$

where $= \frac{Y}{2\,(v+1)}$.

The Hertzian time is the second critical time step used in this study and is given by equation (3-44). The suggested simulation time step which is essential to resolve particle contact, is greater than 5% and less than 15% of the Hertzian time.

$$T_H = 2.87 \left(\frac{m^*}{R^*Y^{*2}v_r}\right)^{\frac{1}{5}} \tag{3-44}$$

where v_r is the maximum relative velocity of either two particles or particle and boundary surface.

Chapter 4 Case studies and results

4.1 Introduction

This chapter consists of three main sections of 4-1: CFD Results and validation cases, 4-2: DEM Results and finally 4-3: CFD-DEM Results; where the first one contains case studies that have been used for validation purposes, the second section indicates results obtained related to particle (sediment) phase only and the last section contains 4-way coupling of fluid-particle interaction at a particle scale.

4.2 CFD results and validation cases

Three different case studies have been modelled and studied numerically. Results in sections below shows the accuracy of the numerical settings and LES turbulence model in the CFD solver i.e. ANSYS FLUENT and OpenFOAM. These have been validated with other available numerical results and also experiments done as part of this research.

4.2.1 Turbulent channel flow ($Re_\tau = 180$)

This benchmark problem has been chosen to show the accuracy of turbulent modelling used in the simulations in this study. Therefore a Large Eddy Simulation (LES) of a turbulent channel flow using OpenFoam 2.3.0 is performed on the geometry set-up shown in Figure 4-1. Numerical results has been compared with Direct Numerical Simulation (DNS) conducted by Kim, Moin and Moser (1987).

4.2.1.1 Problem setup

The geometry and mesh for the simulation is constructed using blockMesh, in which depth $\delta = 2m$, width $z = 2m$ and length $x = 4\,m$ of the geometry are shown in Figure 4-1.
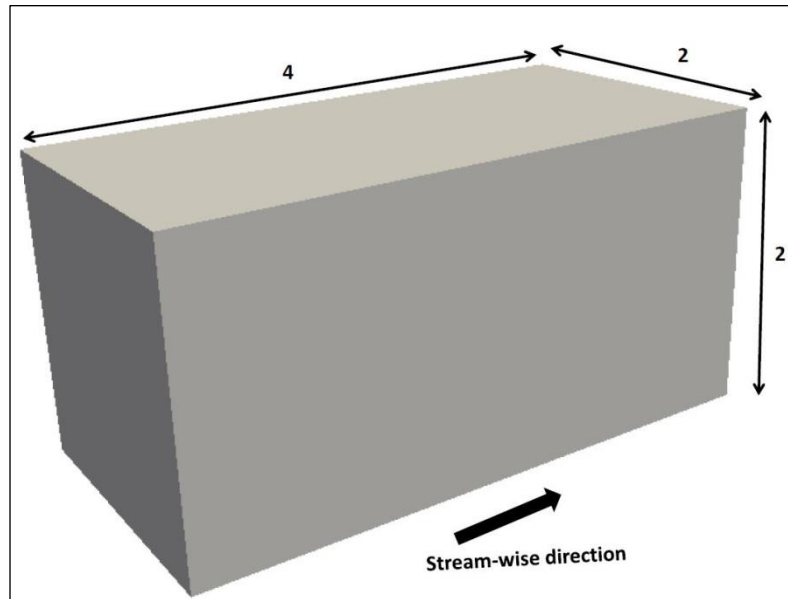
Figure 4-1: Geometry Set-up

The unsteady Navier-Stokes equations are solved numerically at a Reynolds number of 180 ($Re_\tau = 180$), based on the friction velocity and channel half-width, with about 4 x 10^4 grid points (100 x 80 x 50 in x, y, z), depicted in Figure 4-2. In DNS study all essential turbulence scales are resolved on the computational grid and no sub-grid model is used, however using OpenFOAM as a CFD tool for carrying out this test case, the subgrid scale model is chosen to be Smagorinsky model for the LES turbulence model.
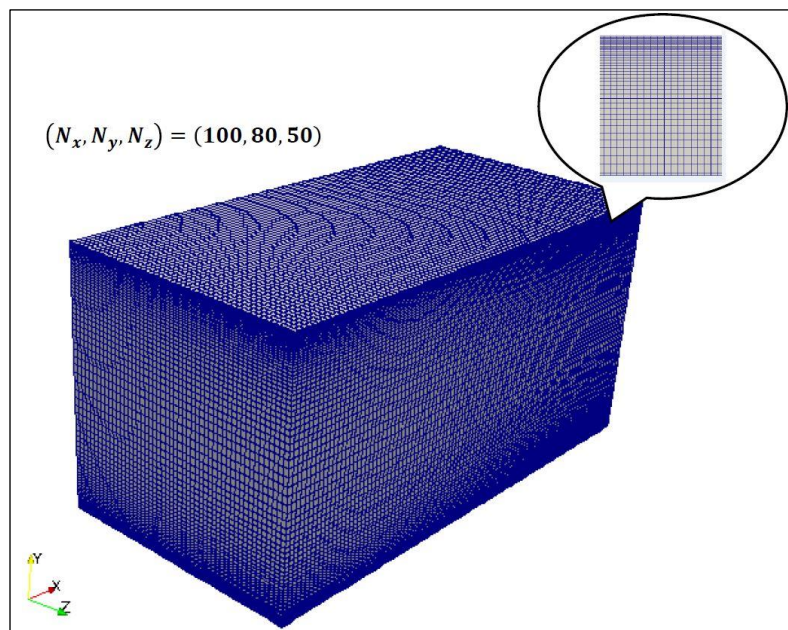

Figure 4-2: Mesh configuration, $\left(N_x, N_y, N_z\right) = (100, 80, 50)$

Periodic boundary conditions in the stream-wise (x,u) and span-wise (z,w) directions and no-slip wall-normal direction is imposed for the channel flow considered. Flow is moving in x-direction as pressure gradient have been implemented in the stream-wise direction.

4.2.1.2 Turbulence statistics

Velocity contour snapshot shown in Figure 4-3 indicates turbulent flow at $Re_\tau = 180$. Numerical results for this test case are stated in the form of statistics of the mean stream-wise velocity and velocity fluctuations. Statistics are achieved by sampling the solution fields at the cell and averaging in the stream-wise and span-wise directions as well as in time. Comparison of the statistical results with the DNS data of Kim, Moin and Moser (1987) is made in order to evaluate the accuracy of the LES turbulence modelling methodology. All results are presented in dimensionless wall units.
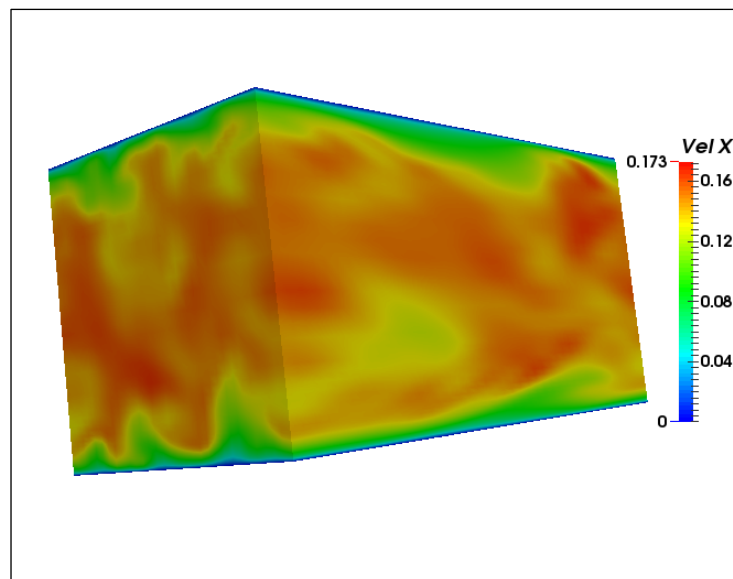

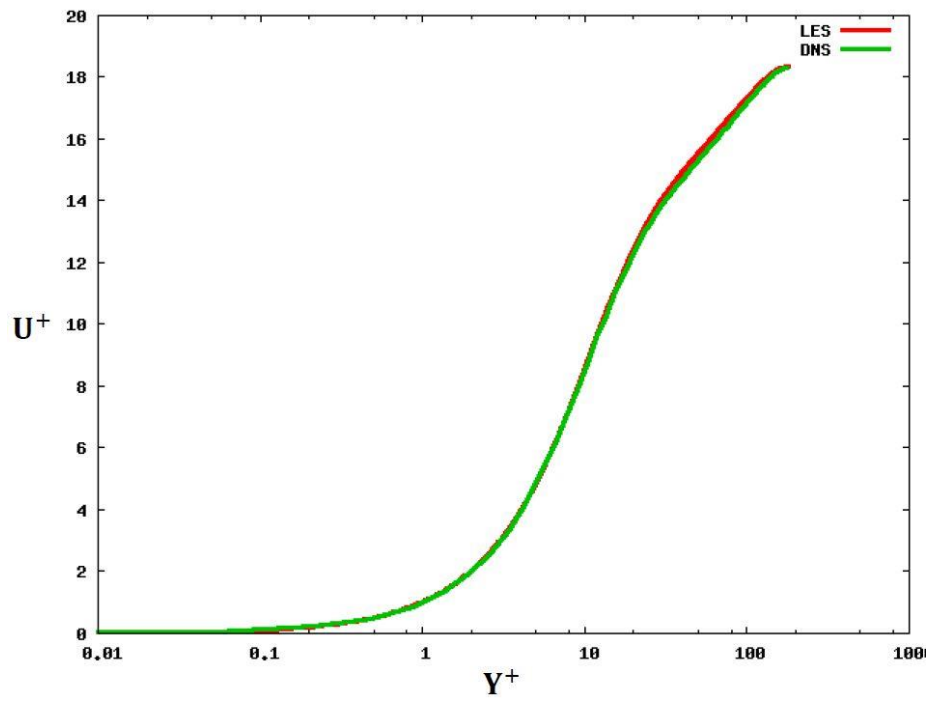Figure 4-3: Velocity snapshot of turbulent flow at $Re_\tau = 180$

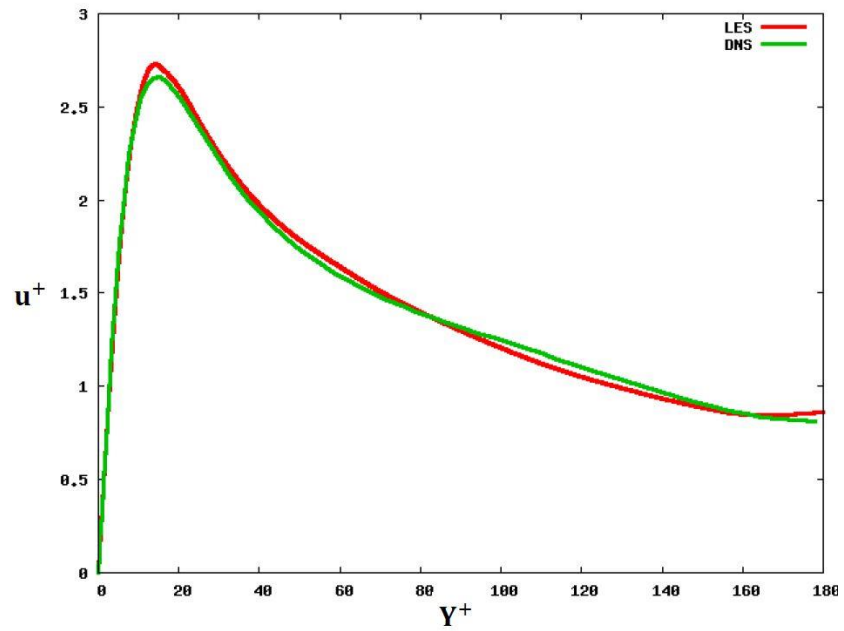Figure 4-4: Mean stream-wise velocity, $U^+ = \frac{\bar{u}}{u_\tau}$ versus $Y^+ = \frac{yu_\tau}{\nu}$

Figure 4-5: Stream-wise velocity fluctuation, $u^+ = \frac{\acute{u}}{u_\tau}$
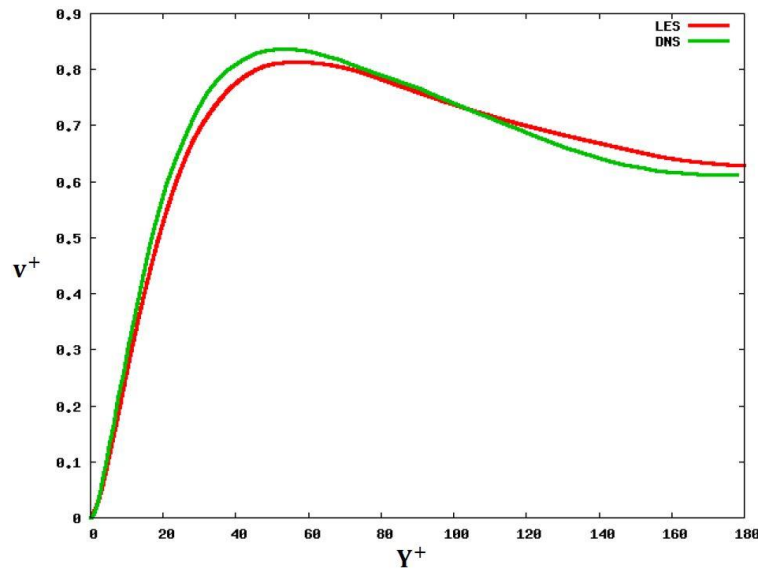
Figure 4-6: Wall-normal velocity fluctuation, $v^+ = \frac{\acute{v}}{u_\tau}$

Figure 4-4 shows mean stream-wise velocity, $U^+ = \frac{\bar{u}}{u_\tau}$, where $\bar{u}$, u_τ are average velocity and friction velocity, respectively. Velocity fluctuations in the stream-wise, wall-normal and span-wise directions are depicted in Figure 4-5, Figure 4-6 and Figure 4-7 respectively. Note that the fluctuation have been non-dimensionalized by dividing by friction velocity, u_τ.
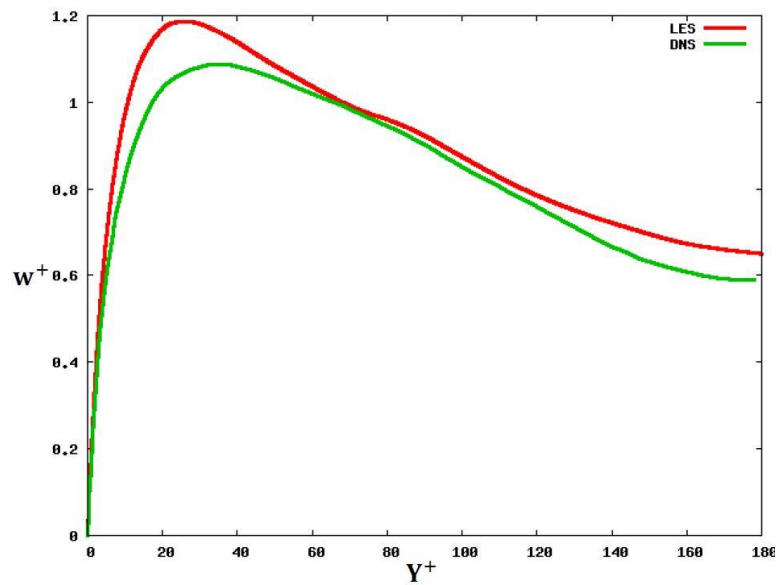

Figure 4-7: Span-wise velocity fluctuation, $w^+ = \frac{\acute{w}}{u_\tau}$

The accuracy of turbulent modelling used in the simulations, i.e. LES modelling has shown to be in very good agreement with the DNS results reported by Kim, Moin and Moser (1987).

4.2.2 Bar-form

4.2.2.1 Geometry set-up

Experimental model set up has been constructed as a bar-form (negative slope) with a height of 0.15m and a 30 degrees angle for the slope. The flume includes the upstream which is set to have a fairly long length of 2 meter and 3 meters long for the downstream. The current investigation has been done with the below specifications: (

Figure 4-8)

- Investigated section of flume dimensions: length = 2.76 m, height = 0.25 m, width = 0.3 m
- Water velocity: 0.5 m/s
- f = 25 HZ
- Inlet upstream water depth: 0.1 meter
- Upstream investigated length: 0.5 meter
- Slope horizontal length: 0.26 meter
- Downstream investigated length: 2 meter
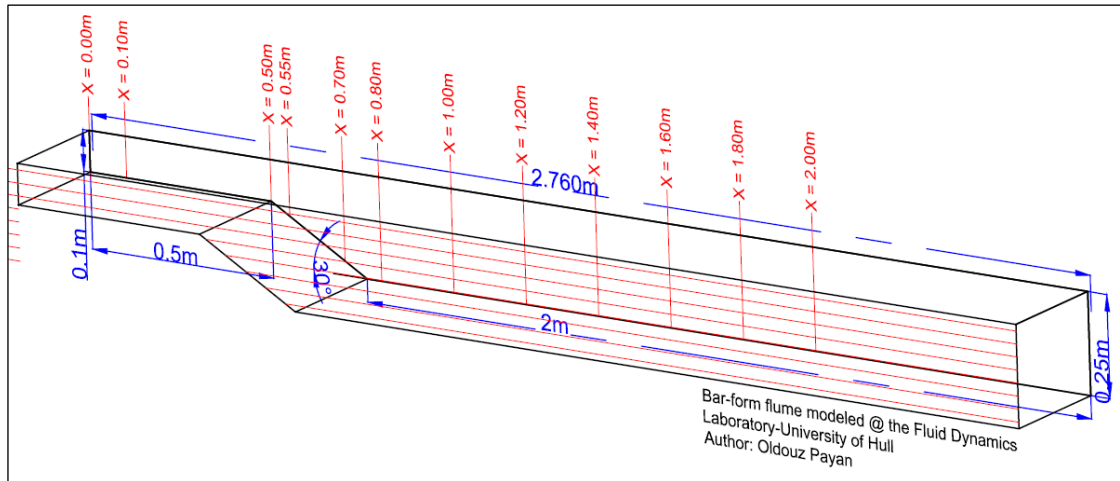- Downstream water depth: 0.25 meter

Figure 4-8: Experimental model set up

Experimental investigation has been carried out in the Fluid Dynamics Laboratory at the University of Hull in the United Kingdom. Knowing that the brink point is at X = 0.5 m; several measurements of velocity values and turbulence statistics have been obtained, using Vectrino-II, which is positioned in on the upstream section (X = 0.5 m), in two locations on the slope (X = 0.55 m & X = 0.7 m), and in six locations (X = 0.8 m, 1.00 m, 1.2 m, 1.4 m, 1.6 m & X=1.8 m) downstream section.

4.2.2.2 Meshing set up and Boundary Condition (BC)

Using Design Modeller (DM) in Workbench 14.0 the same geometry set up was arranged as a 3D model and so ANSYS meshing was used to implement finer bias mesh closer to bed while coarser mesh spreading utilised closer to the surface. (See Figure 4-9 and Figure 4-10)

Figure 4-9: 3D Mesh

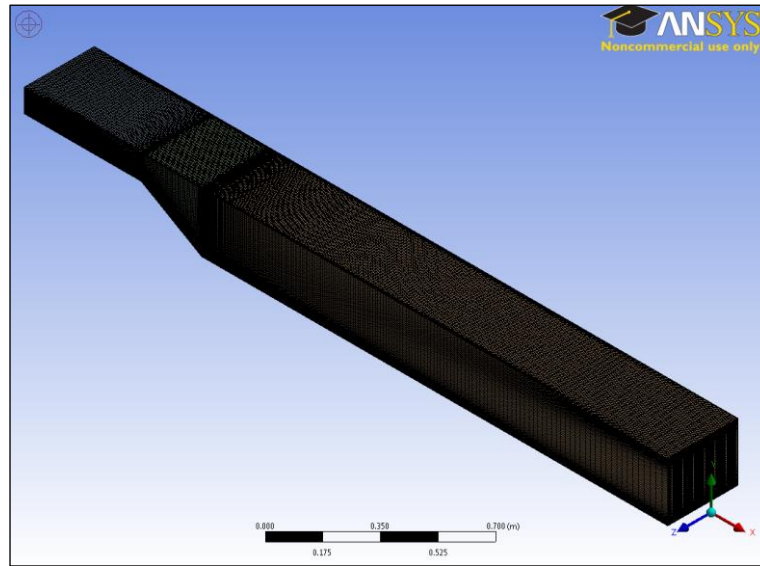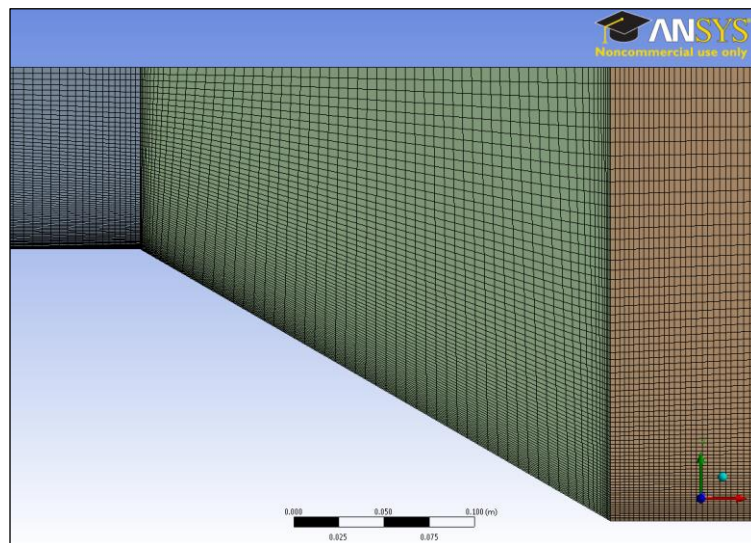Figure 4-10: Mesh refinement

Large Eddy Simulation (LES) set up with the dynamic Smagorinsky subgrid model set up used for solving continuum. Water along with its default characteristics was defined as the fluid in the solver. The boundary condition for the flume has been set up as the physical model.

- Bed and side walls as no-slip wall
- Top surface as zero-shear wall to represent the free surface BC

- Inlet as the velocity inlet
- Outlet as the outflow BC

Many authors studying numerical modelling of open channel flow have used a rigid no-slip boundary condition where the wall-shear is set to be zero (Thomas and Williams 1995b; Shi, Thomas and Williams 1999).

The difference between mean velocity and turbulent quantities distribution using a free surface and a symmetry plane are shown in Figure 4-11 (Rodi 1993). Although implementing a free surface boundary condition in ANSYS FLUENT 14.0 is bound to be resembled by either a zero-shear wall on the top surface or a symmetry boundary condition; It is known that using symmetry boundary condition for the top surface of the flume has direct effect on the stream-wise and lateral velocities of the fluid near the wall where velocity components are mirrored using symmetry boundary condition.
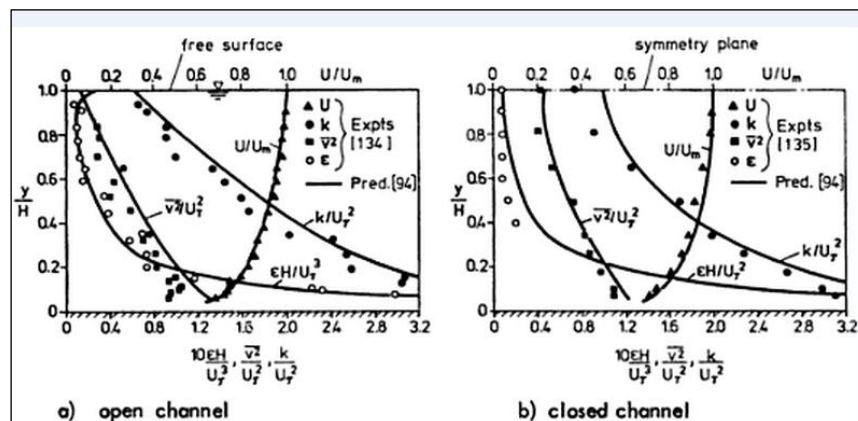
Figure 4-11: Distribution of mean velocity and turbulence quantities in developed two-dimensional channel flow (Rodi 1993)

As ANSYS fluent "User Guide' (2009) which claims that there is no difference between a symmetry BC and a free-surface BC (slip wall with zero-shear), the latter was implemented on the top surface of the geometry.

4.2.2.3 Experiment data as inlet input

Velocity inlet value has been initiated using ANSYS fluent 14.0 for the flume inlet at X = 0.0 m where U = 0.5 m/s which is defined based on the value

used for the experimental study done at the University of Hull Fluid Dynamics Laboratory.

4.2.2.4 Numerical data as inlet input

Following a well validated DNS results of a flat channel by Kim, Moin and Moser (1987), an LES simulation of a flat channel with same dimensions and grid spacing of the upstream of the bar-form flume has been constructed (Figure 4-12). Periodic boundary condition has been imposed between the inlet and outlet assuming the flow field to be periodic in the stream-wise direction. This implementation with a pressure gradient across the channel domain for flow drive along with the sufficient simulation run time to establish stationary conditions certifies that the results are not sensitive to the random initial fluctuations introduced. A fully developed velocity profile was written from the outlet plane after stationary state reached on the flat channel. This numerical logarithmic velocity profile (Figure 4-13) then was read at the inlet of the bar-form geometry as inlet condition.
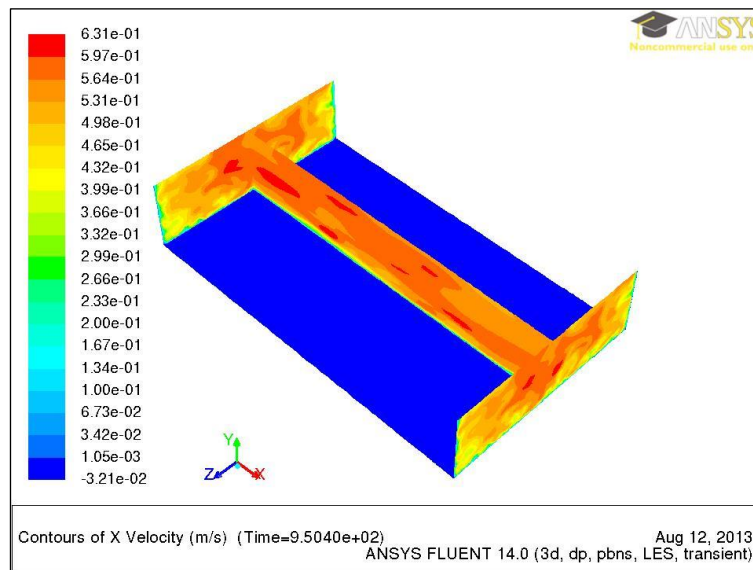

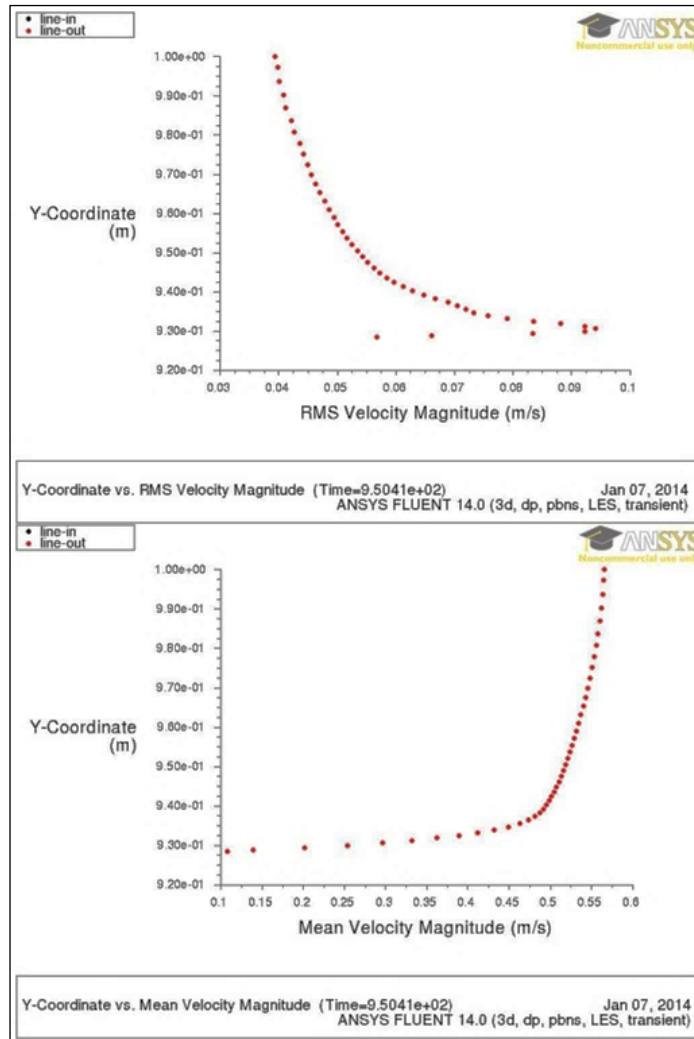Figure 4-12: Numerical Inlet Condition based on flat channel

Figure 4-13: Fully Developed velocity inlet profile (drawn by author)
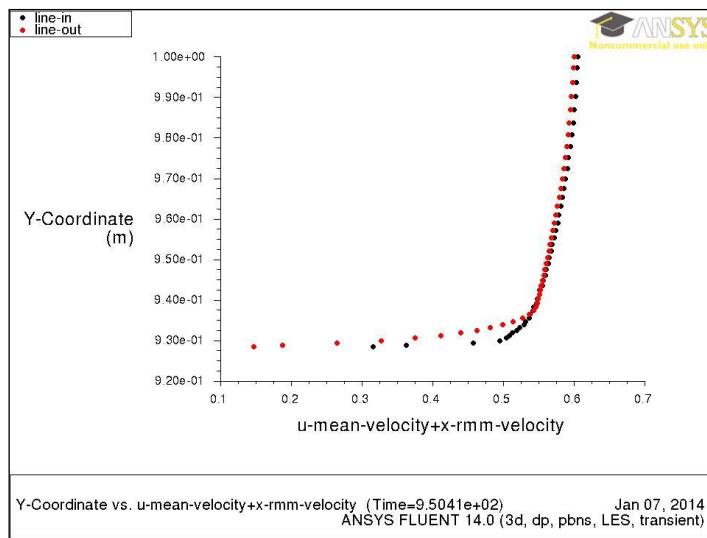

Figure 4-14: Logarithmic Velocity Profile (drawn by author)

4.2.2.5 Numerical results

Using the above specifications, assumptions and the boundary conditions, running the simulations with an average of 16 processors of ANSYS fluent 14.0 on the University of Leeds supercomputers ARC1, stationary point for the flow field reached after 7 months of real time.

Figure 4-15 indicates the seperation point which occures just on the brink point. Looking at the stream-wise velocity profiles that have been shown on two sections of the flume; negative velocity values on the downstream of the flume clearly shows the creation of a vortex with a seperation point at X = 0.55 m as well as attachment point at about X = 2 m (See Figure 4-16 & Figure 4-18). This consistency has been remained at the bottom section of the graphs where the velocities are negative. Negative streamwise velocities are indication of large and small scales eddies generation close to bed at the lee side.
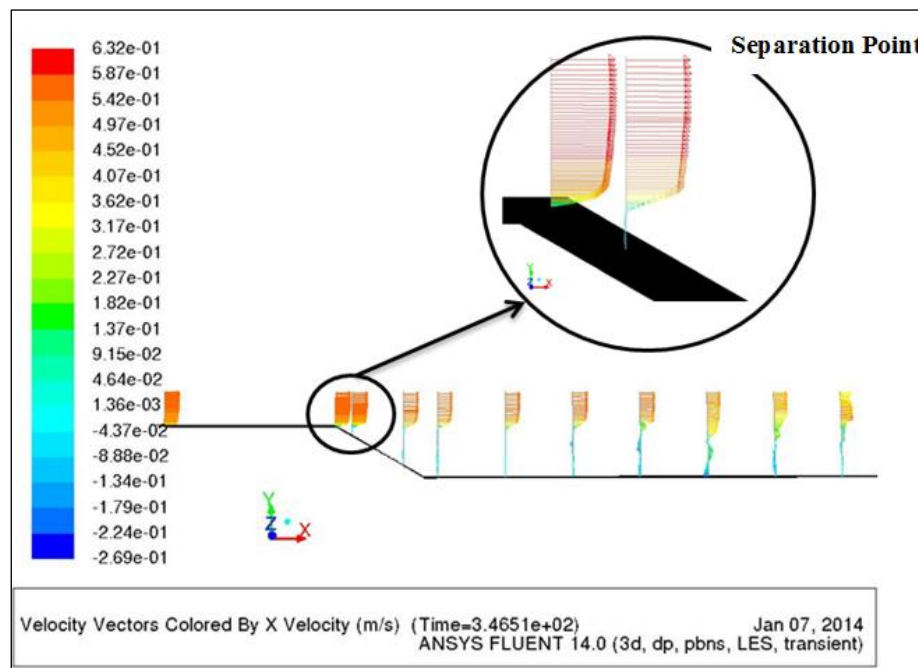

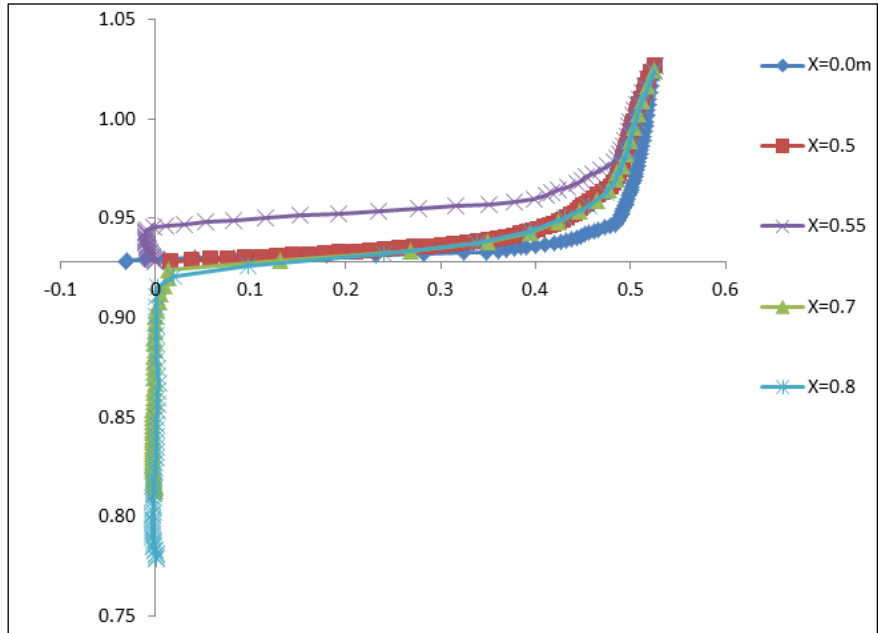Figure 4-15: Separation point after stationary state

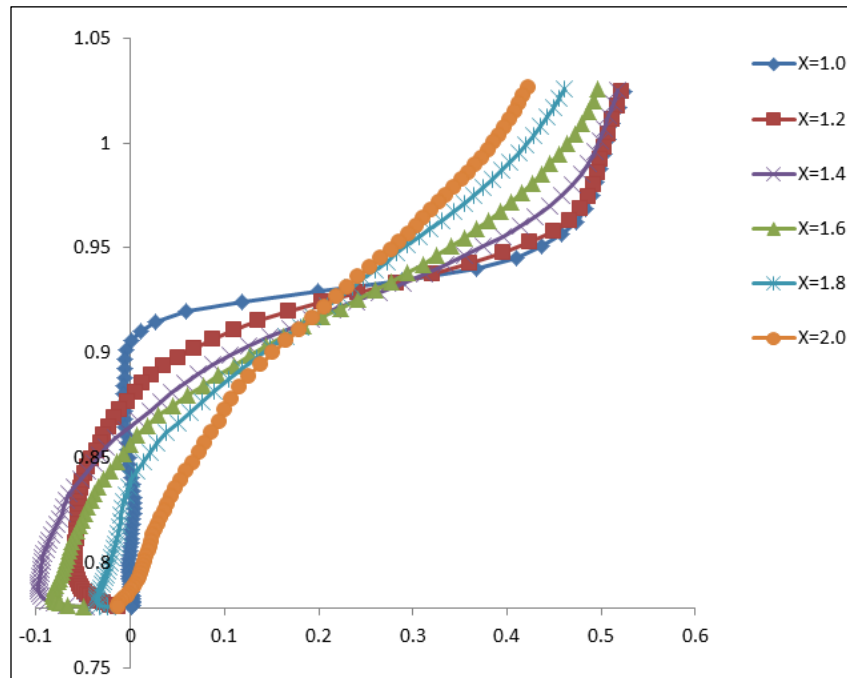Figure 4-16: Upstream Mean Stream-wise Velocity profiles

Figure 4-17: Downstream Mean Stream-wise velocity profiles
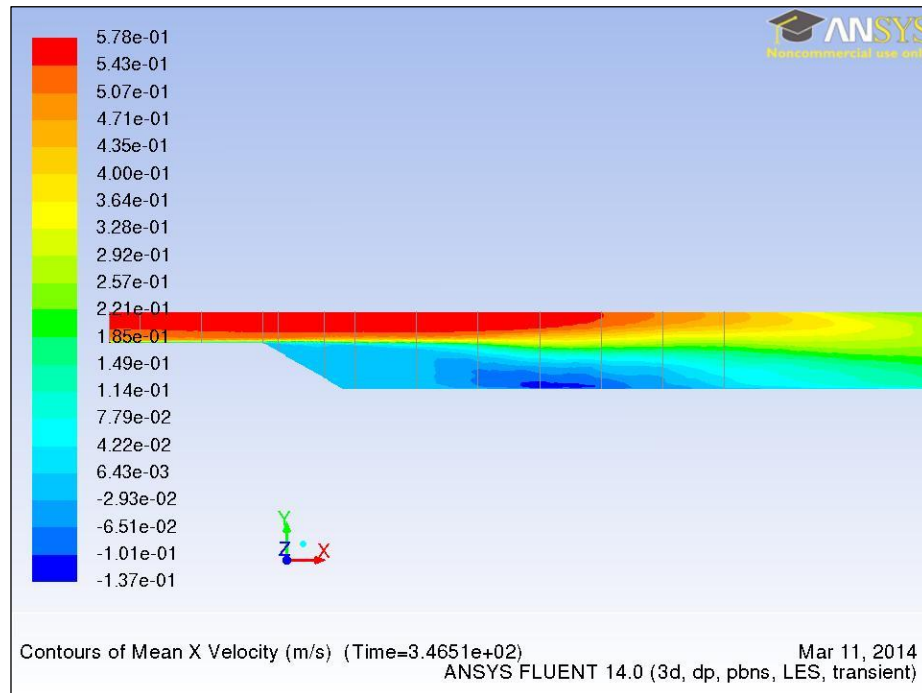
Figure 4-18: Vortex Separation and Reattachment

This results show almost the same trend as the velocity profiles obtained from experimental investigation mentioned in in Chapter 2. These results have been shown and compared in sections below.

4.2.2.6 Experimental results against numerical modelling

After obtaining both experimental and numerical results, the data has been validated. Figure 4-19 to Figure 4-27 show the comparison between three graphs. The first one is the filtered experimental results, the second sets of graphs are the numerical modelling results obtained using the experimental inlet velocity, and the last sets of graphs are the numerical modelling results achieved using the numerical inlet velocity, using previous sections settings for the channel flow.

All graphs clearly shown that the fully turbulent region of flow have been well detected by the use of both numerical and experimental tools. Additionally most of the velocity profiles at the bottom half of the graphs i.e. viscous sub-layer region and parts of buffer-layer, have not been sensitively followed by the experimental readings. This weak trend can be either explained by the poor calibration of the Vectrino-II or by errors in the filtering process. Most

numerically obtained negative velocities at this part of graphs are indicative of the eddy formation at the slope, lee side and downstream of bar-form. Despite the fact that both numerical results with different velocity inlet inputs (red and green lines shown in graphs below) are following very similar pattern in the flow field but justifiably experimental results are shown to be closer to the numerical results with experimental velocity inlet shown with red line in most of the figures, more specifically at the upstream of the flume.

Figure 4-19 which is the readings before formation of eddies close to bed, shows that vectrino-II results follow the numerical outcomes very smoothly. Looking at the flow filed from another perspective, it is witnessed from Figure 4-18 that separation occurs just after the first line of study X = 0.5 m where zero velocities starts to form as a part of separation phenomena. Figure 4-20 that is taken by Vectrino-II at X = 0.55 m of the flume shows an agreeable flow separation results with both numerical results. Although from Figure 4-20, Figure 4-23 and Figure 4-24, it can be seen that zero and very small negative velocities close to bed have been captured well enough with the experimental tool but the rest of velocity profiles at the downstream of flume, close to bed, have not been executed well. This again could be because of the sensitivity of Vectrino close to bed or noise reflection at the beams when is gets close to a solid surface i.e. flume bed.
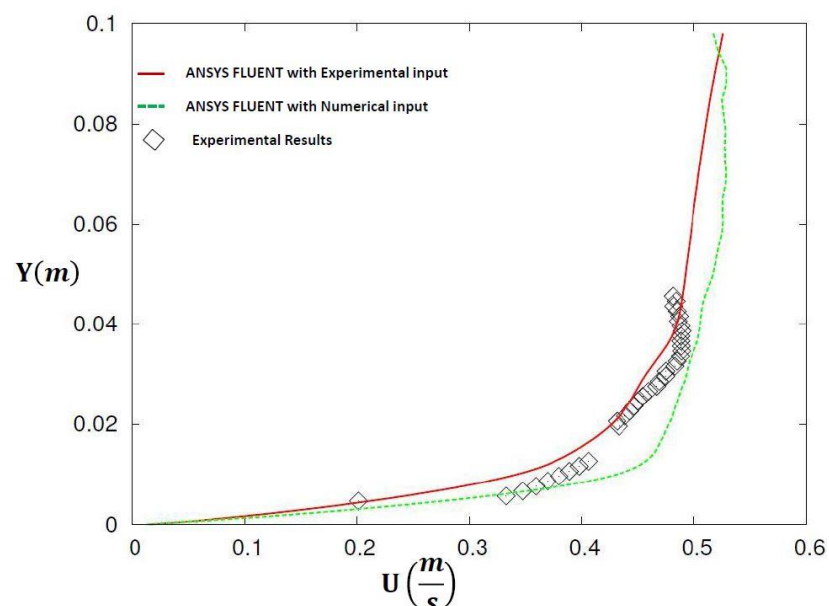
Figure 4-19: Stream-wise velocity at x = 0.5 m
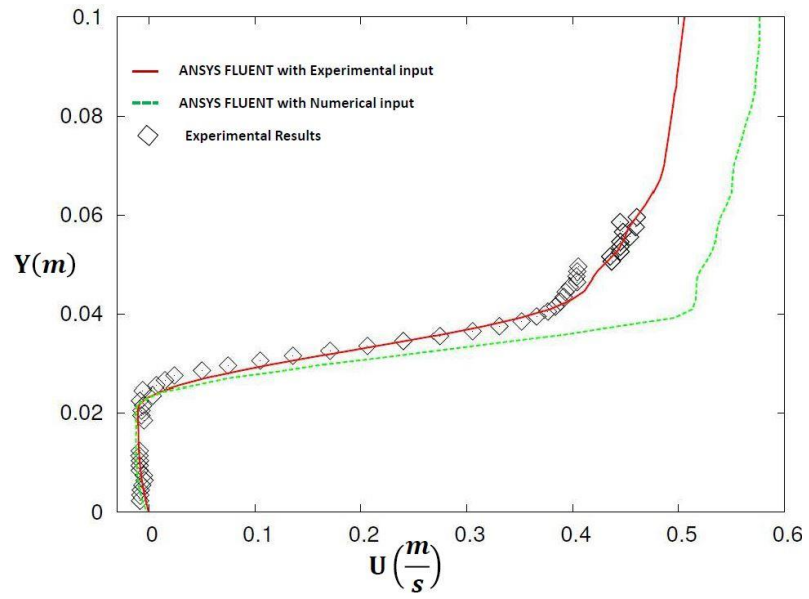
Figure 4-20: Stream-wise velocity at x = 0.55 m
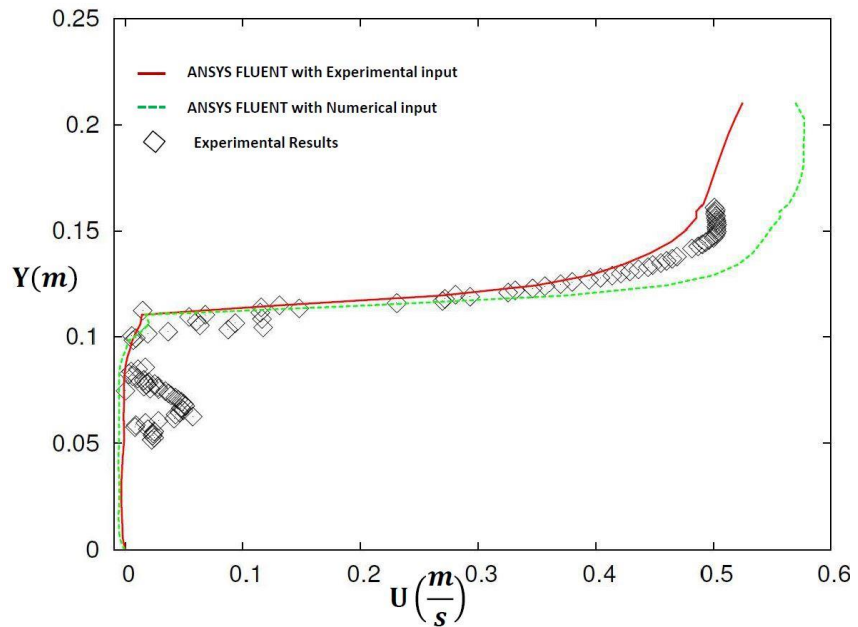
Figure 4-21: Stream-wise velocity at x = 0.7 m
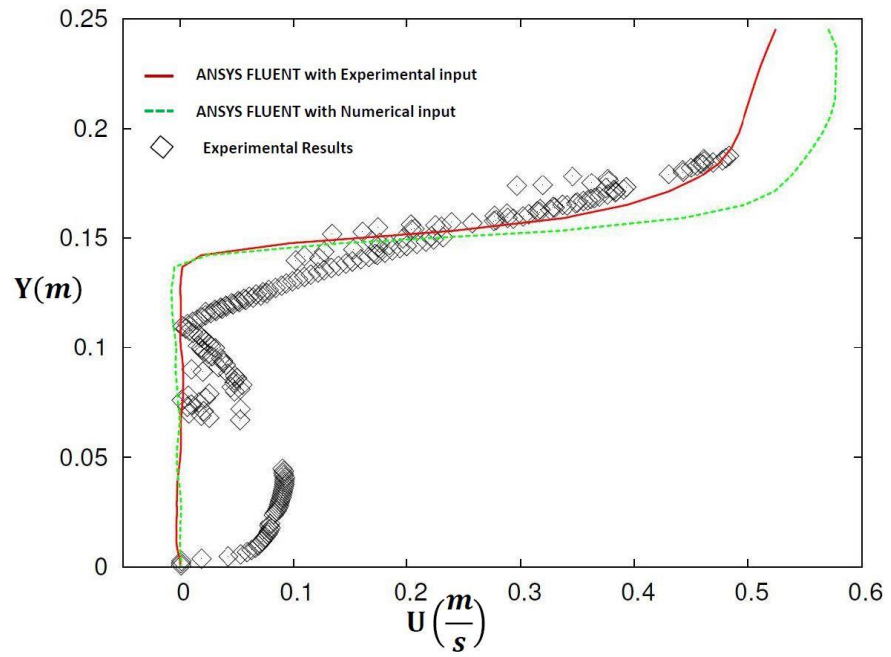
Figure 4-22: Stream-wise velocity at x = 0.8 m
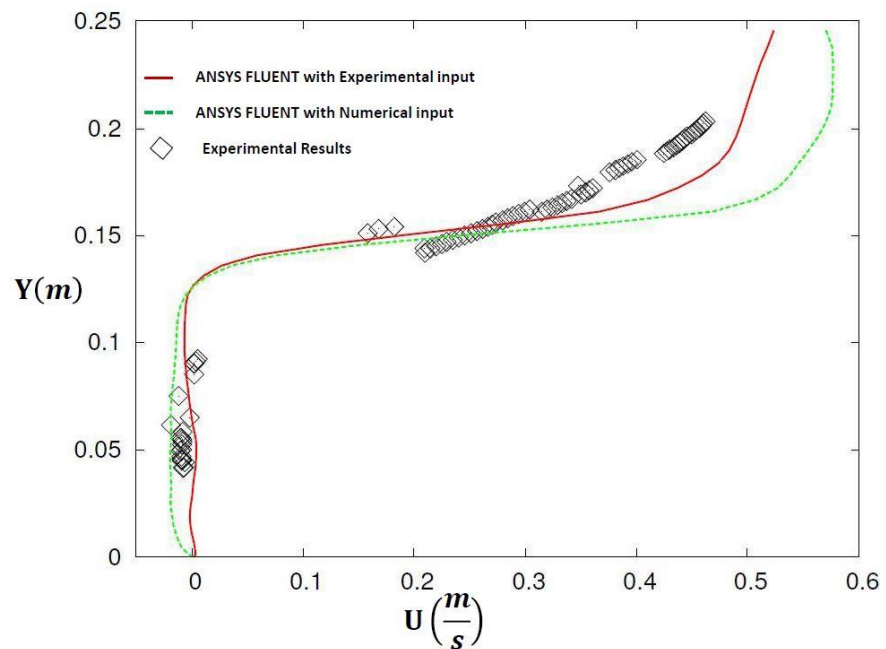
Figure 4-23: Stream-wise velocity at x = 1.0 m
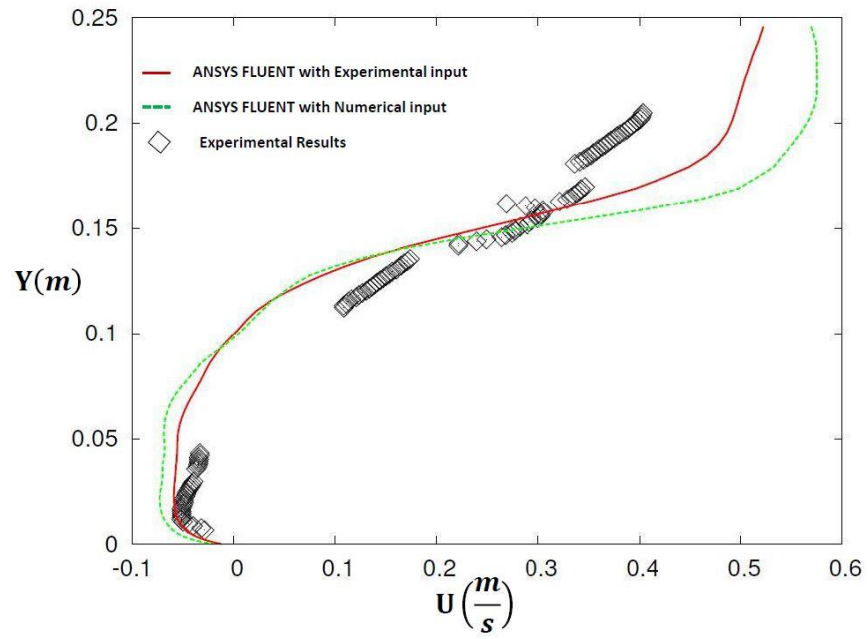
Figure 4-24: Stream-wise velocity at x = 1.2 m
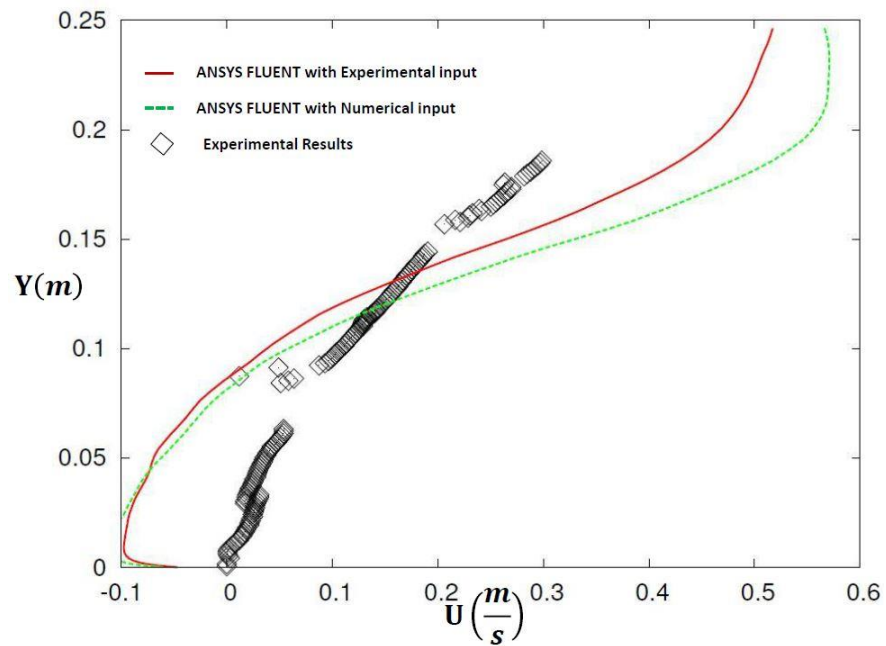
Figure 4-25: Stream-wise velocity at x = 1.4 m
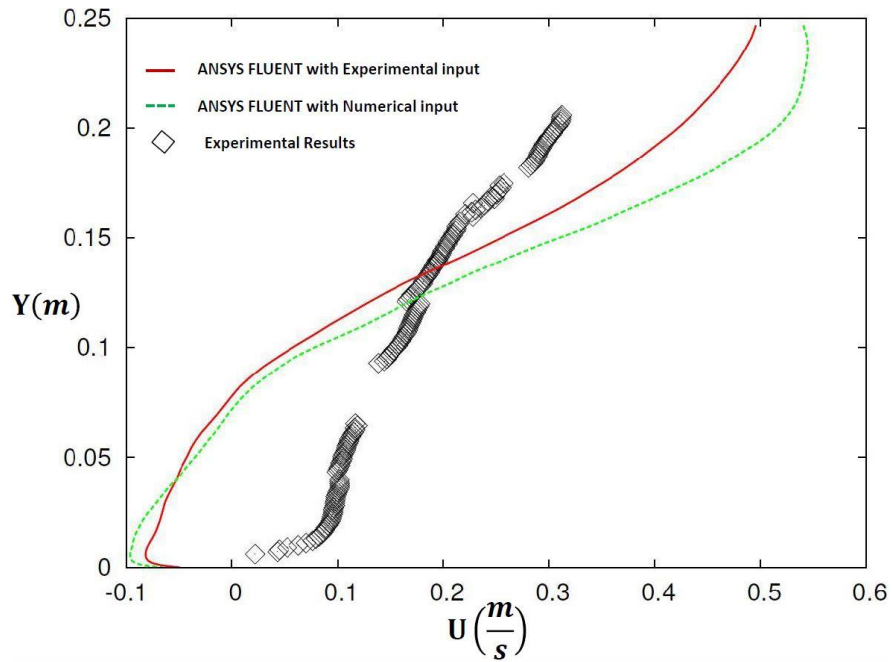
Figure 4-26: Stream-wise velocity at x = 1.6 m
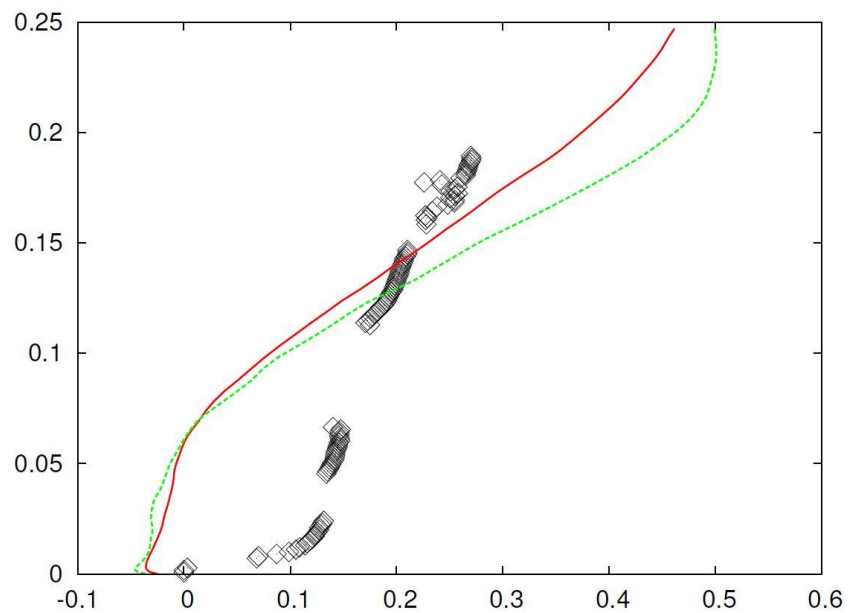
Figure 4-27: Stream-wise velocity at x = 1.8 m

Knowing the capabilities of the Vectrino-II and its sensitivity to water vortex created at the beams of measurements, (See chapter 2), velocity profiles obtained from numerical investigation shows to be in good agreement with

the experimental findings specifically away from the bed. The upstream velocity profiles tends to match better than the downstream velocity profiles.

As the graphs shown a lot of negative velocity values, meaning the presence of large and small eddies close to bed at the downstream, most of the scatter is probably as a result of experimental uncertainty involved in measuring turbulence quantities near the wall. This is where the presence of high shear and small scales of turbulent motions makes measurements extremely difficult.

4.2.3 Dune-form

In this section dune-form problem has been considered to show the accuracy of turbulent modelling used in the simulations with ANSYS FLUENT 14.0 in this thesis. Therefore a Large Eddy Simulation (LES) of a turbulent channel flow using ANSYS FLUENT 14.0 is utilised on the geometry set-up shown in Figure 4-28. Numerical results has been compared with LES conducted by Yue, Lin and Patel (2006) as well as experimental results of Balachandar *et al.* (2002).

4.2.3.1 Problem set up

The geometry is the same as that in the experiments of Balachandar *et al.* (2002) in which Laser-Doppler Velocimetry (LDV) and Particle Image Velocimetry (PIV) measurements were used. The geometry and mesh for this simulation have been generated by ANSYS Design Modeller and ANSYS Mesh. (Figure 4-28 and Figure 4-29) The same geometry constructed using blockMesh and used for the CFD-DEM section of this chapter.
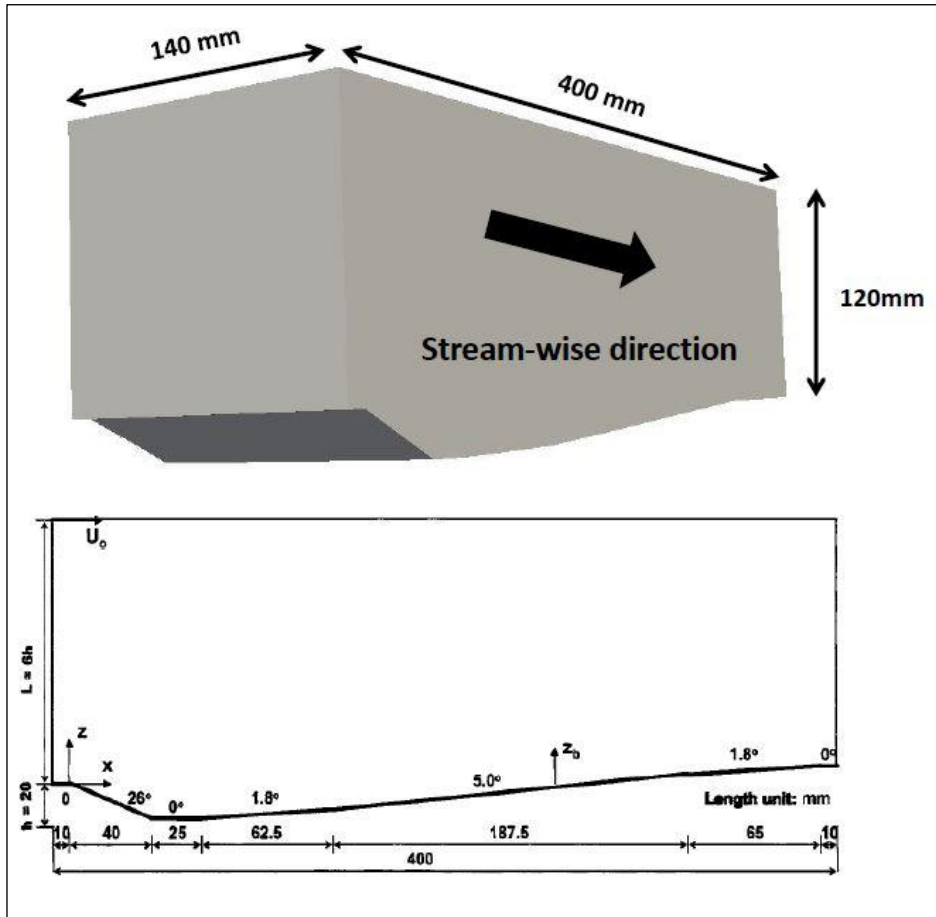
Figure 4-28: Dune geometry (drawn by author)
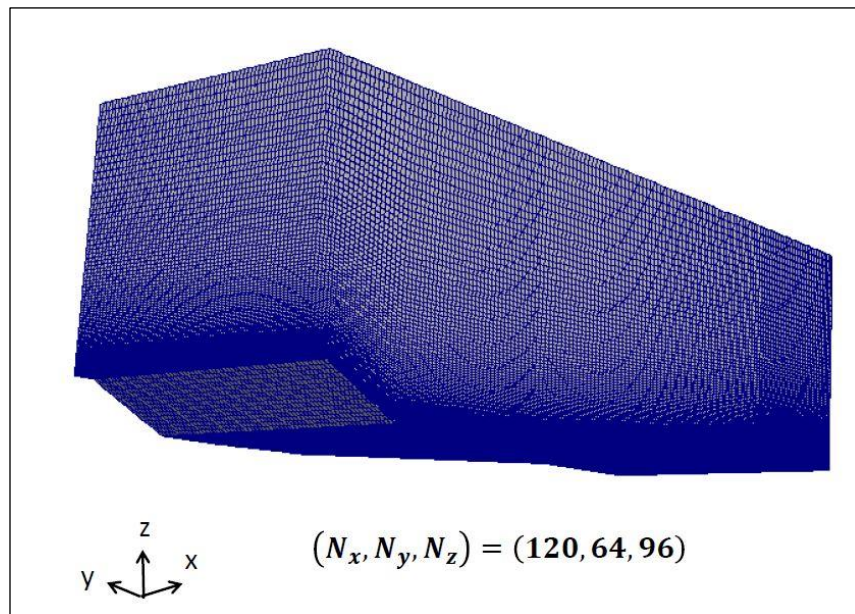
Figure 4-29: Dune mesh (drawn by author)

The origin of the (*x*, *y* , *z*) coordinate system is located at the dune crest, with *x* parallel to the stream-wise direction, *y* in the span-wise direction, and *z* in the wall-normal. The Reynolds number, based on water depth L and free-surface velocity U_0 at the inlet of the solution domain, is 5.7×10^4. Dune height h is$20\ mm$. The grid used is $(120, 64, 96)$ in the stream-wise, span-wise and wall-normal directions, respectively. The spacing is uniform in the stream-wise and span-wise directions. In the vertical direction, the grid points are non-uniformly distributed. Periodic boundary conditions are imposed at the stream-wise and span-wise boundaries, while no-slip boundary condition is applied at the bed. The free surface is treated as a plane of symmetry. The flow is driven by a mean pressure gradient, $\frac{dp}{dx}$, that is determined to match the Reynolds number, $Re = \frac{U_0 L}{\nu} = 5.7 \times 10^4$

4.2.3.2 Numerical results

In order to solve turbulent Navier-Stokes, LES based on the Smagorinsky model is considered (Germano *et al.* 1991; Lilly 1992). Snapshot of velocity contours for $Re = 5.7 \times 10^4$ in depicted in Figure 4-30.
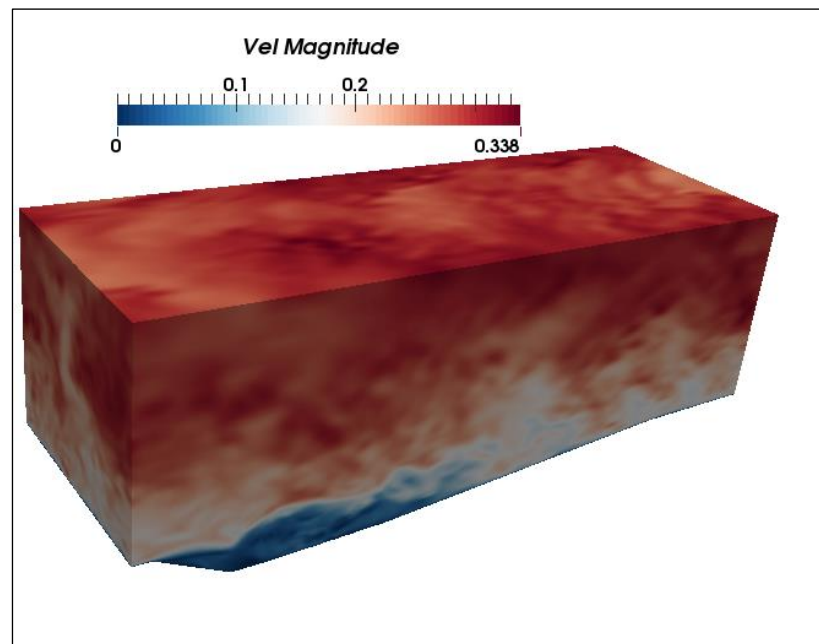
Figure 4-30: Velocity contours for $Re = 5.7 \times 10^4$.

The results are averaged at the mid-plane of the dune, in order to obtain the time-mean values of the velocity components and turbulence statistics. These mean values are normalized by the free surface velocity, U_0 of the top boundary at the inlet of the solution domain and in the profile plots the vertical distance from the bed, z_b, is normalized by the dune height, h. In Figure 4-31 to Figure 4-36 show comparison of mean stream-wise velocity profiles predicted by the present LES modelling with the experimental results of Balachandar *et al.* (2002) and LES modelling results obtained by Yue, Lin and Patel (2006) at six representative stream-wise positions. The overall agreement of the numerical predictions with the experimental data lies within an acceptable range.
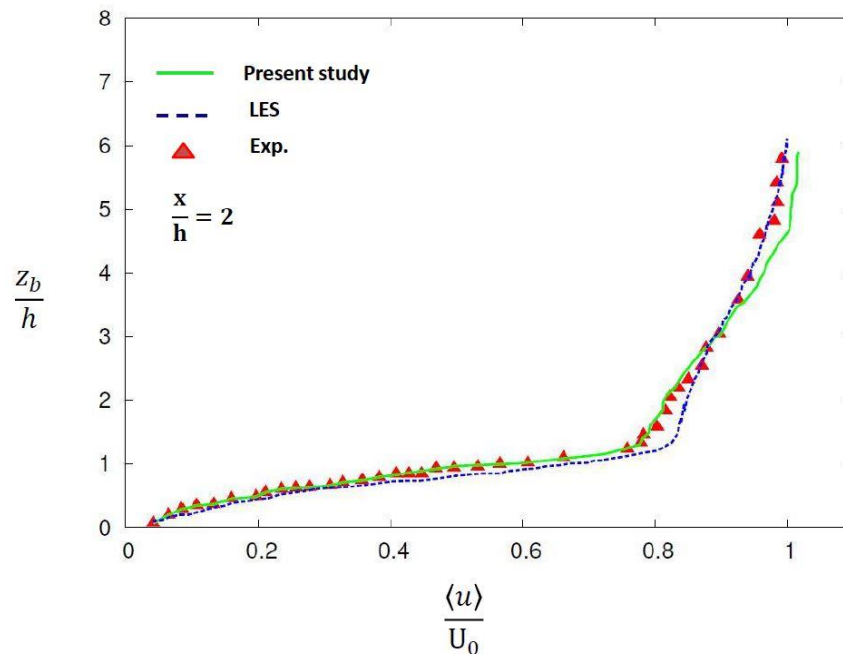
Figure 4-31: Mean velocity profile at $\frac{x}{h} = 2$
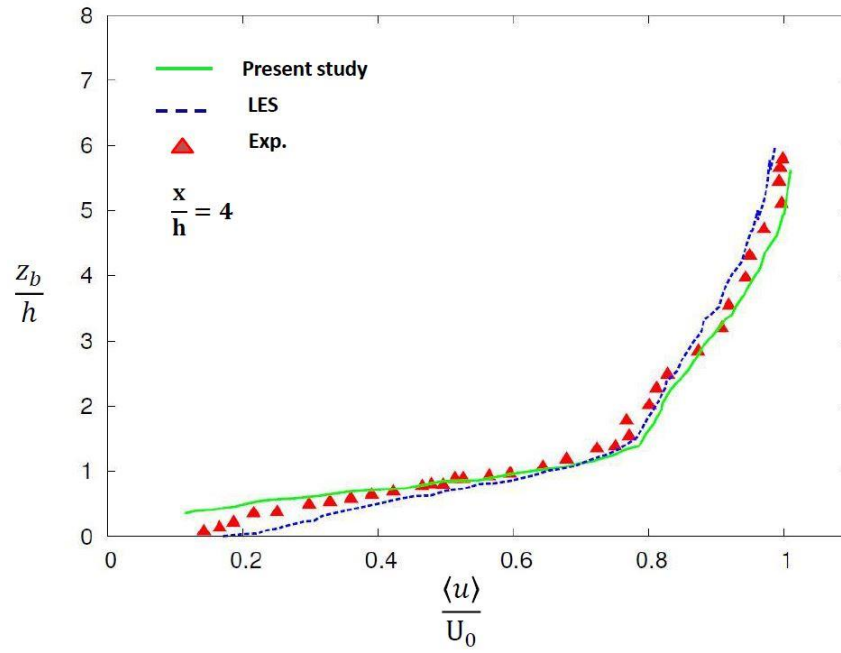
Figure 4-32: Mean velocity profile $\frac{x}{h} = 4$
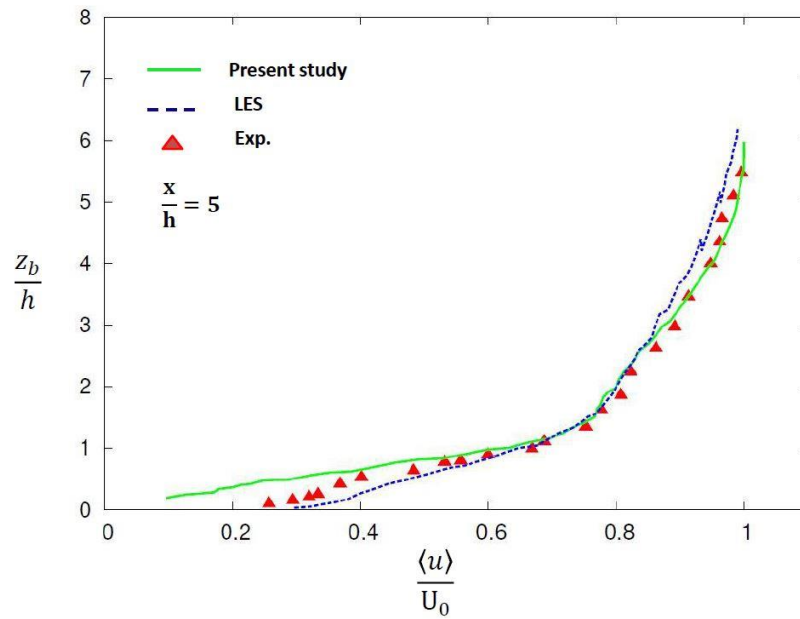
Figure 4-33: Mean velocity profile at $\frac{x}{h} = 5$
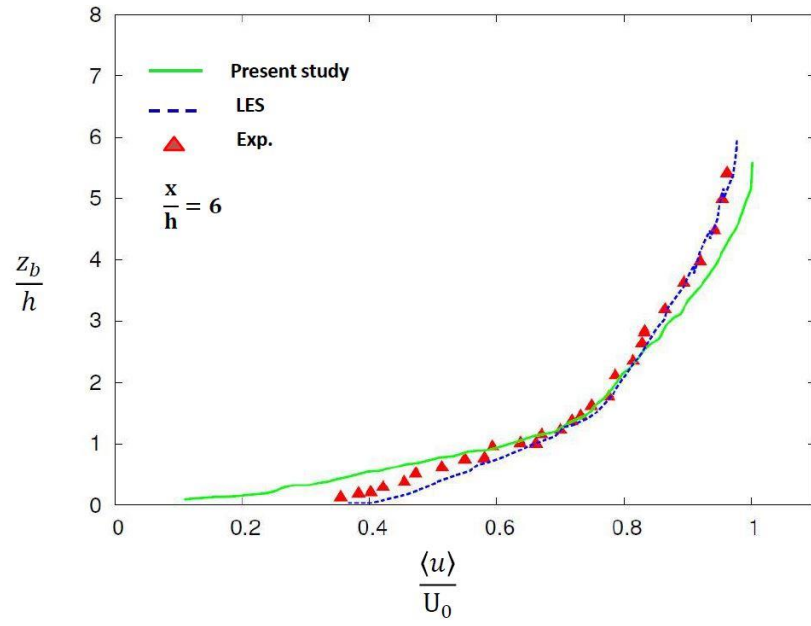
Figure 4-34: Mean velocity profile at $\frac{x}{h} = 6$
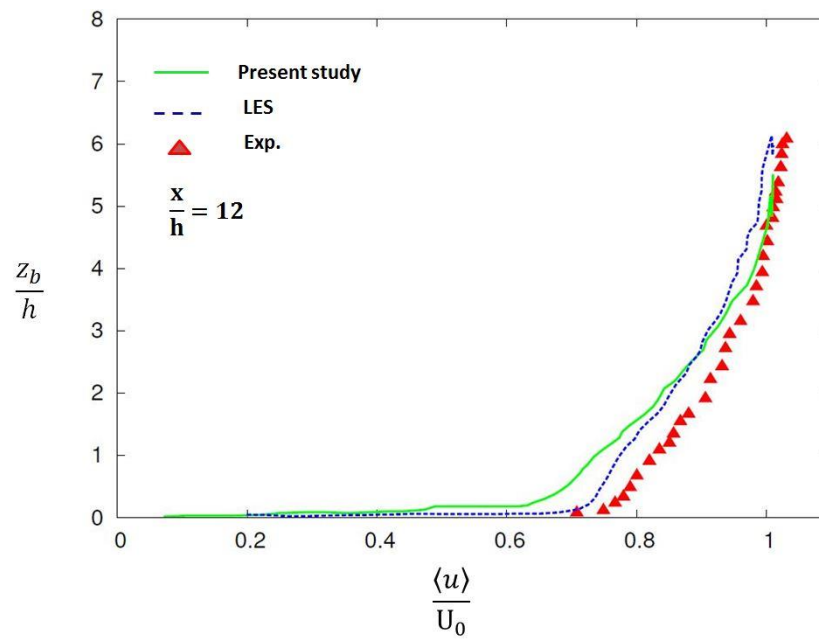
Figure 4-35: Mean velocity profile $\frac{x}{h} = 12$
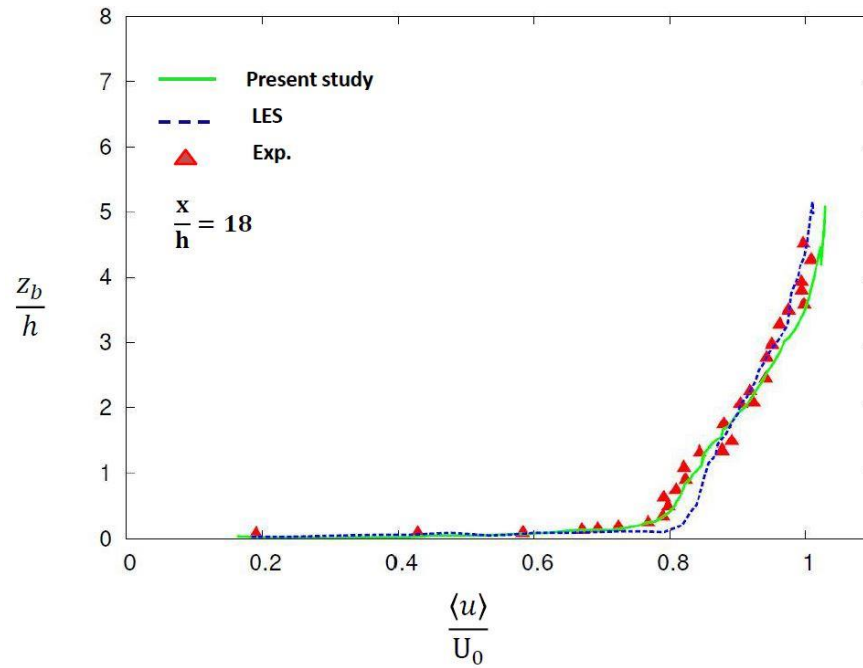
Figure 4-36: Mean velocity profile at $\frac{x}{h} = 18$

Figure 4-37 to Figure 4-39 show superimposed profiles of the three turbulence fluctuations, $\frac{\langle \acute{u} \rangle}{U_0}$, $\frac{\langle \acute{v} \rangle}{U_0}$ and $\frac{\langle \acute{w} \rangle}{U_0}$ in the common vertical coordinate z at the six stream-wise stations. The upper graphs are the predictions of the current study and the lower ones are from LES data conducted by Yue, Lin and Patel (2006). Very similar results are predicted by present study compare with the available LES.
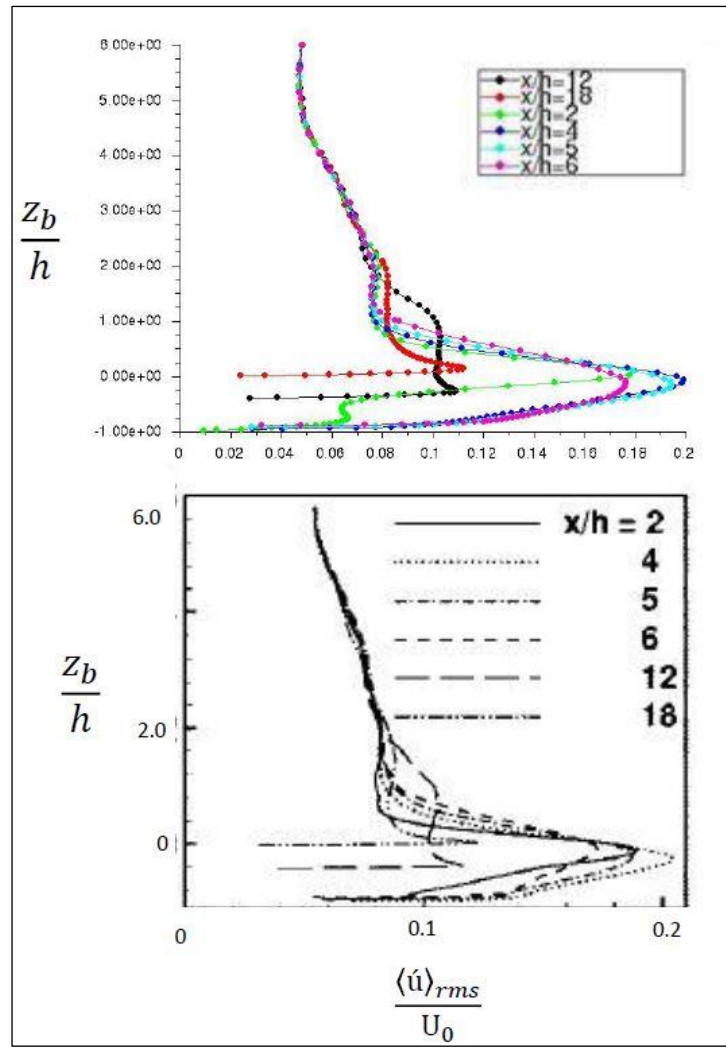
Figure 4-37: Fluctuations in the stream-wise direction
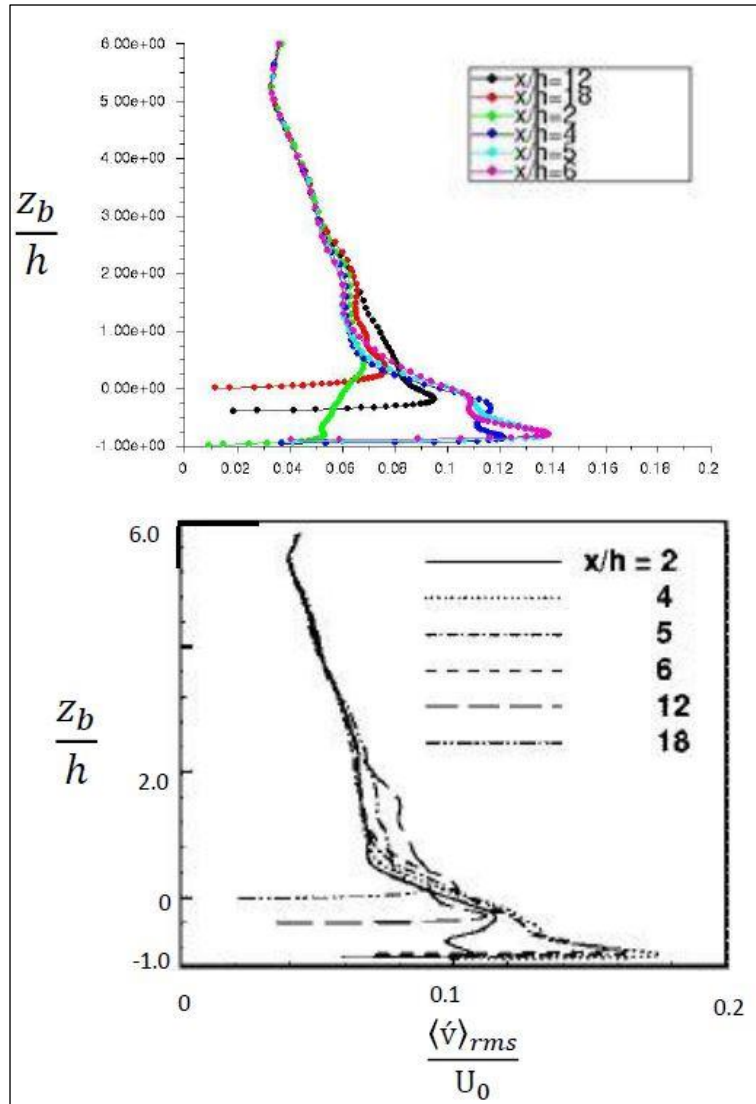
Figure 4-38: Fluctuations in the wall-normal direction
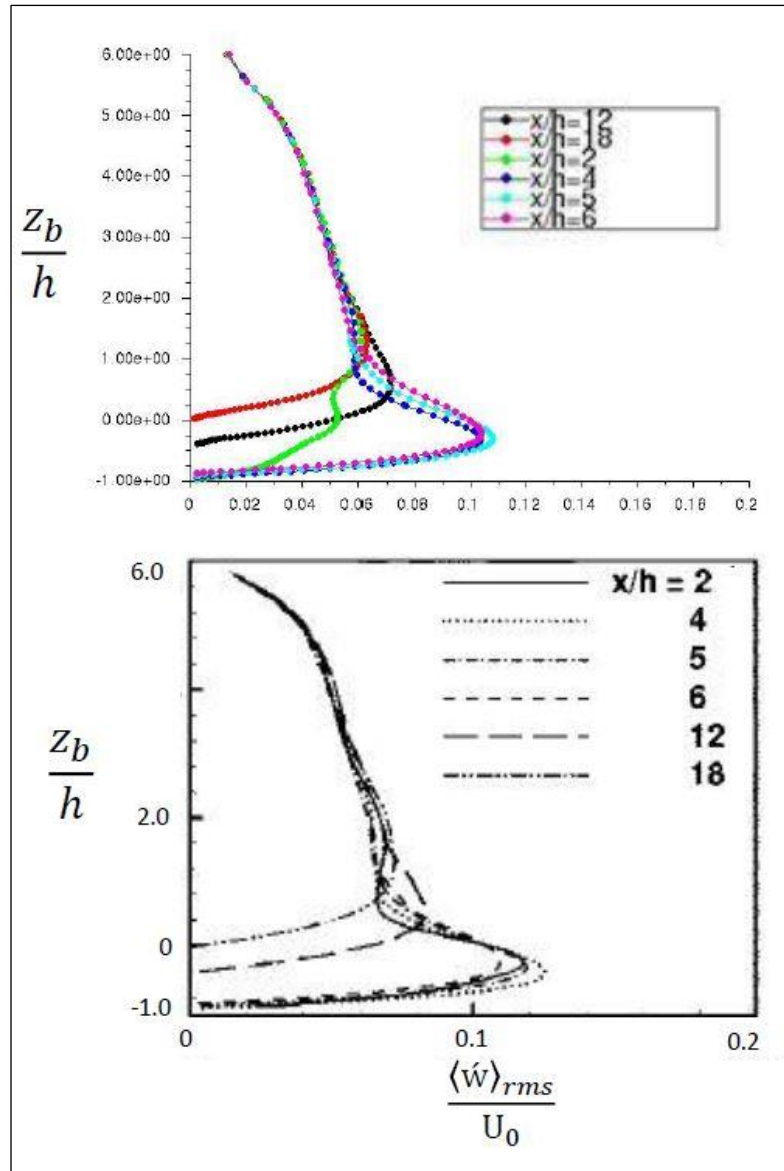
Figure 4-39: Fluctuation in the span-wise direction

CFD tool, i.e. ANSYS Fluent, used for this part of simulation has successfully functioned for both turbulent mean values, e.g. mean velocities and turbulent statistics, e.g. stream-wise, wall-normal and span-wise velocity fluctuations .

4.3 **DEM results**

This section is furnished by Discrete Element Method (DEM) simulation in dune-form case study, to account for particle-particle interaction as well as

providing input file for the next series of numerical modelling which is to couple DEM and CFD using CFD-DEM coupling code.

4.3.1 Dune-form

Output result from simulation of particulate phase without presence of fluid flow in dune-form case has been used as an input file for the coupling code of CFD-DEM used in section 4.1.3 of this chapter. This section includes problem set up and numerical results sub-sections.

4.3.1.1 Problem setup

A geometrical model has been constructed in gmsh open source as a stl file. LIGGGHTS open source code has been used to simulate particle flow based on DEM. Fixed boundary conditions are imposed on the wall-normal direction while periodic boundary conditions are set in stream-wise and span-wise directions. Particle properties shown in Table 4-1. Particles are injected with velocity $1.0\frac{m}{s}$ in the stream-wise direction. Time step is set to 10^{-5}.

Young Modulus	$5 \times 10^6\ Pa$
Poisson Ratio	0.45
Coefficient of restitution	0.3
Coefficient of friction	0.5
Density	$2000\frac{kg}{m^3}$
Radius	$0.0005m$

Table 4-1: Particle properties

4.3.1.2 Numerical results

Positions of particle at different times depicted in Figure 4-40 to Figure 4-44. Particle are released from a plane close to inlet with the velocity of $1.0\frac{m}{s}$, and normal to the plane. Simulated inter-particle collision and also with bed is shown from Figure 4-41 to Figure 4-43 and due to gravity force they fall and

are dispersed on the bed surface. An input file is then exported to the CFD-DEM code for coupling with the fluid phase once these sand-type represented particles eventually distributed on bed.
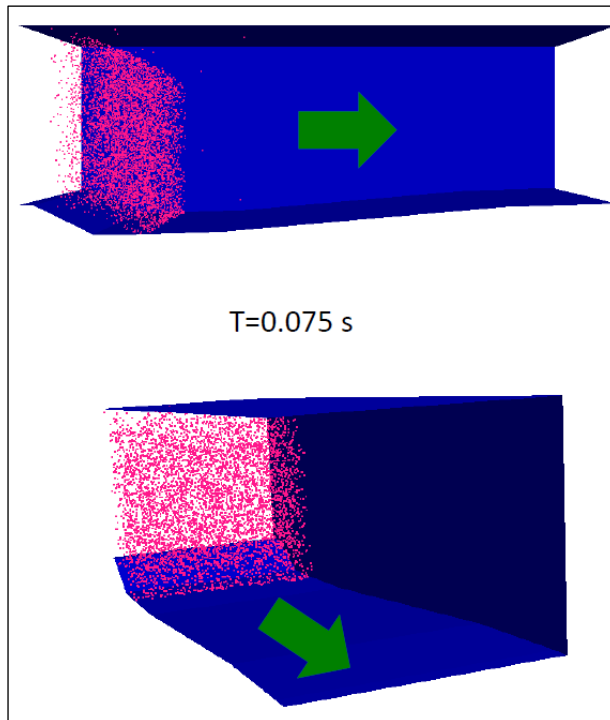
Figure 4-40: Position of particles in dune at t = 0.075 s
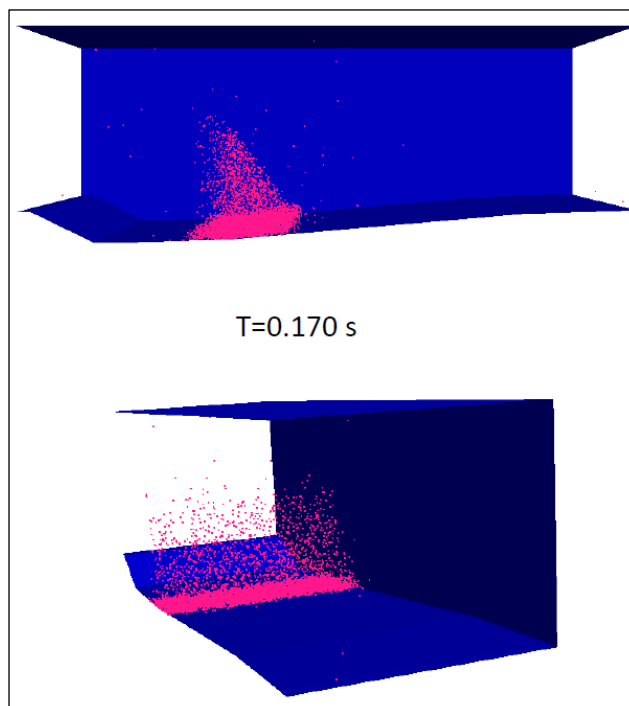
Figure 4-41: Position of particles in dune at t = 0.1705 s
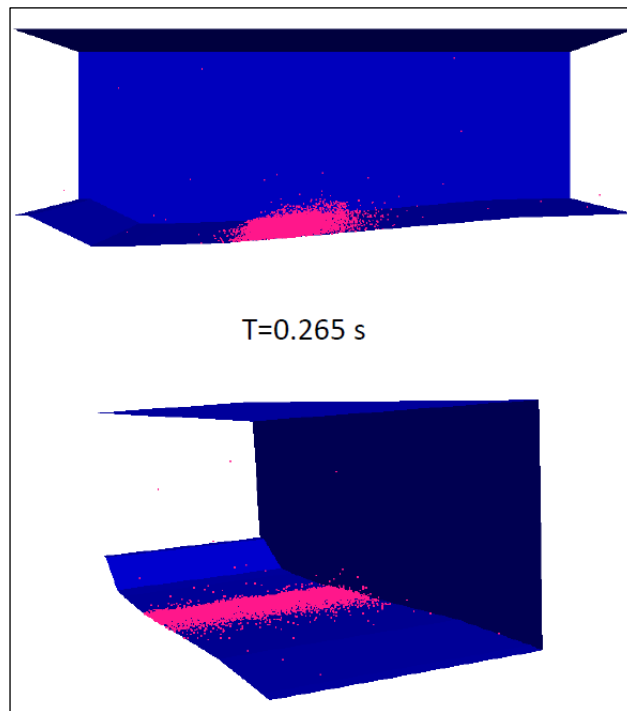
Figure 4-42: Position of particles in dune at t = 0.265 s
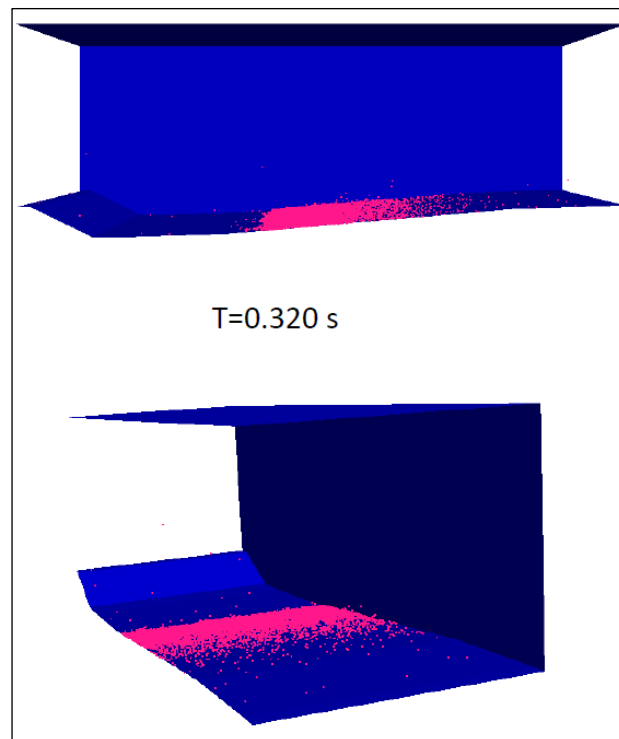
Figure 4-43: Position of particles in dune at t = 0.320 s
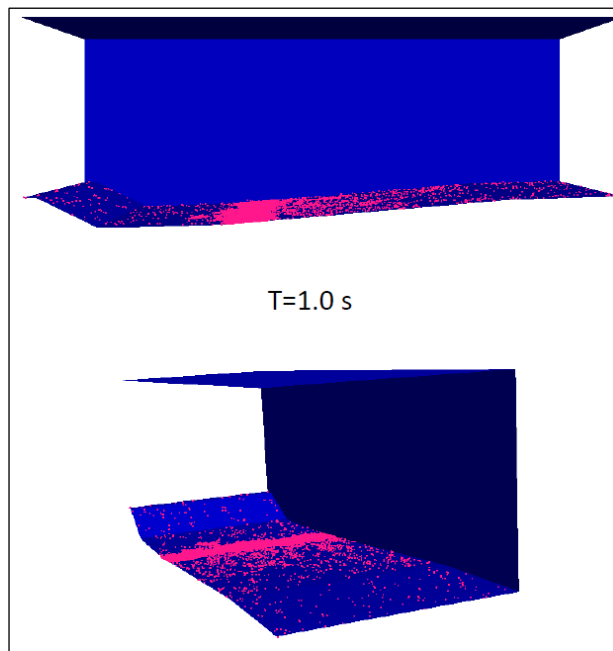
T=1.0 s

Figure 4-44: Position of particles in dune at t = 1.0 s

4.4 CFD-DEM results

To simulate fluid particle flow, OpenFOAM has been coupled with LIGGGHTS. In the section below the four-way coupling results have been presented from two perspectives. Initially the effect of fluid on the particles and subsequently the influence of the particles on the flow field have been shown. In both viewpoints role of inter-particle collision has also been taken into account for detailed modelling of sediment transport problem.

4.4.1 Dune-form

4.4.1.1 Problem setup

In order to carry out the coupling between fluid and particle, first the turbulent flow has been generated in the dune-form geometry. The geometry, boundary condition and the flow Reynolds number set up are based on the case used in section 4.1.1.3.1 of this chapter. For studying bed-load, distributed particles on bed depicted in Figure 4-45 is considered as an input for the coupling process. Properties of particles have been set up as Table 4-1 and particles were injected from the inlet to the flume. Interval

coupling is set to 1 which means every time step CFD solver couples with DEM solver to exchange the data between particle and fluid phases. Time step for CFD and DEM solvers are set to 10^{-5} seconds. Since the void fraction (Figure 1-3) in this case study has been obtained to be defined as a dense phase, based on (Figure 4-46), the dense model in the DEM solver has been selected in place of dilute model.
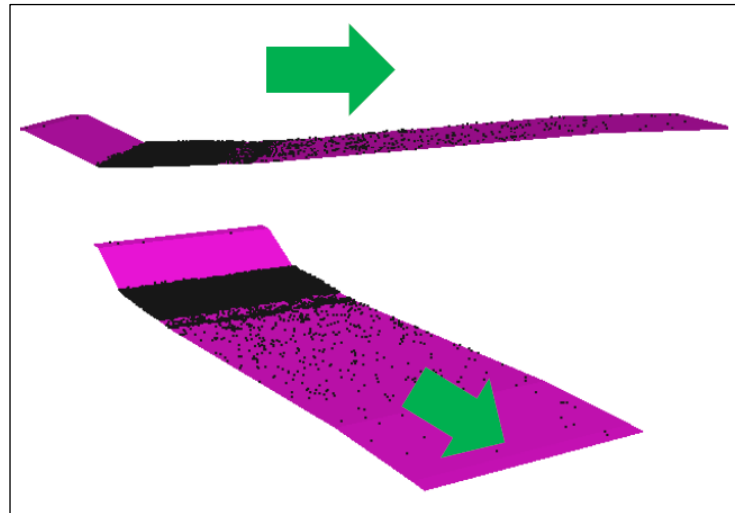
Figure 4-45: Initial position of particles on bed
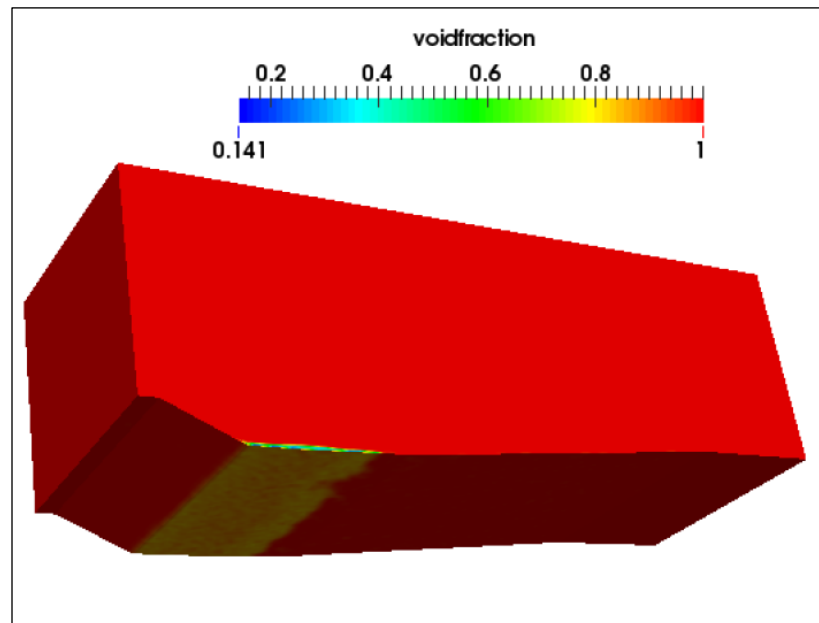
Figure 4-46: Void-fraction contour shows dense presence of particle near the bed

4.4.1.2 Numerical results

Once coupling process initiated, two set of results i.e. fluid-particle and particle-fluid interaction while taking into account of inter-particle collision, have been reported to reveal four-way coupling nature. The former set of results have informed the effect of fluid flow on the particles present in the flume and the latter has been indicating the particles' influence on the fluid current. Just after $t = 0.345$ seconds, the first significant effects of momentum exchange between the fluid and particulate phase have been observed.
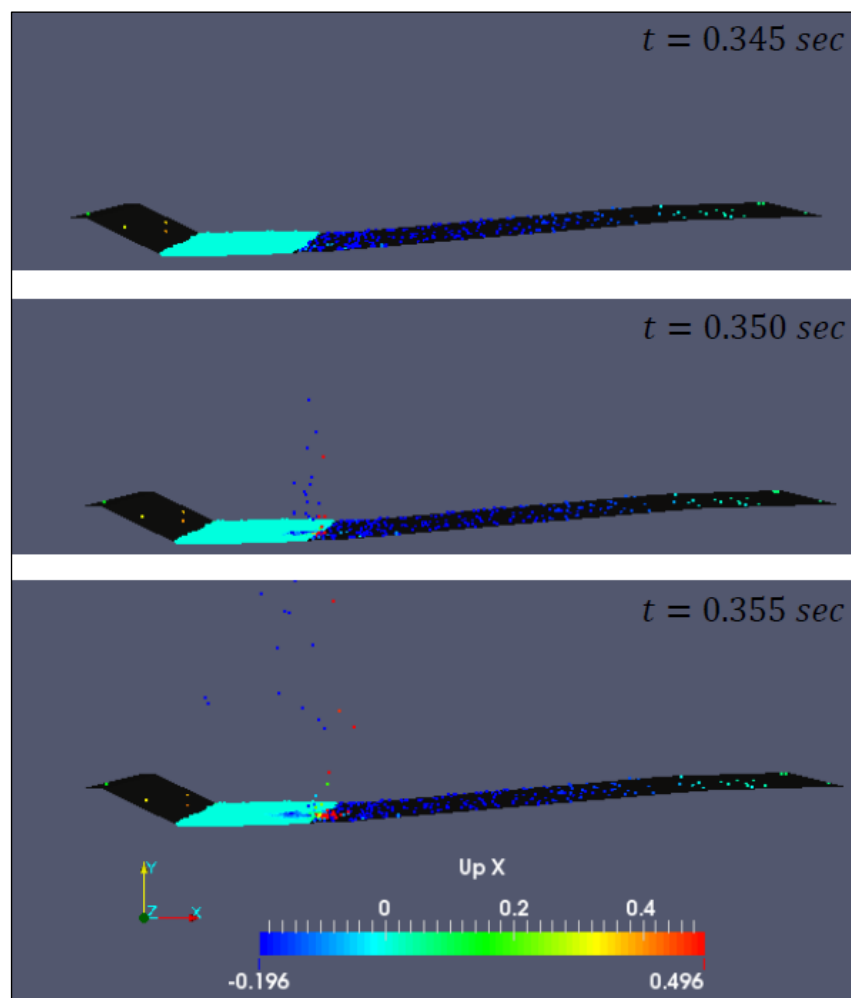
Figure 4-47: Particle position snapshot coloured by stream-wise velocity of particles at 0.345, 0.350 and 0.355 seconds

Figures 4-47 to 4-50 are showing the particle locations at different time intervals close to bed after all forces mentioned earlier including the particle-particle contacts forces have been considered at the coupling stage.
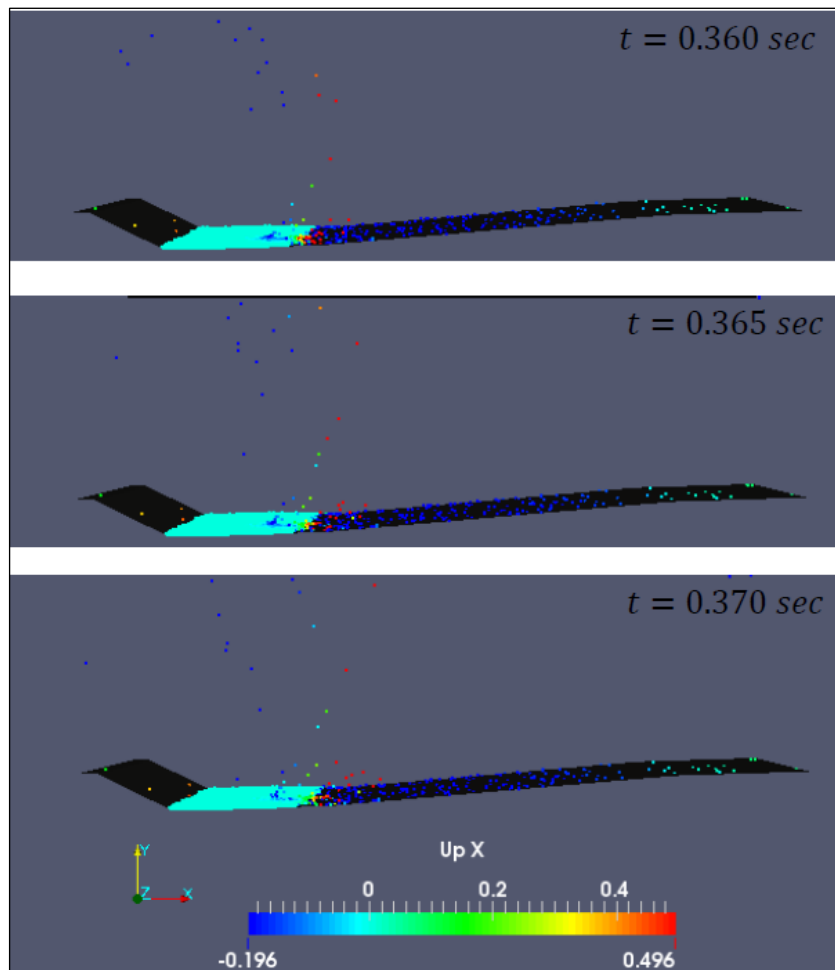
Figure 4-48: Particle position snapshot coloured by stream-wise velocity of particles at 0.360, 0.365 and 0.370 seconds

The red coloured picked up particles with the positive velocities have behaved like projectiles. After each particle reached its summit, they start to descend towards the bed due to exerted gravitational force.
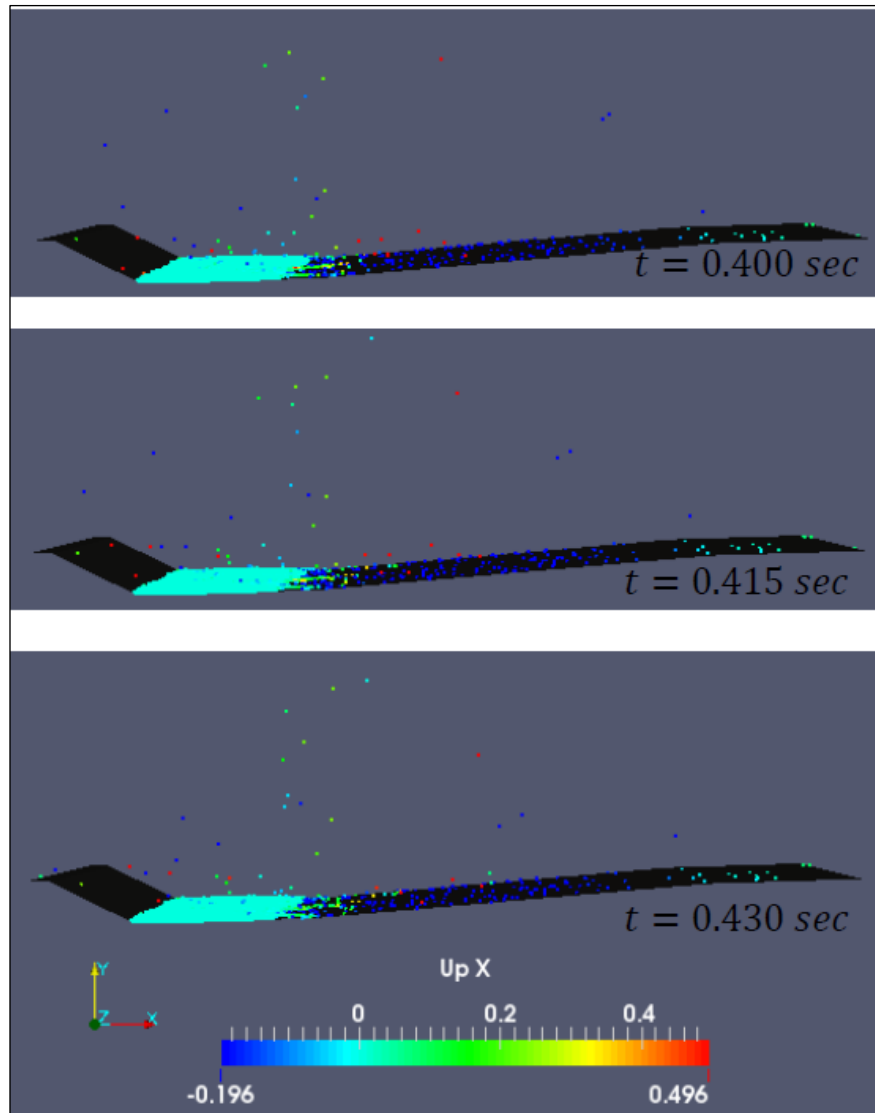
Figure 4-49: Particle position snapshot coloured by stream-wise velocity of particles at 0.400, 0.415 and 0.430 seconds
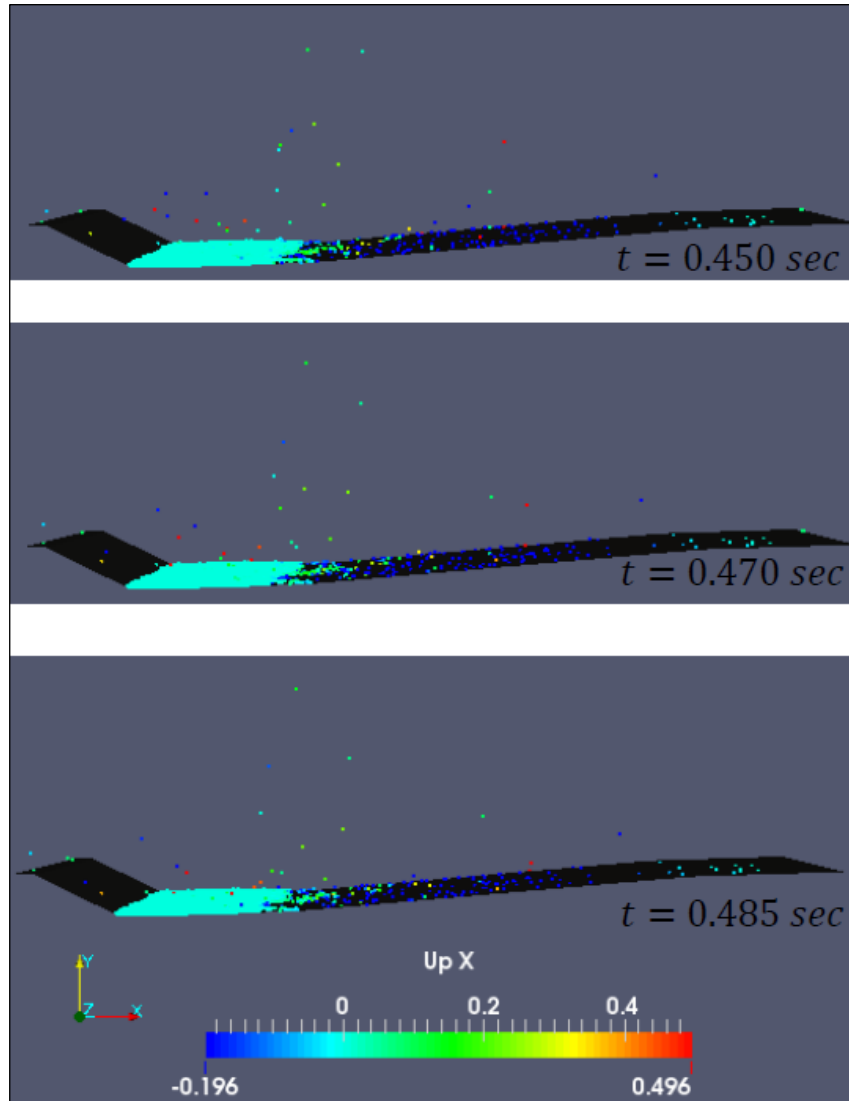
Figure 4-50: Particle position snapshot coloured by stream-wise velocity of particles at 0.450, 0.470 and 0.485 seconds
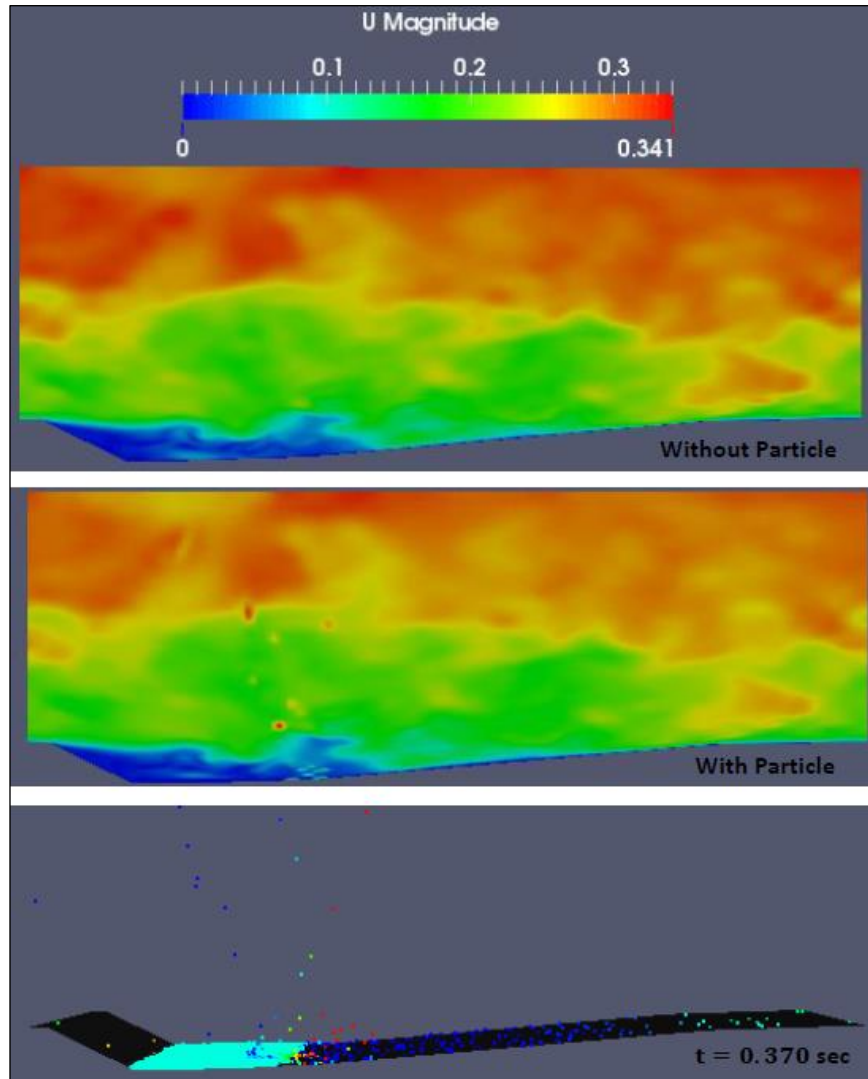
Figure 4-51: Comparison of velocity contours in fluid with and without particles: Upper figure shows velocity contour of flow without particle while the middle figure shows particle-laden velocity contours. The lower figure shows particle position coloured by particle velocities corresponding with the middle figure

Presence of local flow turbulence structures that are termed as coherent flow structures are shown in Figure 4-52 . High fluid velocity is presented with the red colour arrows which is result of the effect of particles interaction with fluid and also adjacent inter-particle collisions.
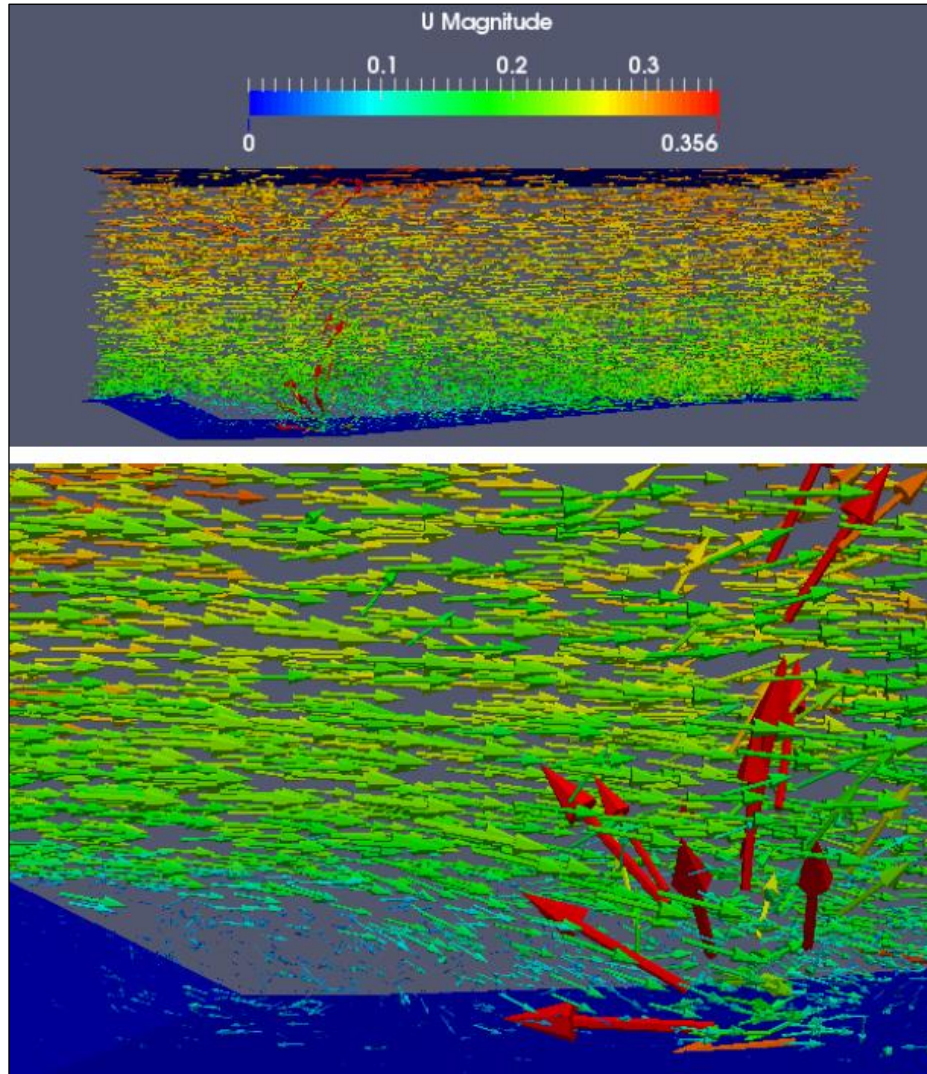
Figure 4-52: Velocity vector field of fluid influenced by particles in a particle-laden flow

As a matter of presentation all of the domain arrows have been scaled up by the same amount so the "sensitively changed features" could be shown noticeably and discussed in Chapter 5 straightforwardly. Figure 4-53 shows vector field of eddy structure in fluid flow and particle-laden flow at the similar time.
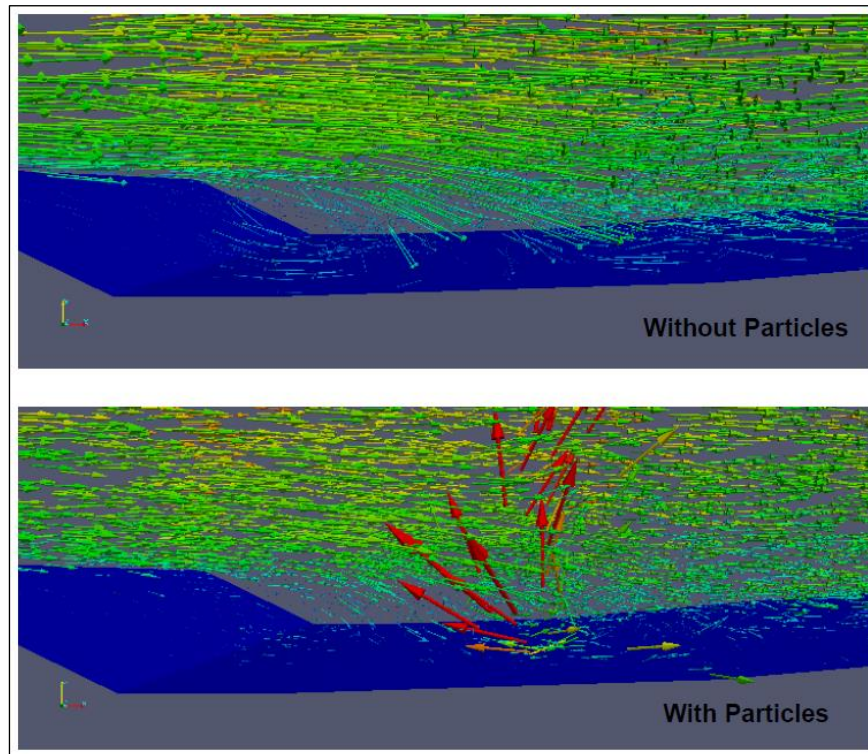
Figure 4-53: Vector field of eddy structure in fluid flow and particle-laden flow

Results obtained have been divided into pre-stationary and stationary states and all figures all included with their discussions in Chapter 5 of this thesis where fluid flow had not reach its fully fluid stationary state at the CFD-DEM coupling occurrence, 6000 particles in the flow were injected. The results contain stream-wise mean velocity and fluctuations on a line of interest and compared in particle-laden flow as opposed to fluid flow.

At the point of stationary state 16000 particles were introduced into the flow to be used at the CFD-DEM coupling stage. Again all results and discussion have been included in Chapter 5.

All mean values have been normalized by the bulk velocity, $U = 0.356\ m/s$ of the solution domain. The vertical distance from the bed, y, is normalized by the dune height, $h = 20\ mm$.

4.5 **Conclusion**

To study fluid particle interaction in sediment transport problems, LES turbulent modelling have been utilised to capture small and large turbulence scales in the particle-laden flow where particles experience high intensity of velocity fluctuations close to bed. Considering that inter-particle collision is inevitable, four-way coupling approach has been utilised with the DEM numerical modelling where effect of fluid on the particles and subsequently the influence of the particles on the flow field have been the focus of this investigation. CFD-DEM open source code has been used to couple the fluid phase with the particulate phase. Using this has given an insight into momentum exchange between both phases at bed-load region. Significant turbulence intensity has been resulted at the locations of particles and subsequently flow velocity fluctuations have experienced disturbance greatly.

Chapter 5 Discussions

In this chapter CFD-DEM findings as the focus of this study from aspects of four-way coupling i.e. the effects of fluid on the particles, particle-particle interactions, and also the influence of particles on the flow field have been discussed in the sections below.

5.1 Fluid-Particle (F-P) & Particle-Particle (P-P) effects

From the qualitative analysis aspect, the effects of fluid on particles and also particle-particle interactions can clearly be understood and witnessed from the figures provided in chapter 4.

It is evident in Figure 4-47 that at $t = 0.350$ seconds due to presence of eddies and vortices close to bed (see Figure 4-53), particle movements have been picked up from bed. Particles are picked up by positive and negative velocities coloured by red and dark blue respectively by adjacent vortices at $t = 0.355$ seconds.

The negative velocities of dark blue coloured particles that picked up from bed, are decreased to zero by the dominant flow field velocity shown in Figure 4-48 . Furthermore these particles start to change direction and move with the positive velocity in the stream-wise direction. Their journey may or may not end when they approach to bed due to dominancy of self-weight or turbulence effects. As these particles are not as speedy as the red coloured particles, therefore it is unlikely that the lifting up process happens again. Consequently the deposition process occurs where majority of particles decelerate to a zero velocity shown in Figure 4-50.

Path of particles that are approaching towards bed and yet again to be bounced off from bed have been witnessed at $t = 0.400$ sec and 0.415 seconds respectively from Figure 4-49. Projectile behaviours due to exerted gravitational force is also seen. Consequently particle-particle interaction is unlikely to occur at the region where dispersed particles are not close to bed but rather near the flume surface. It is worth mentioning that using LES turbulence modelling has surely played a positive role in capturing such detailed features, while if RANS modelling was used this accuracy and comprehensive forceful results could not be gathered.

Moreover using heavy duty DEM modelling has also taken the whole process to the next level of precision.

Figure 4-49 and Figure 4-50 show that there are few red coloured particles on the steep of the dune. Periodic boundary condition set up for the simulation has triggered the particles to be injected from the inlet with the same velocity as they leave the outlet. The fluid velocity then increases the velocity increase of particles and cause their jump from the stoss. They finally deposited at the lee dune where the zero velocity has been coloured as sky blue.

Effect of particles on the fluid phase has been observed from Figure 4-51 just after the deposited particles on bed start to be picked up by the fluid. This interpretation is from the upper and middle snapshots of the aforementioned figure where velocity contours have changed colours significantly at $t = 0.370$ seconds when sediments experience interaction with fluid phase. It should be noted that Inter-particle collision in this process also plays a role in such detailed continuous interaction. This is clearly understood from Figure 4-53 as the turbulence intensity has been increased on the vicinity area of particles' location.

5.2 Particle-Fluid (P-F) effects

From the qualitative analysis aspect, the effects of fluid on particles and also particle-particle interactions can clearly be understood and witnessed from the figures provided in chapter 4.

5.2.1 Qualitative analysis

Figure 4-52 shows the coherent flow structures generated locally. These turbulent structures are located in the separation region very close to dune-bed and are coloured as turquoise. This corresponds with Figure 1-12 in which the principal regions of flow over asymmetrical dunes has been portrayed by Best (2005a) in a schematic diagram. The red colour arrows correspond with high fluid velocity which is result of the effect of particles interaction with fluid and also adjacent inter-particle collisions.

It is perceived that more vortices are also generated due to particle movements, interactions with fluid, and thus turbulence intensity increase on these regions. Upper picture of Figure 4-53 shows the velocity vector maps of fluid in the separation zone where coherent turbulent structures are present. In the near-wall region, eddies' strength are very low and so the turquoise colour shown as smaller arrows. However the below picture of the same figure presents high velocity vectors of fluid when particles are lifted in the flow. It is apparent that these newly high turbulent features shown in the forms of velocity vectors are created due to the momentum exchange that particles experience with time-dependant motions e.g. turbulent scales.

5.2.2 Quantitative analysis

5.2.2.1 Pre-stationary state

Line of interest in Figure 5-1 has been used to compare the stream-wise mean velocity and fluctuations in the particle-laden flow as opposed to the fluid flow without particle. Pre-stationary results, where fluid flow does not reach its fully fluid stationary state at the CFD-DEM coupling occurrence, have been obtained with injecting 6000 particles in the flow.
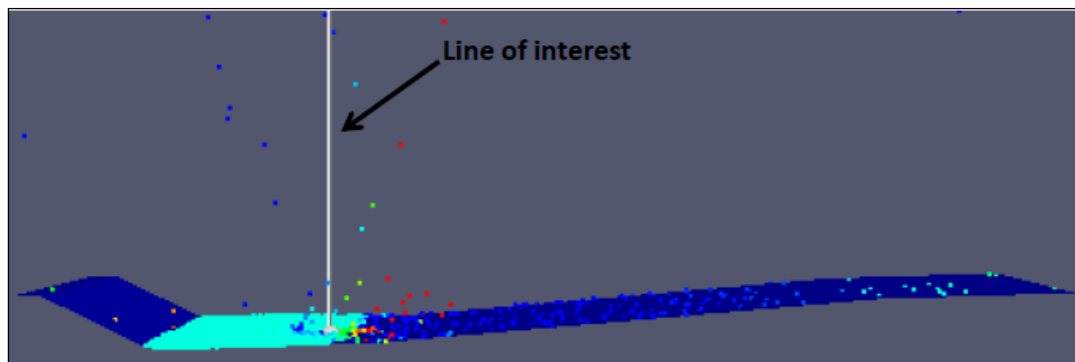
Figure 5-1: Line of interest for the measured turbulent statistics at location X = 0.075

Figure 5-2: Stream-wise mean velocity in fluid flow and particle-laden flow
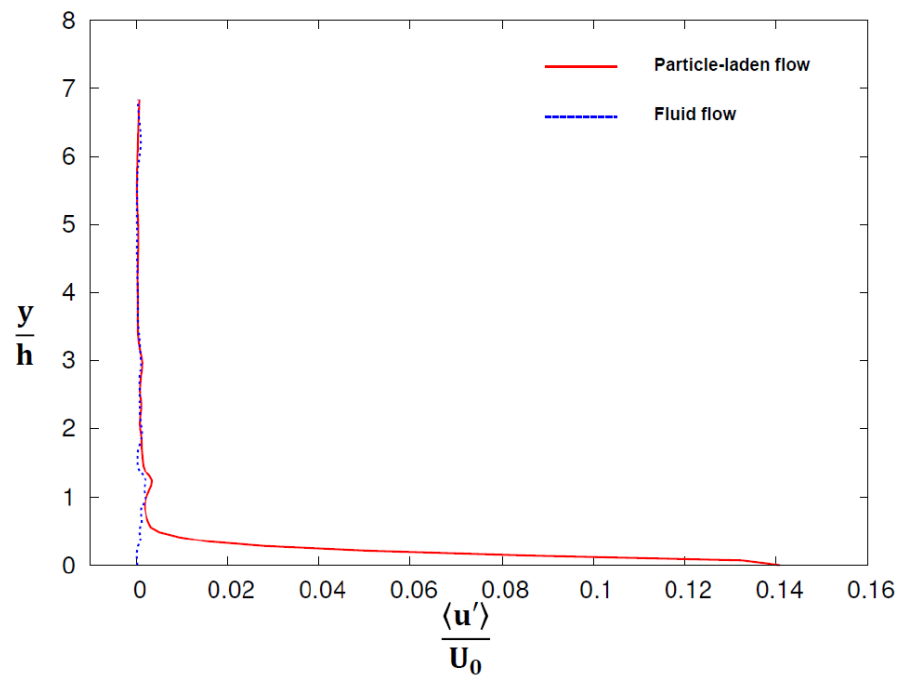
Figure 5-3: Stream-wise velocity fluctuations in fluid flow and particle-laden flow

As shown in Figure 5-2, in the flow with particles, reverse flow has been formed close to bed. This indicates that coherent flow structures i.e. eddies are generated as a result of particles interactions in that specific location.

Nonetheless slight difference between stream-wise mean velocity in the fluid flow and the particle-laden flow are experienced far from the wall-region, but significant change in the velocity profiles are captured in the close to bed region. Moreover stream-wise velocity fluctuations depicted in Figure 5-3 for both flows with and without particles reveals a dramatic increase of velocity fluctuations in the particle-laden flow in comparison with the fluid only flow, particularly near the bed. Intense effect of particles-fluid interaction, hence the momentum exchange between both fluid and particulate phases, is evident from these findings.

5.2.2.2 Stationary state

Lines of interest at four different locations shown on Figure 5-4 has been used to compare the stream-wise mean velocity and fluctuations in the particle-laden flow as opposed to the fluid flow without particle. These locations have been chosen to study close to bed particle-fluid behaviour because at X = 0.05, X = 0.07 and X = 0.1 particles are present. Moreover X = 0.02 is also chosen as particles' upstream line of interest. These results, where fluid flow reaches its fully fluid stationary state at the CFD-DEM coupling occurrence, have been obtained with injecting 16000 particles in the flow.
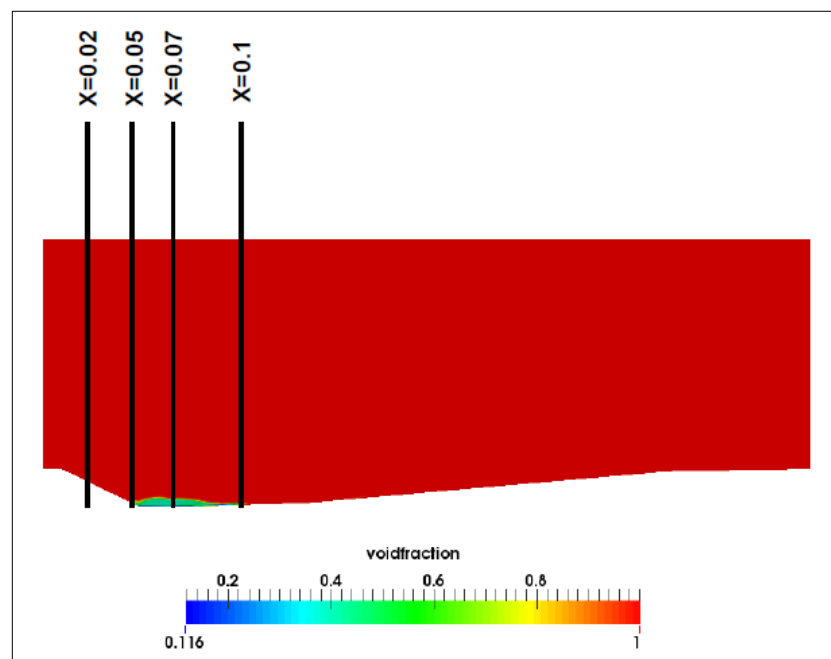
Figure 5-4: Lines of interest for the measured turbulent statistics, where void fraction = 1 indicates fluid only region

The following findings have been obtained at the time where the fluid flow statistics i.e. CFD results have been reached to their stationary state but the CFD-DEM results have not reached to the stationary state. The ideal option would have been to consider the fully stationary state for the coupling phase.

At X = 0.02 where void-fraction = 1 i.e. there are no particles presence in the region; near to wall stream-wise mean velocity graphs shown in Figure 5-5 are analogous. Nonetheless their similarity starts to fade as moving away from the bed. Knowing that particles are present at the downstream of such location, their affects are seen globally on the flow field. This on the other hand can be justified by the stationary state of the coupling phase.
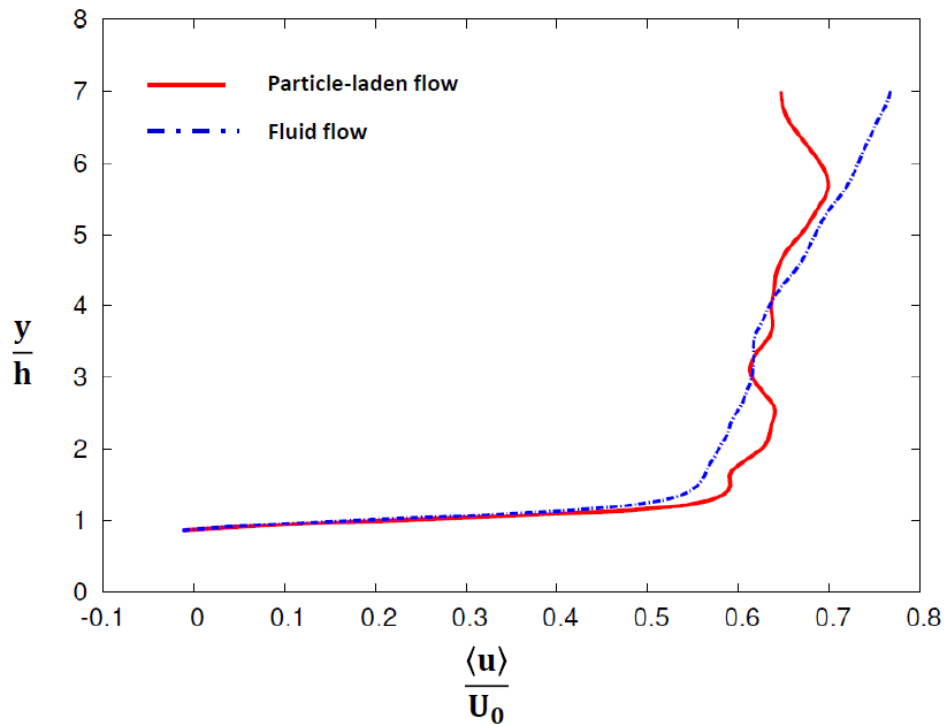
Figure 5-5: Stream-wise mean velocity in fluid flow and particle-laden flow x = 0.02

It can be seen that in Figures 5-6 and Figure 5-7 sediments are present. Studying the near-wall region at X = 0.05 and 0.07, where void fraction is almost 0.6 i.e. 60% water presence in between the solid surfaces, such permeable particles could slide on top of each other. Therefore separation features with higher negative velocities have been captured at bed-load. Another cause of such negative velocities can be due to vortex presence close to bed.
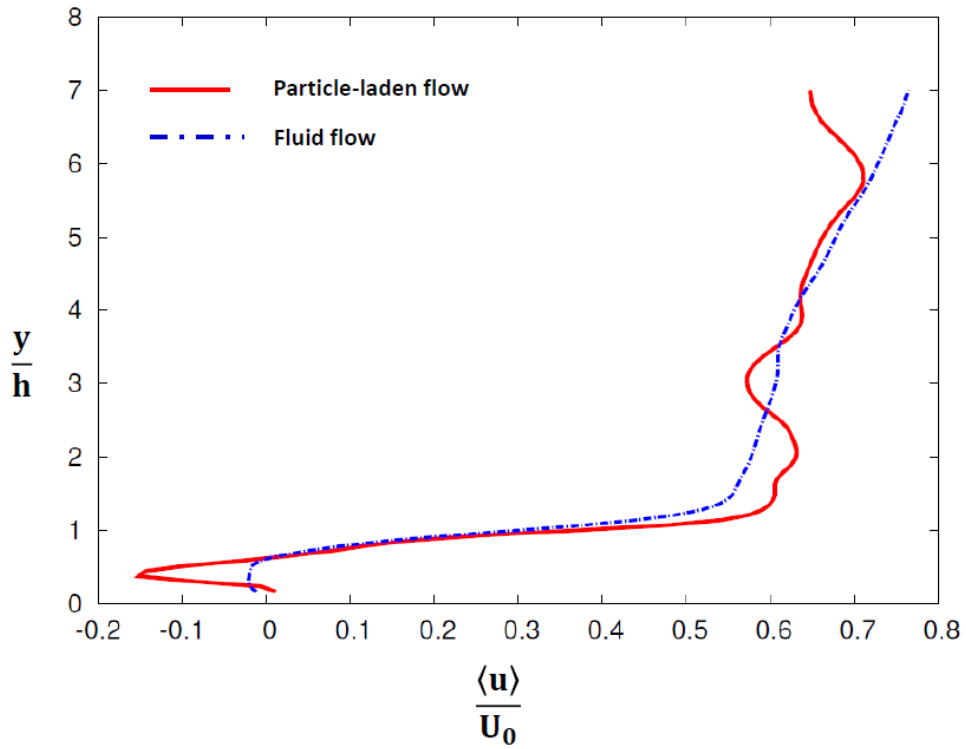
Figure 5-6: Stream-wise mean velocity in fluid flow and particle-laden flow x = 0.05
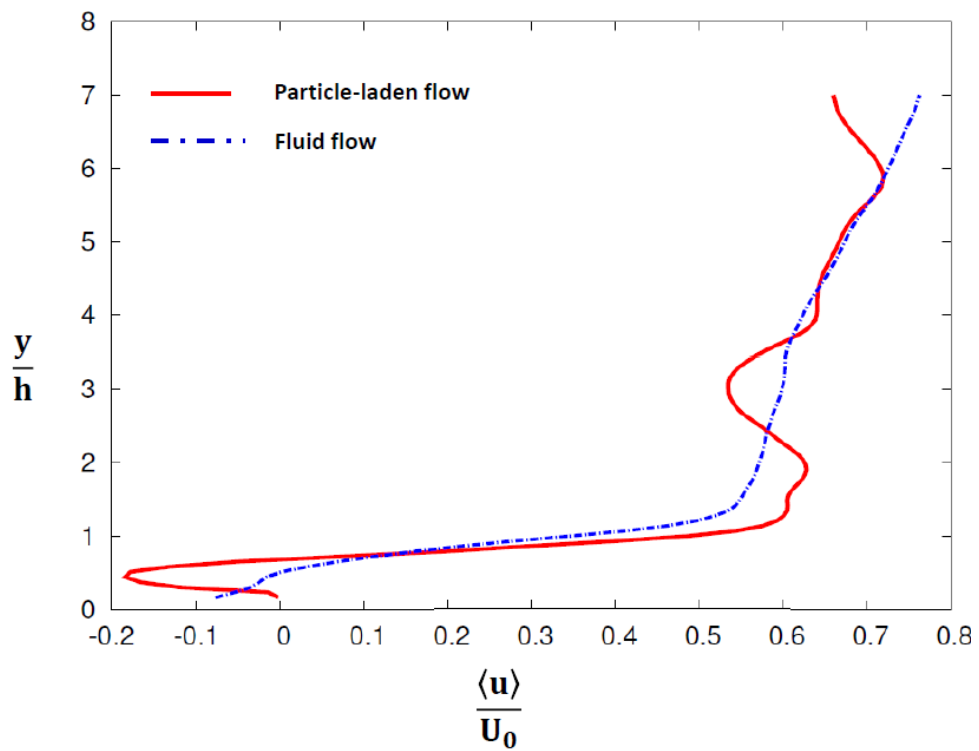
Figure 5-7: Stream-wise mean velocity in fluid flow and particle-laden flow x = 0.07

While near wall stream-wise mean velocities of particle-laden flow follows the fluid-only velocities trend at X = 0.1 in Figure 5-8, they are still under effect of upstream velocities and remained to be negative.
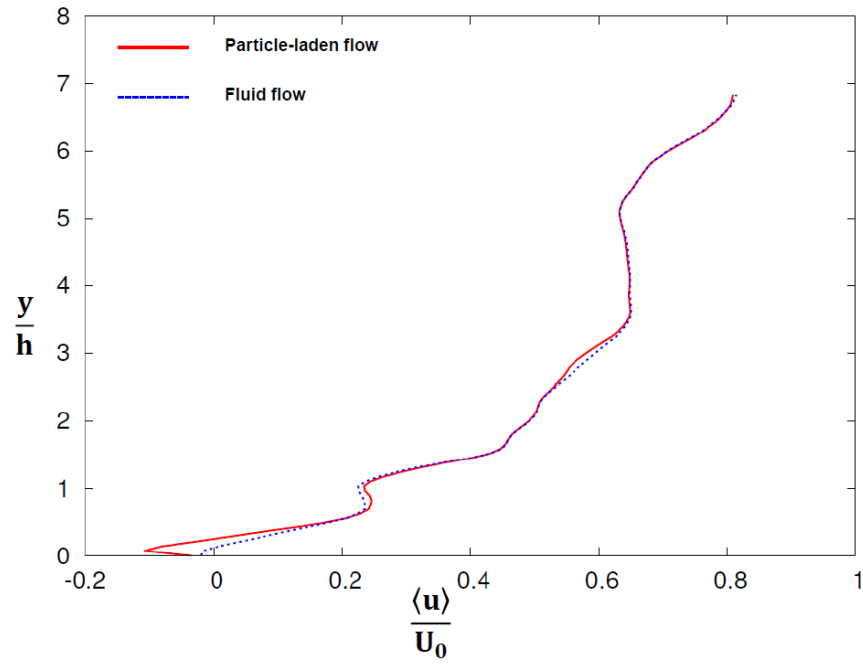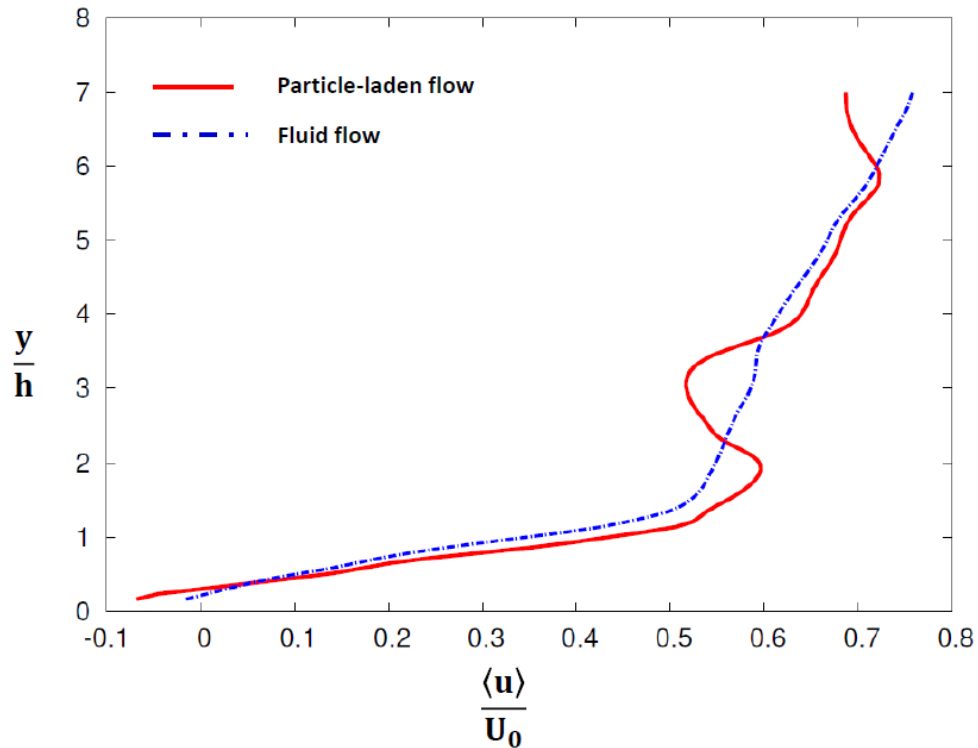

Figure 5-8: Stream-wise mean velocity in fluid flow and particle-laden flow at x = 0.1

Figures 5-9 to Figure 5-11, particle-laden flow's stream-wise fluctuations have been less than flow-only fluctuations. Although velocity graphs in both cases follow the same trend but the turbulence intensities have been decreased significantly in caparison with the pre-stationary results at the same location of X = 0.07. Although it is expected that the difference value between these graphs can be adjusted when the CFD-DEM results reaches its fully stationary state, but this expectation does not deny the convinced difference between the turbulence intensities for the cases of fluid flow with and without particles.
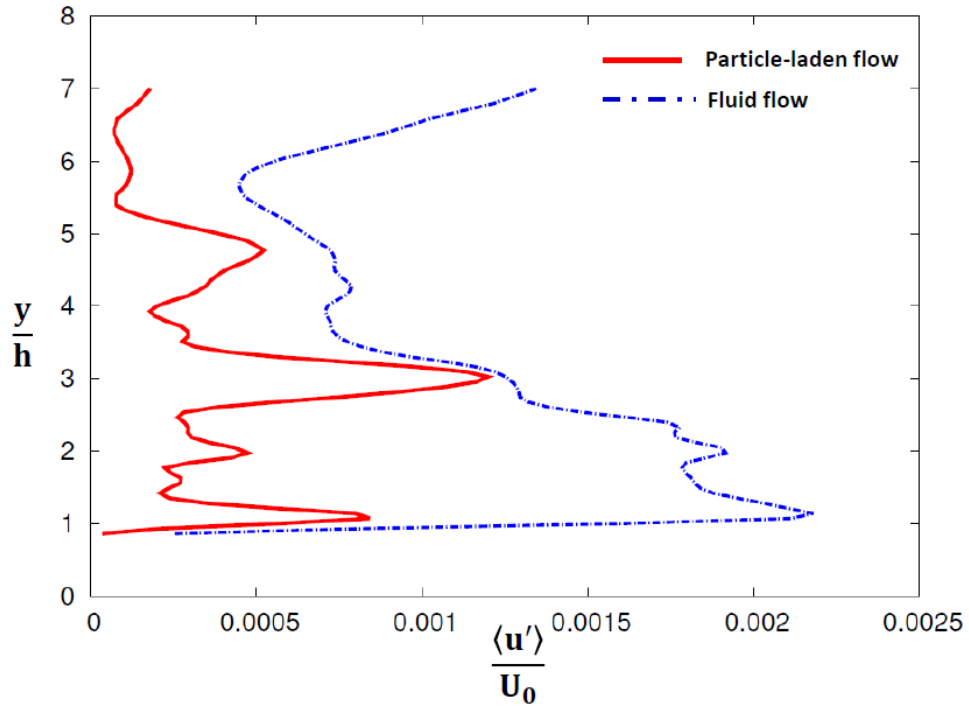
Figure 5-9: Stream-wise velocity fluctuations in fluid flow and particle-laden flow at
x = 0.02
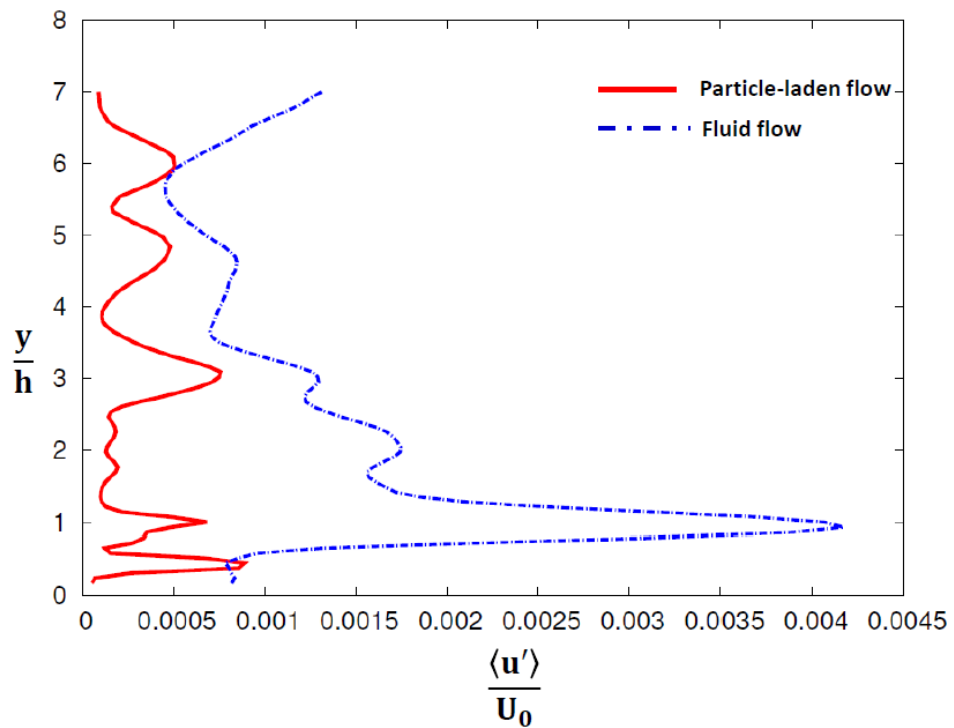
Figure 5-10: Stream-wise velocity fluctuations in fluid flow and particle-laden flow at
x = 0.05
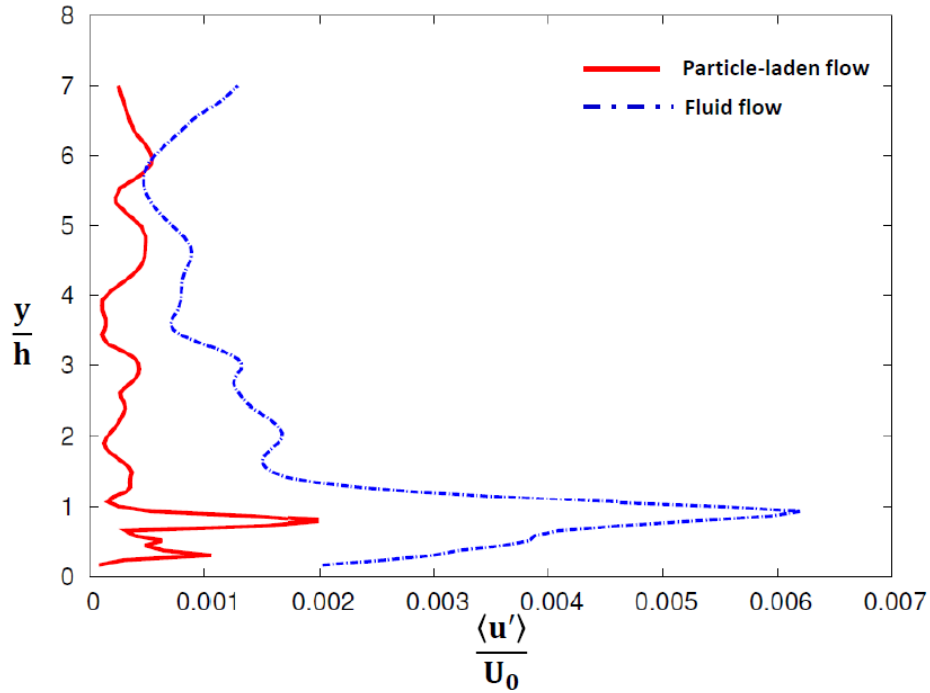
Figure 5-11: Stream-wise velocity fluctuations in fluid flow and particle-laden flow at x = 0.07

Near wall turbulence intensity starts to change in Figure 5-12. It increases in the particle-laden flow slightly and remains less than the fluid flow case as move away from bed.
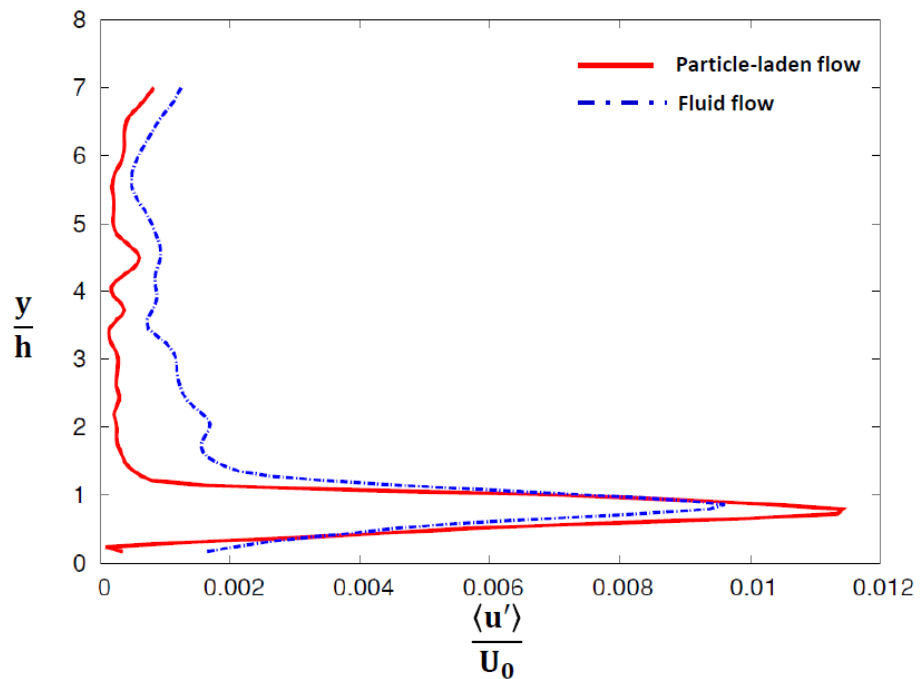
Figure 5-12: Stream-wise velocity fluctuations in fluid flow and particle-laden flow at x = 0.1

Likewise to the study done by Vreman *et al.* (2009) where Large-eddy simulations (LES) of a vertical turbulent channel flow laden with a very large number of solid particles were performed, the method incorporates four-way coupling, i.e. both the particle-fluid and particle-particle interactions are taken into account. Considering the nature of the aforementioned vertical flume with the focus of study on suspended-load, fairly different results on turbulence intensities variations have been achieved in the present research. Unlike the outcomes of the abovementioned work, where increase in stream-wise turbulence intensity of the gas phase and decrease in both normal and span-wise turbulence intensities compared to single-phase turbulent flow is testified; in the current study reduction of turbulence intensities in all three stream, wall normal and span-wise directions have been resulted. On the other hand in both studies similarly it is witnessed that considering collisions between particles is thus essential to be included in the numerical simulations of two-phase flow.

Four-way coupling in the numerical simulations with applications in sediment transport have not been the focus of many researches. The only numerical case study on channel flow has been carried out in 2013 by studying bed-load sediment transport by Furbish and Schmeeckle (2013) and furthermore suspended sediment transport calculations in 2014 by Schmeeckle (2014). Moreover in 2015 same strategy for conducting bed load study has been used by Schmeeckle (2015) with the change in geometrical model to backward facing instead of channel flow. The novelty of the present study can be highlighted by the fact that more realistic river-bed geometry of dune-form has been considered. The similarity in all of these works including the present research is that the coupled LES-DEM model is integrated through the bed of moving and stationary particles. Essentially it resolves for the permeable flow through the bed, driven by the flow. Figure 5-9 to Figure 5-11 clearly show that even though the turbulent velocity fluctuations are increased in the fluid flow, but these fluctuations in the particle-laden flow penetrate the bed and hence are almost completely damped within the particles that are formed the bed. This phenomenon has been observed in all the all above-mentioned recent studies. Additionally it is depicted in both Figures 5-6 and 5-7 that negative velocity near the bed has caused the

negative shear stress where the same outcome has been reported by Schmeeckle (2015).

5.3 **Conclusion**

At pre-stationary state findings show that presence of particles increases intensity of turbulence in comparison with the fluid flow only case. This can be due to the fact that the stationary state has not been reached yet, and so the presence of unsettled particles in the domain can cause some instability in the flow filed.

On the other hand at the stationary state of CFD results it is concluded that turbulence intensity decreases generally knowing that CFD-DEM results still have not reached the fully stationary state. The most important conclusion is at the near the wall region where particle presence and their movements cause in reduction of turbulence intensities, negative shear stress and also damped turbulent velocity fluctuations flow close to bed.

Chapter 6 Conclusion and future works

6.1 Conclusions

Understanding the fluid-particle interaction for application in rivers where the presence of micro and macro-scale features in the fluid plays a significant role, have been the focus of this study. These features are directly and significantly influenced by the chaotic phenomenon of turbulence, which involves a lot of large and small turbulent scales that have been captured in a more precise way than it has already been in the past i.e. LES turbulent modelling techniques. The effect of captured turbulent scales on the particles and vice versa is also demonstrated consequently. Points below are outlined the methods used to carry out this investigation along with the findings.

1. Running 3-D model with LES turbulence model and capturing small and large turbulent scales. The accuracy of turbulent modelling used in simulations of this study, i.e. LES modelling has shown to be in good agreement with different test cases such as DNS results reported by Kim, Moin and Moser (1987), LES results conducted by Yue, Lin and Patel (2006) and also experimental results of Balachandar *et al.* (2002). CFD tools used for numerical simulations have shown to successfully function for both turbulent mean values, e.g. mean velocities and turbulent statistics, e.g. stream-wise, wall-normal and span-wise velocity fluctuations. The first objective of this thesis has successfully been achieved through this section.

2. Experimental tests have been carried out to compare with numerical results obtained for bar-form geometry. With the use of an experimental tool Vectrino-II, considering its sensitivity to water vortex created at the beams of measurements, experimental findings specifically away from the bed have been shown to be in good agreement with the velocity profiles obtained from numerical investigation. All graphs clearly show that the fully turbulent region of flow have been well detected by the use of both numerical and

experimental tools. Additionally most of the velocity profiles at the bottom half of the graphs i.e. viscous sub-layer region and parts of buffer-layer, have not been sensitively followed by the experimental readings. This is where the presence of high shear and small scales of turbulent motions makes measurements extremely difficult. Furthermore this weak trend can be either explained by the poor calibration of the Vectrino-II or by errors in the filtering process. Most numerically obtained negative velocities at this part of graphs are indicative of the eddy formation at the slope, lee side and downstream of bar-form. The upstream velocity profiles tend to match better than the downstream velocity profiles. Such findings covers the 2nd objective this project.

3. Bed-load sediment transport has been studied on a particulate scale. Sediments have been introduced in the aforementioned dune-form model and therefore four-way coupling i.e. fluid-particle, particle-fluid, particle-particle and particle-structure interactions has been studied by the use of numerical modelling. Objective 3 of this study has been met by this approach. To examine the accuracy of the particle-particle interaction, simulation has been conducted by using DEM solver where fluid is not present in this stage. This has shown a faithful behaviour of particles on the bed surface. Hence the effects that flow field has on the particles close to bed, have been evidently witnessed. Through this step the 4th objective has also been achieved. Particles are lifted as a result of applied forces from eddies and therefore significant influence is captured on the moving particles that are in the vicinity of eddies. Moreover effects that sediments apply on the turbulent structures in the flow have also been captured due to momentum exchange between particle and fluid phase. This has been revealed by the means of fluctuation variations at the location of interacting particles in the flume. It is clear that, not only movement of sediments at river beds are influenced by turbulent flows but also in most occasions the solid particles have a direct impact on the flow

regime and fluids motion. This point covers the objective 5 of this study successfully.

6.2 **Future works**

Detailed modelling of fluid-particle interaction with applications in rivers has been the focus of this research with the use of numerical modelling. The following points are outlined to state future works possibilities:

- In this study bed-load sediment transport has been investigated, only by the use of single size and one material. This should be extended by the use of varieties of particle sizes and materials.
- For describing bed-load in a more realistic approach the number of particles should be increased.
- Four-way coupling should also be used for the suspended-load phase of sediment transport.

REFERENCES

ABBOTT, J. and J. R. D. FRANCIS. 1977. Saltation and suspension trajectories of solid grains in a water stream. *Philosophical Transactions of the Royal Society of London. Series A, Mathematical and Physical Sciences,* **284**(1321), p225.

AFKHAMI, M., A. HASSANPOUR, M. FAIRWEATHER and D. NJOBUENWU. 2015. Fully coupled LES-DEM of particle interaction and agglomeration in a turbulent channel flow. *Computers & Chemical Engineering,* **78**, pp.24-38.

ANDERSON JR, J. D. 2005. Ludwig Prandtl's boundary layer. *Physics today,* **58**(12), pp.42-48.

ANSYS FLUENT. 2009. 12.0 User's Guide. *ANSYS Inc.*

ANSYS FLUENT. 2011. 14.0.0 Theory Guide. *ANSYS, Inc.,* **Version 14.0.0, ANSYS, Inc., Canonsburg, PA, USA,**.

Introduction to ANSYS FLUENT. 2010. [CD-ROM].

ANSYS UK, L. 2012. *ANSYS turbulence* [online]. [Accessed]. Available from: http://www.ansys.com/staticassets/ANSYS/Conference/Confidence/San%20 Jose/Downloads/turbulence-summary-4.pdf.

ASCE TASK FORCE, B., E.D. 2002, 2005. Flow and Transport over Dunes. *Journal of Hydraulic Engineering.*

ASHIDA, K. 1972. Study on hydraulic resistance and bed-load transport rate in alluvial streams. *Journal of Civil Engineering, Jpn Soc Civil Engineers,* **206**, pp.59-69.

BAGNOLD, R. A. 1988. An approach to the sediment transport problem from general physics. *The physics of sediment transport by wind and water: a collection of hallmark papers*, p231.

BALACHANDAR, R., C. POLATEL, B. HYUN, K. YU, C. LIN, W. YUE and V. PATEL. 2002. LDV, PIV and LES investigation of flow over a fixed dune. *In: Proc., Symp. Held in Monte Verità: Sedimentation and Sediment Transport*: Kluwer Academic Dordrecht, The Netherlands, pp.171-178.

BATCHELOR, G. K. 1953. *The theory of homogeneous turbulence.* Cambridge university press.

BATCHELOR, G. K. 2000. *An introduction to fluid dynamics.* Cambridge university press.

BEAMAN, F. 2010. *Large eddy simulation of open channel flows for conveyance estimation.* thesis, Nottingham.

BENNETT, S. and J. BEST. 1995. Mean flow and turbulence structure over fixed, two dimensional dunes: implications for sediment transport and bedform stability. *Sedimentology,* **42**(3), pp.491-513.

BERDANIER, R. A. 2011. Turbulent flow through an asymmetric plane diffuser. *Masters, Purdue University.*

BERNARD, P. S. 1986. Limitations of the near-wall k-epsilon turbulence model. *AIAA journal,* **24**(4), pp.619-622.

BEST, J. 2005a. The fluid dynamics of river dunes: A review and some future research directions. *J. Geophys. Res,* **110**(1).

BEST, J. 2005b. Kinematics, topology and significance of dune-related macroturbulence: some observations from the laboratory and field. *Fluvial Sedimentology VII*, pp.41–60.

BOSSE, T., L. KLEISER and E. MEIBURG. 2006. Small particles in homogeneous turbulence: settling velocity enhancement by two-way coupling. *Physics of Fluids,* **18**, p027102.

BRIDGE, J. S. 2003. *Rivers and floodplains: forms, processes, and sedimentary record.* Wiley-Blackwell.

BUICE, C. U. 1997. *Experimental investigation of flow through an asymmetric plane diffuser.* thesis, Stanford University.

BYUN, D. S. and X. H. WANG. 2005. The effect of sediment stratification on tidal dynamics and sediment transport patterns. *Journal of Geophysical Research,* **110**(C3), pC03011.

CALANTONI, J., K. TODD HOLLAND and T. G. DRAKE. 2004. Modelling sheet–flow sediment transport in wave–bottom boundary layers using discrete–element modelling. *Philosophical Transactions of the Royal Society of London. Series A: Mathematical, Physical and Engineering Sciences,* **362**(1822), p1987.

CEA, L., J. PUERTAS and L. PENA. 2007. Velocity measurements on highly turbulent free surface flow using ADV. *Experiments in fluids,* **42**(3), pp.333-348.

CHENG, N.-S. and Y.-M. CHIEW. 1999. Analysis of initiation of sediment suspension from bed load. *Journal of Hydraulic Engineering,* **125**(8), pp.855-861.

CHOU, Y. J. and O. B. FRINGER. 2008. Modeling dilute sediment suspension using large-eddy simulation with a dynamic mixed model. *Physics of Fluids,* **20**, p115103.

CHUNG, T. 2010. *Computational fluid dynamics.* Cambridge Univ Pr.

COLEMAN, N. L. 1967. A theoretical and experimental study of drag and lift forces acting on a sphere resting on a hypothetical streambed.

DAWDY, D. R. and V. A. VANONI. 1986. Modeling alluvial channels. *Water Resources Research,* **22**(9S), pp.71S-81S.

DEY, S. 1999. Sediment threshold. *Applied Mathematical Modelling,* **23**(5), pp.399-417.

DEY, S. and K. DEBNATH. 2000. Influence of streamwise bed slope on sediment threshold under stream flow. *Journal of irrigation and drainage engineering,* **126**(4), pp.255-263.

DEY, S. and A. PAPANICOLAOU. 2008. Sediment threshold under stream flow: a state-of-the-art review. *KSCE Journal of Civil Engineering,* **12**(1), pp.45-60.

DORGAN, A. and E. LOTH. 2004. Simulation of particles released near the wall in a turbulent boundary layer. *International journal of multiphase flow,* **30**(6), pp.649-673.

DRAKE, T. G. and J. CALANTONI. 2001. Discrete particle model for sheet flow sediment transport in the nearshore. *Journal of Geophysical Research,* **106**(C9), pp.19859-19,868.

DWIVEDI, A., B. MELVILLE and A. Y. SHAMSELDIN. 2010. Hydrodynamic Forces Generated on a Spherical Sediment Particle during Entrainment. *Journal of Hydraulic Engineering,* **136**, p756.

EINSTEIN, H. A. 1942. Formulas for the transportation of bed load. *Trans. ASCE,* **107**, pp.575-577.

EINSTEIN, H. A. and E.-S. A. EL-SAMNI. 1949. Hydrodynamic forces on a rough wall. *Reviews of modern physics,* **21**(3), p520.

ELGHOBASHI, S. 1994. On predicting particle-laden turbulent flows. *Applied Scientific Research,* **52**(4), pp.309-329.

ELGHOBASHI, S. and G. TRUESDELL. 1993. On the two-way interaction between homogeneous turbulence and dispersed solid particles. I: Turbulence modification. *Physics of Fluids A Fluid Dynamics,* **5**, pp.1790-1790.

ENGELUND, F. and E. HANSEN. 1967. A monograph on sediment transport in alluvial streams. *MONOGR, DENMARK TECH UNIV, HYDRAUL LAB, 62 P, 1967. 30 FIG, 3 TAB, 31 REF.*

FAN, L.-S. and C. ZHU. 2005. *Principles of gas-solid flows.* Cambridge University Press.

FEDELE, J. J. and M. H. GARCIA. 2001. 3 Alluvial Roughness in Streams with Dunes: A Boundary-Layer Approach. *River, coastal, and estuarine morphodynamics*, p37.

FEURICH, R. and N. R. B. OLSEN. 2011. Three-Dimensional Modeling of Nonuniform Sediment Transport in an S-Shaped Channel. *Journal of Hydraulic Engineering,* **137**, p493.

FLUENT 6.2-USER GUIDE. 2005. 6.2-User's Guide. *Fluent Inc., New Hampshire*.

FRIZELL, K. W. 2004. Effects of aeration on the performance of an ADV. *In*: ASCE.

FURBISH, D. J. and M. W. SCHMEECKLE. 2013. A probabilistic derivation of the exponential-like distribution of bed load particle velocities. *Water Resources Research,* **49**(3), pp.1537-1551.

FUREBY, C., G. TABOR, H. WELLER and A. GOSMAN. 1997. A comparative study of subgrid scale models in homogeneous isotropic turbulence. *Physics of Fluids (1994-present),* **9**(5), pp.1416-1429.

GARCÍA, C. M., M. I. CANTERO, Y. NIÑO and M. H. GARCÍA. 2004a. Acoustic Doppler velocimeters (ADV) performance curves (APCs) sampling the flow turbulence. *In: Critical transitions in water and environmental resources management, proceedings of the 2004 world water and environmental resources congress. ASCE, Salt Lake City*.

GARCÍA, C. M., M. I. CANTERO, C. R. REHMANN and M. H. GARCÍA. 2004b. New methodology to subtract noise effects from turbulence parameters computed from ADV velocity signals. *In: Critical transitions in*

water and environmental resources management, proceedings of the 2004 world water and environmental resources congress. ASCE, Salt Lake City.

GARCIA, M. H. 2008. Sedimentation engineering. *Processes, Measurements, Modeling, and Practice. ASCE Manuals and Reports on Engineering Practice,* (110).

GARCÍA, M. H. 2008. *Sedimentation engineering: processes, measurements, modeling, and practice.* ASCE Publications.

GERMANO, M., U. PIOMELLI, P. MOIN and W. H. CABOT. 1991. A dynamic subgrid-scale eddy viscosity model. *Physics of Fluids A: Fluid Dynamics (1989-1993),* **3**(7), pp.1760-1765.

GEUZAINE, C. and J. F. REMACLE. 2009. Gmsh: A 3-D finite element mesh generator with built-in pre-and post-processing facilities. *International Journal for Numerical Methods in Engineering,* **79**(11), pp.1309-1331.

GONIVA, C., C. KLOSS, A. HAGER and S. PIRKER. 2010. An open source CFD-DEM perspective. *In: Proceedings of OpenFOAM Workshop, Göteborg.*

GORING, D. G. and V. I. NIKORA. 2002. Despiking acoustic Doppler velocimeter data. *Journal of Hydraulic Engineering,* **128**(1), pp.117-126.

GRAF, W. H. 1984. *Hydraulics of sediment transport.* Water Resources Pubns.

HARDY, R., J. BEST, S. LANE and P. CARBONNEAU. 2009. Coherent flow structures in a depth-limited flow over a gravel surface: The role of near-bed turbulence and influence of Reynolds number. *Journal of Geophysical Research,* **114**(F1), pF01003.

HARDY, R., J. BEST, S. LANE and P. CARBONNEAU. 2010. Coherent flow structures in a depth-limited flow over a gravel surface: The influence of surface roughness. *Journal of Geophysical Research,* **115**(F3), pF03006.

HARDY, R., S. LANE, R. FERGUSON and D. PARSONS. 2007. Emergence of coherent flow structures over a gravel surface: A numerical experiment. *Water Resources Research,* **43**(3), pW03422.

HARLOW, F. H. and A. A. AMSDEN. 1968. Numerical calculation of almost incompressible flow. *Journal of Computational Physics,* **3**(1), pp.80-93.

HASBO, P. B. 1995. Flow and sediment transport over oblique bed forms. *Series paper/Institute of hydrodynamics and hydraulic engineering (Lyngby).*

HEALD, J., I. MCEWAN and S. TAIT. 2004. Sediment transport over a flat bed in a unidirectional flow: simulations and validation. *Philosophical Transactions of the Royal Society of London. Series A: Mathematical, Physical and Engineering Sciences,* **362**(1822), p1973.

HSÜ, K. J. 2004. *Physics of sedimentology: textbook and reference.* Springer Verlag.

IKEZAKI, S., M. W. SCHMEECKLE, Y. SHIMIZU, K. HOSHI and H. BABA. 1999. Turbulent Structures and Suspended Sediment Over Two-Dimensional Dunes.

JACKSON, R. G. 1976. Sedimentological and fluid-dynamic implications of the turbulent bursting phenomenon in geophysical flows. *Journal of Fluid Mechanics,* **77**(03), pp.531-560.

JEFCOATE, B. and I. MCEWAN. 1997. Discrete Particle Modelling of Grain Sorting During Bedload Transport. *In*: ASCE, pp.1457-1462.

JOHNSON, K. 1987. *Contact mechanics.* Cambridge university press.

JULIEN, P. Y. 2010. *Erosion and sedimentation.* Cambridge Univ Pr.

KIM, J., P. MOIN and R. MOSER. 1987. Turbulence statistics in fully developed channel flow at low Reynolds number. *Journal of Fluid Mechanics,* **177**, pp.133-166.

KLEINHANS, M. 2004. Sorting in grain flows at the lee side of dunes. *Earth-Science Reviews,* **65**(1-2), pp.75-102.

KLEINHANS, M. G. and L. C. VAN RIJN. 2002. Stochastic prediction of sediment transport in sand-gravel bed rivers. *Journal of Hydraulic Engineering,* **128**(4), pp.412-425.

KLOSS, C., C. GONIVA, G. AICHINGER and S. PIRKER. 2009. Comprehensive DEM-DPM-CFD simulations-model synthesis, experimental validation and scalability. *In: Proceedings of the Seventh International Conference on CFD in the Minerals and Process Industries, CSIRO, Melbourne, Australia.*

KLOSS, C., C. GONIVA, A. HAGER, S. AMBERGER and S. PIRKER. 2012. Models, algorithms and validation for opensource DEM and CFD–DEM. *Progress in Computational Fluid Dynamics, an International Journal,* **12**(2), pp.140-152.

KLOSS, C., P. SEIL, S. A. AMBERGER and A. AIGNER. 2011. *CFDEM* [online]. [Accessed 30/12/2014]. Available from: http://www.cfdem.com/liggghts-open-source-discrete-element-method-particle-simulation-code.

KOLMOGOROV, A. 1942. Equations of turbulent motion of an incompressible fluid. *Izv. Akad. Nauk SSSR, Ser. Fiz,* **6**(1/2), pp.56–58.

KOLMOGOROV, A. N. 1941. The local structure of turbulence in incompressible viscous fluid for very large Reynolds numbers. *In*, pp.9–13.

KOSTASCHUK, R., P. VILLARD and J. BEST. 2004. Measuring velocity and shear stress over dunes with acoustic Doppler profiler. *Journal of Hydraulic Engineering,* **130**, p932.

KRAUS, N. C., A. LOHRMANN and R. CABRERA. 1994. New acoustic meter for measuring 3D laboratory flows. *Journal of Hydraulic Engineering,* **120**(3), pp.406-412.

KRUGGEL-EMDEN, H., M. STURM, S. WIRTZ and V. SCHERER. 2008. Selection of an appropriate time integration scheme for the discrete element method (DEM). *Computers & Chemical Engineering,* **32**(10), pp.2263-2279.

LANE, S., P. BIRON, K. BRADBROOK, J. BUTLER, J. CHANDLER, M. CROWELL, S. MCLELLAND, K. RICHARDS and A. ROY. 1998. Three-dimensional measurement of river channel flow processes using acoustic Doppler velocimetry. *Earth Surface Processes and Landforms,* **23**(13), pp.1247-1267.

LEE, H. A. H., I.S. 1994. Investigation of saltating particle motions. *Journal of Hydraulic Engineering,* **120**, p831.

LILLY, D. K. 1992. A proposed modification of the Germano subgrid-scale closure method. *Physics of Fluids A: Fluid Dynamics (1989-1993),* **4**(3), pp.633-635.

LING, C.-H. 1995. Criteria for incipient motion of spherical sediment particles. *Journal of Hydraulic Engineering,* **121**(6), pp.472-478.

LIU, M., D. Z. ZHU and N. RAJARATNAM. 2002. Evaluation of ADV measurements in bubbly two-phase flows. *In: Hydraulic measurement and experiment methods 2002, proceedings of the specialty conference July*.

LOHRMANN, A., R. CABRERA and N. C. KRAUS. 1994. Acoustic-Doppler velocimeter (ADV) for laboratory use. *In: Fundamentals and advancements in hydraulic measurements and experimentation*: ASCE, pp.351-365.

LOTH, E. and A. DORGAN. 2009. An equation of motion for particles of finite Reynolds number and size. *Environmental fluid mechanics,* **9**(2), pp.187-206.

LU, S. and W. WILLMARTH. 1973. Measurements of the structure of the Reynolds stress in a turbulent boundary layer. *Journal of Fluid Mechanics,* **60**(03), pp.481-511.

MADDUX, T., J. NELSON and S. MCLEAN. 2003a. Turbulent flow over three-dimensional dunes: 1. Free surface and flow response. *Journal of Geophysical Research,* **108**(F1), p6009.

MANSOUR, N., J. KIM and P. MOIN. 1989. Near-wall k-epsilon turbulence modeling. *AIAA journal,* **27**(8), pp.1068-1073.

MCEWAN, I. and J. HEALD. 2001. Discrete particle modeling of entrainment from flat uniformly sized sediment beds. *Journal of Hydraulic Engineering,* **127**(7), pp.588-597.

MCEWAN, I., J. HEALD and D. GORING. 1999. Discrete Particle Modelling of Entrainment from a Mixed Size Sediment Bed ". *In*, pp.75-84.

MCLEAN, S., J. NELSON and S. WOLFE. 1994. Turbulence structure over two-dimensional bed forms: Implications for sediment transport. *Journal of Geophysical Research,* **99**(C6), pp.12729-12,747.

MCLEAN, S., S. WOLFE and J. NELSON. 1999a. Predicting boundary shear stress and sediment transport over bed forms. *Journal of Hydraulic Engineering,* **125**, p725.

MCLEAN, S., S. WOLFE and J. NELSON. 1999b. Spatially averaged flow over a wavy boundary revisited. *Journal of Geophysical Research,* **104**(C7), pp.15743-15,753.

MCLEAN, S. R. 1990. The stability of ripples and dunes. *Earth-Science Reviews,* **29**(1-4), pp.131-144.

MCLEAN, S. R. and J. D. SMITH. 1979. Turbulence measurements in the boundary layer over a sand wave field. *Journal of Geophysical Research,* **84**(C12), pp.7791-7808.

MEYER-PETER, E. and R. MÜLLER. 1948. Formulas for bed-load transport. *In*, pp.39–64.

MIDAS DATA ACQUISITION SOFTWARE. 2012. Nortek Software User Guide. [online].

MONIN, A. S. and A. M. YAGLOM. 2007. *Statistical fluid mechanics: mechanics of turbulence.* Courier Dover Publications.

MURPHY, P. J. and H. HOOSHIARI. 1982. Saltation in water dynamics. *Journal of the Hydraulics Division,* **108**(11), pp.1251-1267.

NABI, M., H.J. DE VRIEND, E. M. &, C.J. SLOFF and Y. SHIMIZU. 2010. Simulation of subaqueous dunes using detailed hydrodynamics.

NELSON, J. M., S. R. MCLEAN and S. R. WOLFE. 1993. Mean flow and turbulence fields over two-dimensional bed forms. *Water Resources Research,* **29**(12), pp.3935-3953.

NELSON, J. M., R. L. SHREVE, S. R. MCLEAN and T. G. DRAKE. 1995. Role of near-bed turbulence structure in bed load transport and bed form mechanics. *Water resources research,* **31**(8), pp.2071-2086.

NIKORA, V. and D. GORING. 2000. Flow turbulence over fixed and weakly mobile gravel beds. *Journal of Hydraulic Engineering,* **126**(9), pp.679-690.

NIKORA, V. I. and D. G. GORING. 1998. ADV measurements of turbulence: Can we improve their interpretation? *Journal of Hydraulic Engineering,* **124**(6), pp.630-634.

NIÑO, Y. and M. GARCÍA. 1994. Gravel saltation: 2. Modeling. *Water Resources Research,* **30**(6), pp.1915-1924.

NORTEK AS. 2013. *Acoustic Doppler Velocimeters* [online]. [Accessed 30/09/2013]. Available from: http://www.nortek-as.com/en/products/velocimeters.

NORTEK AS USER GUIDE. 2012. Vectrino Velocimeter User Guide. *Nortek AS, Vangkroken, Norway* [online].

PAINTAL, A. 1971. Concept of critical shear stress in loose boundary open channels. *Journal of Hydraulic Research,* **9**(1), pp.91-113.

PAPANICOLAOU, A., P. DIPLAS, C. DANCEY and M. BALAKRISHNAN. 2001. Surface roughness effects in near-bed turbulence: Implications to sediment entrainment. *Journal of Engineering Mechanics,* **127**(3), pp.211-218.

PAPANICOLAOU, A., P. DIPLAS, N. EVAGGELOPOULOS and S. FOTOPOULOS. 2002. Stochastic incipient motion criterion for spheres under various bed packing conditions. *Journal of Hydraulic Engineering,* **128**(4), pp.369-380.

PAPANICOLAOU, A. N., M. ELHAKEEM, G. KRALLIS, S. PRAKASH and J. EDINGER. 2008. Sediment transport modeling review—current and future developments. *Journal of Hydraulic Engineering,* **134**(1), pp.1-14.

PAPHITIS, D. 2001. Sediment movement under unidirectional flows: an assessment of empirical threshold curves. *Coastal Engineering,* **43**(3), pp.227-245.

PARKHURST, J., G. PRICE, P. SHARROCK and C. MOORE. 2011. Phase unwrapping algorithms for use in a true real-time optical body sensor system for use during radiotherapy. *Applied optics,* **50**(35), pp.6430-6439.

PATANKAR, S. V. and D. B. SPALDING. 1972. A calculation procedure for heat, mass and momentum transfer in three-dimensional parabolic flows. *International Journal of Heat and Mass Transfer,* **15**(10), pp.1787-1806.

PEDINOTTI, S., G. MARIOTTI and S. BANERJEE. 1992. Direct numerical simulation of particle behaviour in the wall region of turbulent flows in horizontal channels. *International journal of multiphase flow,* **18**(6), pp.927-941.

PLIMPTON, S., R. POLLOCK and M. STEVENS. 1997. Particle-Mesh Ewald and rRESPA for Parallel Molecular Dynamics Simulations. *In: PPSC*: Citeseer.

PLIMPTON, S., A. THOMPSON, P. CROZIER and A. KOHLMEYER. 1990. *LAMMPS* [online]. [Accessed 30/12/2014]. Available from: http://lammps.sandia.gov/.

POPE, S. B. 2000. *Turbulent flows.* Cambridge Univ Pr.

PRANDTL, L. 1945. Uber ein neues Formelsystem für die ausgebildete Turbulenz. Math. *Phys. Klasse*, p6.

PUERTAS, J., L. PENA and T. TEIJEIRO. 2003. Experimental approach to the hydraulics of vertical slot fishways. *Journal of Hydraulic Engineering,* **130**(1), pp.10-23.

PYE, K. 1994. *Sediment transport and depositional processes.* London.

REYNOLDS, O. 1895. On the dynamical theory of incompressible viscous fluids and the determination of the criterion. *Philosophical Transactions of the Royal Society of London. A*, pp.123-164.

RICHARDSON, L. F. 2007. *Weather prediction by numerical process.* Cambridge University Press.

RODI, W. 1993. *Turbulence models and their application in hydraulics: a state-of-the art review.* Aa Balkema.

ROTTA, J. 1951. Statistische theorie nichthomogener turbulenz. *Zeitschrift für Physik,* **129**(6), pp.547-572.

SAGAUT, P. 2001. *Large eddy simulation for incompressible flows.* Springer.

SALIM, S. M. and S. CHEAH. 2009. Wall y Strategy for Dealing with Wall-bounded Turbulent Flows. *Proceedings of the International MultiConference of Engineers and Computer Scientists,* **2**.

SCHMEECKLE, M. 1999. A dynamic boundary condition for bedload sediment transport in non-uniform, hydraulically rough turbulent boundary layers. *Annual Journal of Hydraulic Engineering, Japan Society of Civil Engineers,* **42**, pp.653-658.

SCHMEECKLE, M. 2015. The role of velocity, pressure, and bed stress fluctuations in bed load transport over bed forms: numerical simulation downstream of a backward-facing step. *Earth Surface Dynamics,* **3**(1), pp.105-112.

SCHMEECKLE, M. and J. NELSON. 2003. Direct numerical simulation of bedload transport using a local, dynamic boundary condition. *Sedimentology,* **50**(2), pp.279-301.

SCHMEECKLE, M., J. NELSON, J. PITLICK and J. BENNETT. 2001. Interparticle collision of natural sediment grains in water. *Water Resources Research,* **37**(9), pp.2377-2391.

SCHMEECKLE, M., J. NELSON and R. SHREVE. 2007. Forces on stationary particles in near-bed turbulent flows. *Journal of Geophysical Research,* **112**(F2), pF02003.

SCHMEECKLE, M. W. 2014. Numerical simulation of turbulence and sediment transport of medium sand. *Journal of Geophysical Research: Earth Surface,* **119**(6), pp.1240-1262.

SCKINE, M. 1992. Mechanics of saltating grains. II.

SHI, J., T. THOMAS and J. WILLIAMS. 1999. Large-eddy simulation of flow in a rectangular open channel. *Journal of Hydraulic Research,* **37**(3), pp.345-361.

SHIELDS, A. 1936. Anwendung der Ähnlichkeitsmechanik und der Turbulenz Forschung auf die Geschiebe Bewegung, Mitt, der Preuss. *Versuchsanst. für Wasserbau und Schiffbau,* (26).

SHIMIZU, Y., M. SCHMEECKLE and J. NELSON. 2001. Direct Numerical Simulation of Turbulence Over Two-Dimensional Dunes Using CIP Method. *Journal of Hydroscience and Hydraulic Engineering,* **19**(2), pp.85-92.

SMAGORINSKY, J. 1963. General circulation experiments with the primitive equations. *Monthly weather review,* **91**(3), pp.99-164.

STOESSER, T., J. FROHLICH and W. RODI. 2003. Identification of coherent flow structures in open-channel flow over rough bed using Large Eddy Simulation. *In.*

TAYLOR, G. I. 1938. The spectrum of turbulence. *Proceedings of the Royal Society of London. Series A-Mathematical and Physical Sciences,* **164**(919), pp.476-490.

TENNEKES, H. and J. L. LUMLEY. 1972. *A first course in turbulence.* MIT press.

THOMAS, R. E., S. J. MCLELLAND and L. E. FROSTICK. 2013. The Impact of Macroalgae on Mean and Turbulent Flow Fields. *In: 2013 IAHR Congress,* Tsinghua University Press, Beijing.

THOMAS, T. and J. WILLIAMS. 1995b. Large eddy simulation of turbulent flow in an asymmetric compound open channel. *Journal of Hydraulic Research,* **33**(1), pp.27-41.

TOWNSEND, A. A. 1980. *The structure of turbulent shear flow.* Cambridge university press.

TSUJI, Y. 2000. Activities in discrete particle simulation in Japan. *Powder technology,* **113**(3), pp.278-286.

VAN RIJN, L. C. 1984-a. Sediment transport, part I: bed load transport. *Journal of Hydraulic Engineering,* **110**(10), pp.1431-1456.

VAN RIJN, L. C. 1984-b. Sediment transport, Part II: Suspended load transport. *Journal of Hydraulic Engineering,* **110**(11), pp.1613-1641.

VAN RIJN, L. C. 1993. *Principles of sediment transport in rivers, estuaries and coastal seas.*

VANONI, V. A. 2006. *Sedimentation engineering.* ASCE Publications.

VENDITTI, J. G. and S. J. BENNETT. 2000. Spectral analysis of turbulent flow and suspended sediment transport over fixed dunes. *Journal of Geophysical Research,* **105**(C9), pp.22,035-22,048.

VERSTEEG, H. K. and W. MALALASEKERA. 2007. *An introduction to computational fluid dynamics: the finite volume method.* Prentice Hall.

VILLARD, P. and R. KOSTASCHUK. 1998. The relation between shear velocity and suspended sediment concentration over dunes: Fraser Estuary, Canada. *Marine geology,* **148**(1-2), pp.71-81.

VON KARMAN, T. 1930a. *Calculation of pressure distribution on airship hulls.* National Advisory Committee for Aeronautics.

VON KARMAN, T. 1930b. Mechanische änlichkeit und turbulenz. *Nachrichten von der Gesellschaft der Wissenschaften zu Göttingen, Mathematisch-Physikalische Klasse,* **1930**, pp.58-76.

VON KARMAN, T. 1948. Progress in the statistical theory of turbulence. *Proceedings of the National Academy of Sciences of the United States of America,* **34**(11), p530.

VOULGARIS, G. and J. H. TROWBRIDGE. 1998. Evaluation of the acoustic Doppler velocimeter (ADV) for turbulence measurements. *Journal of Atmospheric and Oceanic Technology,* **15**(1), p272.

VREMAN, B., B. J. GEURTS, N. DEEN, J. KUIPERS and J. KUERTEN. 2009. Two-and four-way coupled Euler–Lagrangian large-eddy simulation of turbulent particle-laden channel flow. *Flow, turbulence and combustion,* **82**(1), pp.47-71.

WAHL, T. L. 2000. Analyzing ADV data using WinADV. *In: Proc., Joint Conf. on Water Resources Engineering and Water Resources Planning and Management*. ASCE Reston, Va., pp.1-10.

WAHL, T. L. 2003. Discussion of "Despiking acoustic doppler velocimeter data" by Derek G. Goring and Vladimir I. Nikora. *Journal of Hydraulic Engineering,* **129**(6), pp.484-487.

WANG, L. P. and M. R. MAXEY. 1993. Settling velocity and concentration distribution of heavy particles in homogeneous isotropic turbulence. *Journal of Fluid Mechanics,* **256**(-1), pp.27-68.

WELLER, H., C. GREENSHIELDS and M. JANSSENS. 2014. *OpenFOAM User Guide* [online]. [Accessed 01/01/2015]. Available from: http://www.openfoam.org/docs/user/blockMesh.php.

WELLER, H. G., G. TABOR, H. JASAK and C. FUREBY. 1998. A tensorial approach to computational continuum mechanics using object-oriented techniques. *Computers in physics,* **12**(6), pp.620-631.

WHITE, C. 1940. The equilibrium of grains on the bed of a stream. *Proceedings of the Royal Society of London. Series A. Mathematical and Physical Sciences,* **174**(958), pp.322-338.

WIBERG, P. L. and J. D. SMITH. 1985. A theoretical model for saltating grains in water. *Journal of Geophysical Research,* **90**(C4), pp.7341-7354.

WIBERG, P. L. and J. D. SMITH. 1987. Calculations of the critical shear stress for motion of uniform and heterogeneous sediments. *Water Resources Research,* **23**(8), pp.1471-1480.

WILCOX, D. C. 1993. *Turbulence modeling for CFD.* La Canada, CA: DCW Industries, Inc, 1993.

WRIGHT, N. and A. CROSATO. 2011. The Hydrodynamics and Morphodynamics of Rivers. *In:* P. WILDERER, ed. *Treatise on water science.* Oxford: Elsevier Ltd., pp.135-156.

WU, F.-C. and Y.-J. CHOU. 2003. Rolling and lifting probabilities for sediment entrainment. *Journal of Hydraulic Engineering,* **129**(2), pp.110-119.

WU, W., W. RODI and T. WENKA. 2000. 3D numerical modeling of flow and sediment transport in open channels. *Journal of Hydraulic Engineering,* **126**, p4.

YANG, C. and U. LEI. 1998. The role of the turbulent scales in the settling velocity of heavy particles in homogeneous isotropic turbulence. *Journal of Fluid Mechanics,* **371**(-1), pp.179-205.

YEOH, G. H., C. P. CHEUNG and J. TU. 2013. *Multiphase flow analysis using population balance modeling: Bubbles, drops and particles.* Butterworth-Heinemann.

YUE, W., C. LIN and V. PATEL. 2006. Large-eddy simulation of turbulent flow over a fixed two-dimensional dune. *Journal of Hydraulic Engineering,* **132**, p643.

ZANKE, U. 1990. Der Beginn der Sedimentbewegung als Wahrscheinlichkeitsproblem. *Wasser & Boden,* **42**(1), pp.40-43.

ZEDEL, L. and A. E. HAY. 2010. Resolving velocity ambiguity in Multifrequency, pulse-to-pulse coherent Doppler sonar. *Oceanic Engineering, IEEE Journal of,* **35**(4), pp.847-851.

ZEDLER, E. A. and R. L. STREET. 2001. Large-eddy simulation of sediment transport: currents over ripples. *Journal of Hydraulic Engineering,* **127**, p444.

ZEDLER, E. A. and R. L. STREET. 2006. Sediment transport over ripples in oscillatory flow. *Journal of Hydraulic Engineering,* **132**, p180.